Mechanical shock values applied in condition monitoring of bearings operating under variable speed and load conditions.

Dissertation submitted for the degree of Magister Technologiae in

Mechanical Engineering

Allan Andre Olivier

Student No: 8086

Vaal University of Technology

August 2014

Supervisor: Prof. A.A. Alugongo

Co-Supervisor: Prof. L.M. Masu

DECLARATION

I, Allan Andre Olivier, declare that the material in this dissertation is my work. I confirm that this work has not been submitted to another institution for any other degree.

Signed _____  ____

AA Olivier

Student no: 8086

Date: August 2014

Place: Vanderbjilpark

DEDICATION

I dedicate this work to my soul mate and friend, Susan, who motivated me and supported me during this research, and to my children Wayne, Shaun and Ashley for all the hours they allowed me to work on my studies.

ABSTRACT

Monitoring the condition of equipment in industry is very important to prevent unplanned breakdowns and to prolong their life. This is necessary, since it is not always economically viable to stop equipment at regular intervals to do maintenance. Failure on machines can lead to high repair costs and production losses. It is thus of paramount importance that early failure symptoms be identified by means of condition monitoring.

This study in the field of condition monitoring is performed to determine if the mechanical shock values induced in defect bearings could be used to measure the condition of a bearing while operating under variable speed and variable load. Variable speed and variable load is becoming more popular in industry because variable speed drives applications ensure effective process control. Variable speed application, cause fault frequencies to fluctuate and therefore vibration applications for constant speed applications, which are speed-dependent, can no longer apply.
Vibration-monitoring techniques that have applied for many years have now become obsolete in these variable speed applications.

Methods such as Short Time Fourier Transformation (STFT), time scale like wavelet transform, and Order tracking has been applied in variable speed applications with some success. These methods analyses the vibration phases on the signal buy compensating for the speed changes. In this thesis, the Shock pulse method is selected as the analyses tool to measure the mechanical shock. Shock pulse monitoring does not focus on the vibration phases but measures in a small-time window when mechanical shocks are induced in the bearing material before the vibration phase.

There is very little documented research in the field of mechanical shock pulse monitoring for conditions of variable speed and variable loads, and therefore this research focuses on recording these mechanical shock values by empirical tests. The tests were performed on a bearing with an induced defect on the

outer race. The rolling element of the bearing strikes the defect and the mechanical shock value (dBsv) is measured. The mechanical shock is measured with the Shock pulse method in a small-time window before vibration occurs. In this time window, the dBsv is recorded over time to provide diagnostic information of the bearing during acceleration, deceleration and various loading conditions. These mechanical shocks are elastic waves that mirror the impact-contact-force's time function and the Shock pulse monitoring accelerometer, which is tuned to 32 kHz, will respond to the elastic wave fronts with transient amplitudes proportional to the square of the impact velocities.

The mechanical shock values were analysed and reoccurring fault levels were identified on each empirical test. These recurring events from the empirical tests were used as primary data for analysis in this research. Theses test were performed on a bearing with an induced failure and it was found that the dBsv measured over time could not be used to monitor the condition of the bearing under variable speed applications. This was because the dBsv changed as the speed increased. To overcome this problem Sohoel's theory was applied and the initial mechanical shock value (dBi) was calculated for the bearing. The dbi value was subtracted from the dBsv and a value called the maximum mechanical shock value (dBm) was obtained. The dBm values stayed constant for the duration of the test and this allowed the condition of the bearing to be measured under variable speed and variable load conditions with some exception.

The exception to the findings was that the dBm values stayed constant during acceleration phases, but during the deceleration phases the values were erratic and scattered. At speed below 200rpm the dBm values did not stay constant and therefore it was concluded that the dBm value recorded the best results only when thrust on the bearing was maximum. The other exception was under no-load conditions. The the values were erratic and scattered, and therefore the results were not a true reflection of the bearing condition. The third exception was that the results on bearings with various loads remained constant during increased load changes unless the loading was erratic. During

erratic load changes, the results were affected. The results also indicated that the larger the defect on the bearing raceway, the higher the dBm values were. Multipil defects on the bearing race ways were not part of this thesis and this gives an opertunity for futher research.
The Shock pulse monitoring technique was 100% successful in monitoring the bearing condition only while the speed of the bearing was increasing.

The results obtained in this work demonstrated that the condition of bearings can be monitored in applications of variable speed and variable load if the exception are eliminated and to obtain conclusive results the mechanical shock pulses should be measured over time and not be used as once-off value.

TABLE OF FIGURES

DEFINITIONS

Accelerometer: An instrument used for measuring acceleration.

Amplitude modulation: Multiplication of time-based signals of different amplitudes and frequency.

Ball pass frequency inner: Is the calculated fault frequency at which the inner race fault will occur with relation to the running speed of the shaft.

Ball pass frequency outer: Is the calculated fault frequency at which the outer race fault will occur with relation to the running speed of the shaft.

Ball spin frequency: Is the calculated fault frequency at which a roller fault will occur with relation to the running speed of the shaft.

Chattering: Noise in a bearing that is caused by the movement of roller elements inside bearings due to no load conditions.

Decibel initial (dBi): Calculated normalized shock value depended on the bearing rotational speeds and the inside diameter of the bearing.

Decibel maximum (dBm): Measured shock value indicating the severity of damage on the bearing rolling surface.

Decibel carpert value (dBc): Measured shock value indicating the bearing surface roughness and lubrication condition.

Decibel normalized (dBn): Calculated value that represents the difference in decibels of an old bearing compared to a new bearing

Dragline: An excavating machine in which the bucket is attached by cables to the hoist drum and operates by being drawn toward the machine

Distributed defects: Are classified as surface roughness, waviness, misalignment and off-size rolling elements.

Friction forces: Are forces generated in a bearing within the rolling elements.

Hoist motor: Is a device used for lifting or lowering a load by means of a drum or lift-wheel around which rope or chain wraps

Kurtosis: Is any measure of the peakedness of the probability distribution function.

Linear systems: A system is linear if for every element in the system the response is proportional to the excitation.

Localised defects: Are defined defects found on the bearing raceway and typically includes cavities, pits, cracks, spalls or protrusions.

Pressure wave: Are defined as a series of shock pulses that travel through the material.

Shock: Shock is defined as energy that is created when a rolling element strikes a localised defect.

Shock pulses: Are defined as the energy waves that occur after rolling element strikes a localised defect.

Shock pulse monitoring: Is a technique used to measure shock pulse severity in a bearing.

Fundamental Train Frequency: Is the calculated fault frequency at which the Train/cadge fault will occur in relation to the running speed of the shaft.

Transient vibrations: Are temporarily sustained vibration of a mechanical system.

Variable speed: Is defined as the changing operating speed of the machine.

Variable load: Is defined as the changing load on the machines.

LIST OF ABBREVIATIONS

BPFI	Ball Pass Frequency Inner
BPFO	Ball Pass Frequency Outer
BSF	Ball Spin Frequency
CF:	Crest Factor
CWT:	Continuous Wavelet Transformation
dBc:	decibel carpet value
dBi:	decibel initial
dBm:	decibel maximum
dBsv:	decibel shock value
dBn:	decibel value normalised
FTF	Fundamental Train Frequency
HFRT:	High Frequency Resonance Technique
kN:	kilo Newton
K:	Kurtosis
MEPA:	Monitoring Effects Pulse Analyser
PK:	Peak

PLC:	Programmed Logic Controller
rpm:	Revolutions per minute
RMS:	Root Mean Square
SAE:	Society of Automotive Engineers
SPM:	Shock Pulse Monitoring
STFT:	Short Time Fourier Transform
WVD:	Wigner-Ville Distributions

LIST OF SYMBOLS

Bd	Ball diameter
Pd	Pitch diameter
S	Speed
Nb	Number of balls
α	Roller contact angle
FTF	Fundamental Train Frequency
BPFI	Ball Pass Frequency Inner
BPFO	Ball Pass Frequency Outer
BSF	Ball Spin Frequency
E	Electric voltage
Vs	Impact velocity
Vw	Tangential velocity
Ni	Shaft speed
N	Ball rotational speed
D_B	Spherical roller diameter
D_i	Inner race diameter
V	peripheral velocity
Y	Ball depth in cavity
X	Cord $\underline{AB}$
Mc	Material constant
cSt	Centistokes
cP	Centipoise

TABLE OF CONTENTS

CHAPTER 1: INTRODUCTION AND PROBLEM STATEMENT

1.1 INTRODUCTION

Bearing failure analysis under constant speed and steady state applications has been based on the Fast Fourier Technique for years, and has used the fault frequency formulation to determine bearing faults (Stack, Habetler & Harley 2004). The fault frequency formulas and parameters used are shown here as equations 1.1 to 1.4. A schematic layout of the bearing configuration is given in Figure 1.1 (Taylor & Kirkland 2004:26)

Fundamental train frequency; $$FTF = \frac{S}{2}\left(1+\frac{Bd}{Pd}\cos\alpha\right) \quad (1.1)$$

Ball pass frequency inner race; $$BPFI = S\frac{Nb}{2}\left(1+\frac{Bd}{Pd}\cos\alpha\right) \quad (1.2)$$

Ball pass frequency outer race; $$BPFO = S\frac{Nb}{2}\left(1-\frac{Bd}{Pd}\cos\alpha\right) \quad (1.3)$$

Ball rotational frequency; $$2BSF = S\left(\frac{Pd}{Bd}\right)\left(1-\frac{Bd^2}{Pd^2}\cos^2\alpha\right) \quad (1.4)$$

Pd is the pitch diameter, *Bd* is the ball diameter, S is the shaft rotation speed, *Nb* is the number of balls, *cos* α is the contact angle between the roller and raceway.

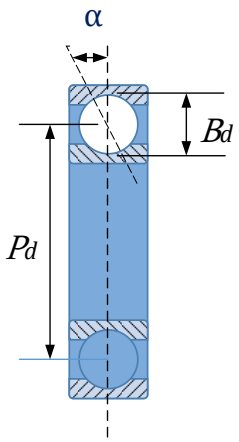

Figure 1.1 Schematic layout of rolling element

Seker and Ayaz (2003) stated that in applications of variable speed and load condition, transient vibration formulae cannot be used unless some alterations

are incorporated. Rai and Mohanty (2007) showed that when a non-stationary system undergoes a transient, the fast fourier technique does not provide correct information about the signal. Spanjaard and Elton (1996) also found out that, the measurements of speed of shafts that accelerated rapidly was characterised by loses of pulses.

It is evident from the equations 1.1 to 1.4 that the various fault frequencies are dependent on the shaft speed and because the motor's speed varies, the fault frequency will therefore also vary.

Taylor and Kirkland (2004:32) state in the Bearing Analysis Handbook that an increase in the load will cause the contact angle to change. A change in the contact angle will increase the value of the Ball Pass Frequency Outer (BPFO), the Ball Spin Frequency (BSF), and the Fault Train Frequency (FTF) for a bearing with an inner race rotating. If the outer race rotates, the Ball Pass Frequency Inner (BPFI) and the FTF values will decrease.

In bearing vibration-monitoring applications, where the speed is varied and the load changed, new vibration analysis techniques have been developed. Zhen, Zhengjia, Yanyang and Xuefeng (2008) used methods such as Short Time Fourier Transformation (STFT), Time scale like Wavelet Transform, Order tracking and Shock Pulse Monitoring in variable speed applications. Other motor condition monitoring techniques also used to identify bearing failure in motors are fault frequency spectral analysis, electrical motor stator current fluctuations and air gap torque monitoring.

These vibration-monitoring applications have been researched since the 1960 and research papers published by Stronach, Cudworth and Johnston (1984), Tandon and Nakra (1992), Ray (1980) are significant in this area. The results of research in this area have develop state of the art vibration technology machines and software, which was proven successful in laboratories. However, the number of failures on bearing on electrical motors in industry is still high. Thoresen and Dalva (1998) commented that, even though there were all these

techniques available to monitor motor conditions, failure of motor bearing still occurred. Many researchers have concluded that bearing failures are the main cause of motor failures. (Thoresen & Dalva 1999; Schoen, Habetler, Kamran and Bartheld 1995; Bisbee 1994).

New Vaal Collieries is a company that have been experiences failures of bearing on their motors, which could not be identified by their condition monitoring systems. The condition-monitoring department of New Vaal Collieries, which have a close working relationship with the Vaal University of Technology, requested assistance in researching the application of shock pulse monitoring to determine bearing failure. The motors on which the failure of bearings occurred were their DC drive dragline motors. These DC drive motors are crucial to the movement of dragline rope drums and any unplanned downtime is not affordable. The draglines are situated at New Vaal Colliery opencast mines, and they are on the doorstep of the university. This critical machine is the heart of the opencast mining process, and determines the success of mining operations. The dragline is one of the largest mechanical engineering machines found in the mining industry in the country and any failures on these machines are costly. Koellner (2006) reported that scheduled maintenance on the dragline rotating equipment cost more than a million dollars per year.

It is very important to have effective condition monitoring equipment on critical machines in industry because it is not always economically viable to conduct maintenance shutdowns at regular intervals, neither is it economical to undertake unplanned plant outages. Condition monitoring is one of the maintenance strategies that can help to protect machinery assets and prevent unplanned failure (Barkov 1998). Critical components on the dragline are the drag and hoist drive units as shown in Figure 1.2. Eight 1045kW DC variable speed motors drive the drums. Four of the motors are used to drag the bucket, and four are used to lift the bucket. The motors are driven at varying working speeds, and the load on the motor is changed continuously, as the rope is wound and unwound. Thorsen and Dalva (1999) found out that when motors

are started under load they experience large torque pulsations, which may lead to the failure of the bearings. A failure of the motor drive bearings leads to increased rotational friction of the rotor, which intern may lead to stator winding or rotor bar failures, and consequent excessive downtime. Thus, it is of paramount importance that failure symptoms are identified early to arrange for planned shutdowns.

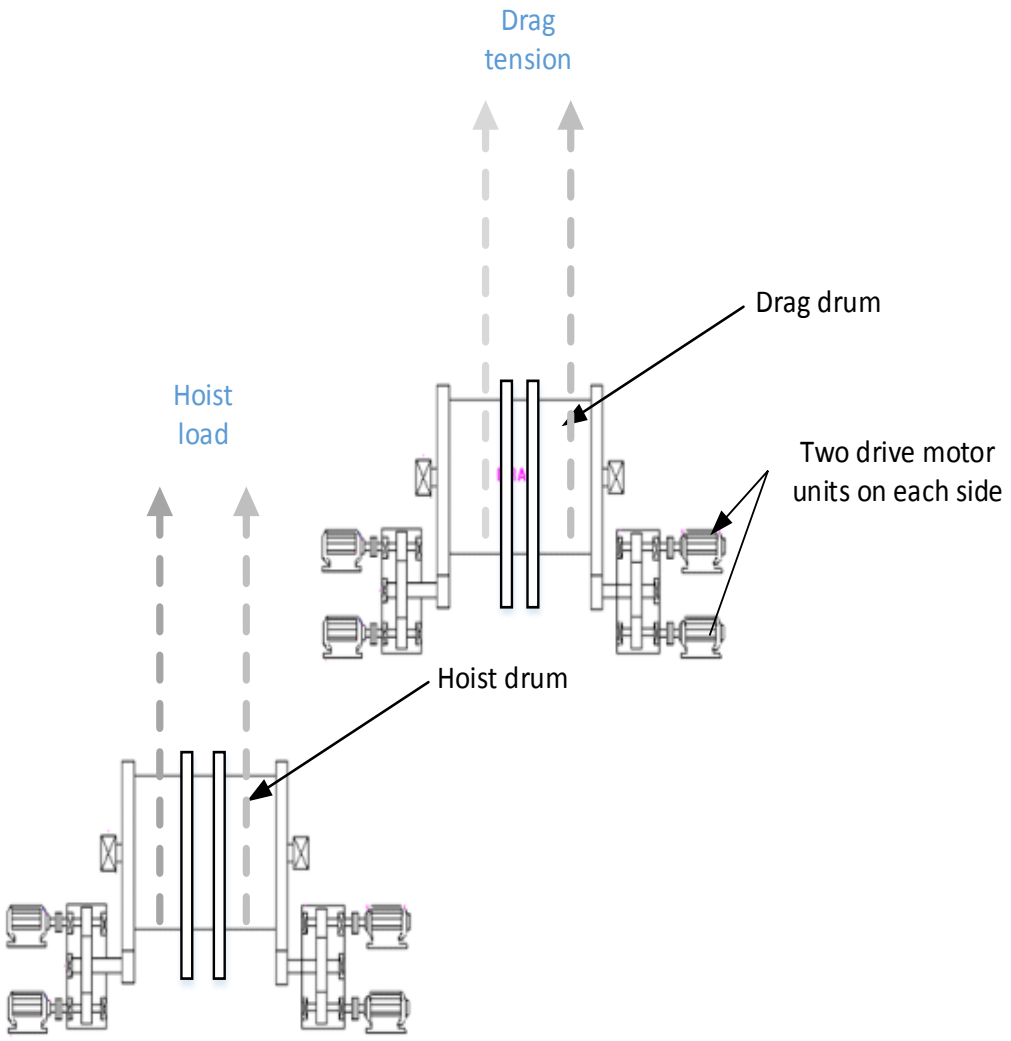

Figure 1.2 Schematic layout of dragline hoist and drag drum driven by eight 1045 kW DC motors

1.2 PROBLEM STATEMENT

Existing bearing vibration-monitoring techniques in industry have not been successfully in monitoring failures of bearings in application of variable speed and variable load. This implies continued and sudden occurrences of failure of bearings and high cost of unplanned shutdowns.

1.3 JUSTIFICATION OF THE STUDY

Zhen *et al.* (2008) observed that SPM had achieved wide acceptance as a quantitative method for detecting defects on rolling-element bearings, and that the maximum normalised shock value was used as a measure of the condition a bearing. The method gives a single value indicating the bearing condition without the need for elaborated data interpretation as required in some other methods. Rai and Mohanty (2007) reported that techniques that measured vibration using suitable transducers, and which measured high frequencies like the SPM, could measure the presence of impulses due to defects in bearings at an early stage. Tandon and Nakar (1992) affirmed that the SPM could detect damage in bearings at a very early stage of failure.

Various authors have compared different condition monitoring techniques to variable speed and load applications. Thorsen and Dalva (1999) found that the pulse intensity was independent of the bearing load in applications where damage was in the fixed outer race. In bearings with damage in rotating raceways, the pulse intensity varied with the change in load. Dyer and Stewart (1978) carried out a study on roller element bearings and concluded that if the changing speed and changing load could be compensated in the existing techniques; better vibration data could be captured to help in diagnosing bearing faults.

1.4 MAIN OBJECTIVE

The main objective of this research is to advance the shock pulse monitoring method for use in capturing values of the mechanical shock in testing bearings operating under variable speed and variable load conditions in order to monitor damage in bearings.

1.3.1 Specific objectives

1. To determine the decibel shock value (dBsv), trended over time, in order to provide diagnostic information of the condition of a bearing.
2. To determine how the decibel normalised value (dBm), trended over time, in order to provide diagnostic information of the condition of the bearing during acceleration and deceleration.
3. To determine how the dBm, trended over time, in order to provide diagnostic information of the condition of the bearing when the applied load is varied.
4. To determine how, the dBm, trended over time, in order to provide diagnostic information of the condition of the bearing, during variable speed and varying load conditions.

1.4 SCOPE OF THE WORK

The work focuses on the application of shock pulse monitoring on bearings operating under variable speed and variable load conditions. Literature survey conducted presently here indicates that, research on Shock Pulse Monitoring is limited. The main research reports and papers existing on SPM are Zhen *et al.* (2008), Rai and Mohanty (2007), Tandon and Nakar (1992), Stewart (1978), Boto (1971) and Sohoel (1984). Due to this, the scope of the work has focused on empirical tests of SPM.

Dissertation outline

Chapter 1 : Introduction, background, problem statement, justification of the study and objectives

Chapter 2 : Literature review

Chapter 3 : Experimental procedures

Chapter 4 : Experimental results

Chapter 5 : Discussion of results

Chapter 6 : Conclusion.

CHAPTER 2: LITERATURE REVIEW

2.1 VIBRATIONS GENERATED IN A BEARING

According to Randall and Antoni (2011), one of the first papers on bearing diagnostics was by Balderston (1969) in which he reported that bearing faults were primarily to be found in the high frequency region. However, Bartel (1977) observed that vibrations in bearings can be caused by various factors and have many symptoms, and the existence and progression of the vibration may be displayed in a vibration spectrum. Taylor and Kirkland (2004:55) observed that the magnitudes and frequencies of these vibrations depended on the bearing's mechanical condition as well as the operating conditions. Randall and Antoni (2011) stated that the frequency at which these vibrations occurred was important in diagnosing the problem as it indicated which component or fault was causing the vibration. In the vibration spectrum, there are three distinctive frequency bands where the condition of the bearing can be monitored (Taylor & Kirkland 2004:57).

The first frequency band where vibrations appear is in the high frequency band of 50kHz-100kHz range (Barkov, Barkova & Azovtsev 1997). At some point the signals that appear in the high frequency band of the vibration spectrum that are caused by cracks and pits become distorted, and the bearing defects are then monitored in the lower frequency band from 10kHz to 50kHz, or even at the very low frequency band from 10Hz to 10kHz (Tandon & Choundhury 1999). Barkov *et al*. (1997) demonstrated that only once the defects becomes severe, would low frequency analysis techniques be effective in picking up vibrations. The lower frequency vibration bands are referred to as the steady state vibrations (Barthel 1977).

Steady state vibrations measured on the bearing housing consist of all of the system's natural frequencies and its harmonics, and are dominant in the power spectrum. Majority of these vibrations originate outside the bearing and are introduced as modulations of the carried load, and are propagated through the

steel body of the machine into the bearing housing and bearing. Steady state vibrations generated within the bearing assembly originate from the imperfections in the bearing, bearing housing, and the shaft (Sohoel 1994). The bearing's geometrical size and operating speed determine the frequency value of vibration. The fundamental frequency components of this spectrum are defined by the formulas, 1.1.to 1.4

Taylor and Kirkland (2004:55) noted that that defects are classified as localised and distributed. Localised defects are classified as cracks, pits, and spalls, and distributed defects are classified as surface roughness, waviness, misalignment, and off-size rolling elements.

One drawback that has been experienced with vibration monitoring is that steady state vibrations cannot be recorded under variable speed and variable load conditions (Gluzman 2001). Steady state vibrations generated by the bearing are also small in amplitudes compared to other machine vibration amplitudes and therefore blend into the system's natural frequencies undetected. To carry out vibration analysis under these conditions, requires special techniques to monitor vibration successfully. Barthel (1977) proved that a change of speed, mass or alignment of any part of the machine would cause some change in its vibration spectrum. Observing that a change has taken place is quite simple with reliable vibration equipment; however, providing reasons for the change is not so easy.

One option to consider when operating at variable speed and load conditions is the high frequency vibration methods like shock pulse monitoring where incipient bearing damage like mechanical shock can be viewed. Butler (1973) found that the magnitude of the shock pulse was not affected so severely by the speed and load on the bearing. Neville (1979) proved that conventional measurement methods provided little or no effect on measuring the vibration in the high frequency band, but that the shock pulse method can discriminate between damaged and undamaged bearings in the high frequency bands. Elbestawi and Tait (1985) carried out tests under which the load and speed

were changed, and they observed that the shock pulse method showed reasonable stability with changes in speed and load.

2.2 THE DEVELOPMENT OF MECHANICAL SHOCK IN BEARINGS

Distinctive bearing damages like spalling, rust, cracks, and pits will create mechanical shocks with regular occurrence. Taylor and Kirkland (2004) found out that the mechanical shocks developed within the bearing have many origins and create a variety of signatures in the frequency spectrum. Shock pulses are caused by various conditions within the bearing and have various amplitudes.

Spalling of the bearing's load carrying surfaces creates cavities and the dislodged particles circulate in the bearing. These particles then lodge onto the surfaces, creating protrusions on the surfaces of the raceways and the rolling elements. Since protrusions appearing on the bearing's load carrying surfaces, the resulting shock pattern becomes random in nature. Figure 2.1 illustrates protrusions and cavities.

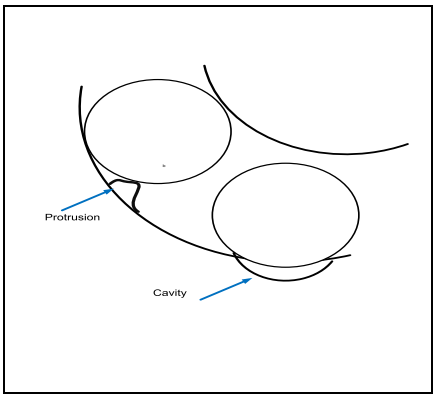

Figure 2.1 Protrusions and cavities

Thorsen and Dalva (1999) proved that cracks in rotating races created shock pulses that varied in intensity with changes in load, and cracks in stationary races caused pulses that were independent of the bearing load. Barkov *et al*. (1997) showed that the high frequency vibration that is induced in bearing components is due to the forces in a roller bearing. In a new bearing, the main type of high frequency oscillating forces that appear are due to friction forces.

In a damaged bearing, the high frequency forces that occur are due to the shock pulses.

The impact velocities developed in rolling element bearings depend on:

- The depth of penetration into the surface cavity. Boto (1971) explains the geometry with respect to velocity impact.
- The height of protrusions on the rolling surface. Protrusions create higher impact velocities than cavities do.
- The type and the diameter of the rolling elements, as well as on the bearing's load. According to Daadbin and Wong (1990) the shock velocity is related to geometrical configuration of the bearing.
- Bearing load. The loads have a stronger effect on ball bearings than on roller bearings. Boto (1971) observed that an accelerometer would respond to the elastic wave fronts with transient amplitudes proportional to the square of the impact velocities and independent of the masses of the impacting bodies.
- The rotational speed of the bearing. Consequently, the accelerometer will output transient amplitudes that vary proportionally with the square of any variation in speed. Sohoel (1984) found that the doubling of the bearing's rotational speed would increase the amplitude of recorded transients four times. Daadbin and Wong (1991) observed that the peak acceleration varied in the same manner as the square of the shock velocity.
- The lubricant film thickness in the rolling interface. The thicker the lubricant film, the greater the reduction of the impact velocity. The results of a research program show that the analyser is capable of measuring the load carrying oil film thickness and the degree of lubrication starvation (Anon 1984).

2.3 VIBRATION MONITORING UNDER CONSTANT SPEED

Barthel (1977) observed that a pressure wave was initiated when a ball in a bearing passed over an irregularity, and that this pressure wave was transient. Shortly after the initial pressure wave passes through the bearing material, deformation of the material occurs and it is this deformation that is measured normally by standard vibration techniques.

The standard frequency domain method is the most widely used approach in determining bearing defects. In this method, the data captured in the time domain is converted into the frequency domain. The data thus captured and displayed in the frequency domain represents amplitude as a function of frequency. In the frequency domain, often the vibration signal is referred to as the spectra and the spectra is defined by the frequency bandwidth. The spectra can be processed either in the high or low frequency bands, or over the whole frequency spectrum. The choice depends on the application and the speed of the bearing.

The free structural rotational resonant frequencies of the individual bearing elements can be calculated theoretically, and compared to measured values on the vibration spectrum. Igarashi and Hamada (1982), McLain and Hartman (1980), and Taylor (1980) have all had success in rotational resonant frequency bearing defect detection. Osuagwu and Thomas (1982) experienced difficulty in detecting defects in the low frequency range because low frequencies are easily masked by other machine frequencies. Osuagwu and Thomas (1982) found the cepstrum method more applicable in such a case. Collacto (1979) stated that in order to improve the signal to noise ratio, and to improve the spectral analysis, the averaging technique, the enveloping technique, band-passing technique, and high frequency resonance technique can be used.

Braun (1975) found that the averaging technique gave good results of the spectral frequency data. Burchill, Frarey and Wilson (1973), McFadden and Smith (1984; 1985), Prasad, Ghosh and Biswas (1985), and Tandon and Choudhury (1999) carried out research with the high frequency techniques with good success. Randall (2007) found that random slip, while small, gives a

fundamental change in the character of the signal, and was the reason why envelope analysis extracts diagnostic information was not obtainable from frequency analyses of the raw signal.

In the seventies and early eighties Glew (1974) carried out research on the octave band analysis, by making use of parallel filtering and obtained some useful results by comparing the change in each band level and by comparing the levels exceeding the predetermined values. Alfredson and Mathew (1985), Osuagwu and Thomas (1982) carried out research in the narrow band analysis, by making use of fast fourier transform and found that if the speed of the bearing was included , better results could be obtained for the condition of the bearing.

Tandon and Choudhury (1999) carried out an intensive review on 137 documented articles on vibration measurement techniques. They concluded that kurtosis is the most effective bearing condition monitoring technique and that shock pulse monitoring has gained wide industrial acceptance. Tandon and Choudhury (1999) conclude that most research work was conducted in the low frequency vibration band.

Liu, Ling and Gribonval (2001) applied matching pursuit on bearing defect detection and concluded that this method works better than Wavelet and enveloping detection, and it was able to identify failure at the early stage of such failure.

According to Gluzman (2001), failing bearings emit low energy, and the signals can be obscured easily by other vibration signals. Popular techniques used to determine bearing condition are demodulation, acceleration enveloping, spectral emitted energy and spike energy, which are able to measure the high frequency resonance generated by rolling element-bearing defects.

Azovtsev, Barkov and Carter (1996) commented on the influence of other vibration components that may spoil the results of rolling element-bearing diagnostics. These include random vibration components from other machine

components, groups of small harmonic components that do not significantly influence the overall vibration level in the frequency band selected for demodulation, and harmonic components that determine the overall vibration level in the frequency band selected for envelope detection.

2.4 VIBRATION-MONITORING TECHNIQUES APPLIED IN VARIABLE SPEED AND VARIABLE LOAD CONDITIONS

Under variable speed, the natural frequency of a bearing does not change. Under variable load conditions, the natural frequency or free structural resonance of a bearing continuously changes. When monitoring mechanical shock on a bearing under constant speed, a periodical sequence of excited vibrations is produced in the time spectrum. These vibrations decay partially or completely until the next mechanical shock appears. The pulse frequency is specific to damage in the bearing and can be calculated if the bearing geometry and the rotational speed are known. Depending on the location of the damage, like the inner ring, outer ring, bearing race or rolling element, different pulse frequencies are produced. Once the signal is filtered, and enveloped in its frequency bands, the information is transformed into a frequency range. This enveloped information is then diagnosed and linked to specific damage in bearings.

Under variable speed conditions, the impulses are not periodic and processing this signal provides no diagnosable data. Standard vibration techniques for constant speed and load conditions cannot be used here, and alternative methods of processing the captured signal must be used.

Normally the signal recorded is captured in the acceleration mode, and then integrated with care to give velocity or displacement values. These signals contain an enormous amount of information, and to appreciate the information fully, the signals must be processed in the time or frequency domain.

The signal captured and displayed in the time domain represents the physical motion, wherein motion is quantified as a set of amplitudes as a function of time. In the time domain, the vibration signal can be quite complex and not easily analysed but it is a very useful diagnostic tool.

The acceleration time signal of a bearing in a good condition is broad banded and random. The amplitude of a good bearing is much lower than that of a damaged bearing. When the first defect appears on the raceway of the bearing, an impulse is generated in the time signal at once per revolution excitation. Elbestawi and Tait (1985) reported that, the time domain signal is most effective in applications where impacts occur in roller bearings.

Several parameters can be extracted from the time domain of a vibration signal. The simplest form of measurement is the peak level, peak to peak, overall root-mean square (RMS) level, averaging, and the crest factor. Elbestawi and Tait (1985) found that, the peak level is effective in indicating short duration shocks, the peak to peak level is effective in measuring of maximum stress for design purposes, averaging has no direct relationship with any physical quantity but does take time into account, the RMS level takes time history and gives an amplitude value, which is directly related to the energy content.

2.4.1 Peak (Pk) method

This is the maximum deviation from a mean value during a time period and increases as soon as the first spalling appears. Stronach, Cudworth and Johnston (1984) found that a baseline peak level is established and variations from this norm are indicative of changes in the signal, and could be due to the occurrence of impacts in the vibration signal. Resonant behaviour could dominate the vibration signal that may hide the effect of transient impacts on the peak values. According to Martins and Gerges (1984), variable operating conditions affect the level of the peak values, and the peak value alone is not sufficient to detect incipient damage. Elbestawi and Tait (1985) reported peak value insensitivity to variations in speed and load for an outer race crack. For a spall on one ball, minimal variation in peak values were observed for speed and

load variation. Miyachi and Seki (1986) found that, the peak level values fluctuated violently in radial loaded bearings with or without damage, thus making it difficult to determine peak values accurately. They instead used the root mean square values to give them accurate values of the frequency signal from 30 to 20000Hz.

2.4.2 Root Mean Square (RMS) method

Tandon and Nakra (1992) and Ray (1980) performed vibration measurements with the RMS values, with limited success in detection of localised defect, but Monk (1972) did have success in applying the RMS value. Stronach *et al*. (1984) stated that the RMS method was useful in industry for monitoring the condition of bearings at the later phases of degradation and was not sufficient in detecting incipient damage. They also observed that the RMS value was unfortunately highly dependent on operating conditions like varying speed and load, and for this reason alone was RMS insufficient on its own. Results from various tests by Elbestawi and Tait (1985) showed little variation in the values obtained from the RMS method, with changes in load and speed for a bearing with damages. Rush (1979) found that in cases of severe damage in bearings, the combination of the RMS and kurtosis method gave a success rate of 96 percent. Miyachi and Seki (1986) found that the RMS level does not always show appreciable changes in the early stages of bearing damage, and that the crest factor is therefore more suitable for the early stages of damage.

2.4.3 Crest factor (Cf):

The crest factor is the quotient of the peak value of the vibration signal divided by the RMS value and hence, the crest factor is less sensitive to variable speed and load conditions since it is a normalised value. Stronach *et al*. (1984) demonstrated that the crest factor gave a qualitative assessment of the condition of the bearing. Elbestawi and Tait (1985) reported crest factor insensitivity to variations in speed and load for an outer race crack, and for a spall on one ball, minimal variation in the values of the crest factor were observed for varying speeds and loads. Weichbrodt and Bowden (1970) also noted that the crest factor was not sensitive to speed and load changes.

Shiroishi, Li, Liang Kurfess and Danyluk (1997) found that the crest factor is insensitive to the severity of the defects.

Weichbrodt and Bowden (1970) found that the crest factor was not sensitive to speed and load changes, and that changes in peak level over a frequency range of 10kHz was a good indication of incipient damage of the bearing. This they exploited through measurements of crest factor and found to be unaffected by changes in speed.

2.4.4 Kurtosis (K)

The amplitude characteristics of bearing vibration signals can be expressed in terms of a probability density function. Kurtosis is defined as the fourth statistical moment of the probability density function normalised with respect to the standard deviation. Dyer and Stewart (1978) reported kurtosis values in specific frequency bands to be a potentially powerful measure of the condition of bearings. The advantage of kurtosis was noted by the author to lie in its insensitivity to changes in load and speed for undamaged bearings and the ability to predict the extent of damage. Rush (1979) compared RMS, peak and kurtosis values on variable speed and load conditions, and found that the kurtosis method had the least variation of the three results under variable speed and load conditions. Martins and Gerges (1984) found that, kurtosis values presented a large enough variation to indicate the presence of incipient defects where values for a normal bearing were 3.

According to Stronach *et al*. (1984), the initial appearance of defects is sensed by an increase in the kurtosis value in the low frequency bands, and as degradation develops and damage becomes more severe, kurtosis values increase in the higher frequency bands. Kurtosis increases as the bearing degrades, and is a measure of how spiky a probability distribution of a vibration signal is, particularly at the extremes of the distribution when compared to the Gaussian curve.

Results from Elbestawi and Tait (1985) show a decrease in the kurtosis values for a bearing with an outer race crack and increasing speed. For a bearing with an inner race crack the kurtosis values decrease for an increase in the radial load, while minimum variation occurred due to changes in speed. For a randomly pitted section on the outer race, the kurtosis values increased slightly with increasing speed. For a spall on the inner race, the kurtosis values decreased for increasing speed where the changes become more dramatic in the higher frequency range. A sharp decrease in the kurtosis values were recorded in the 15 to 20 kHz range for a bearing with a spall on one ball and increasing radial load. For a spall on the outer race, minimal changes were observed for changing speed and load when compared to kurtosis baseline values, typically around 3.5.

According to Shiroishi, Liang, Kurfess and Danyluk (1997), kurtosis is a statistical measure based on the shape of the waveform. A good bearing with a random distribution of asperities has a theoretical kurtosis value of three, regardless of the amplitude of the signal. A bearing with debris denting is essentially the same as a good bearing only with asperities on a large scale. Therefore, the signal level is increased and the kurtosis value remains unchanged.

The instantaneous probability density function of the vibration amplitude is approximately gaussian for an undamaged bearing. The forth moment normalised with respect to the standard deviation gives a value of three. Elbestawi and Tait (1985), Rush (1979) and Dyer and Stewart (1978) carried out research on the kurtosis method and concluded that for an undamaged bearing with a kurtosis value of three, speed and load changes did not affect this value. Should the kurtosis value change due to bearing failure, the speed and load influence the reading.

2.4.5 Order tracking

Order tracking can be used to monitor the condition of a rotating machine, especially during run-ups and run-downs. Order tracking uses frequency as a

base for analysing speed related vibrations. Vold, Mains and Blough (1997) carried out research with order tracking, making use of the Vold-Kalman tracking filter and had success in radical rpm changes of transmissions.

Lyon, Sherrard and Sherman (2000) carried out research on nominally constant speed machines by making use of software-based order tracking. Qian (2003) carried out research with Gaberson expansion order tracking on a four-pole electrical motor, with a varied speed. Wu, Huang and Huang (2004) found that order tracking with the recursive Kalman filtering algorithm is effective in running up or casting down applications. Blough (2003) experimented with a new time variant discrete fourier transform order tracking, of which the bandwidth could be either constant frequency or constant order.

2.4.6 Wavelets

Wavelets have been researched extensively in applications with transient vibration. Transient vibrations are generated in bearings when a ball rolls over a defect. Seker and Ayaz, (2003); Peng and Chu, (2004); Gaberson, (2002); Prabhakar, Mohanty and Sekhar (2002), and Mori, Kasashima, Yoshioka and Ueno (1996) used wavelet transformation in bearings with defects. Schneider, Seeliger, Martin and Mackel (2000) carried out tests on a roughing mill with unstable speeds. They compared the short-term fourier transformation and the wavelet transformation with a common statistical method. The wavelet transformation presented a better result with increasing bearing wear, compared to the short-term fourier transformation, but the results are not an effective indication of the quantitative condition of the bearing. Lou, Loparo, Discenzo, Yoo and Twarowski (2002) carried out tests on an induction motor, of which the load could be varied. They analysed the results with the statistical method and the fast fourier transformation did not give effective results in a damaged bearing. The time-frequency distribution obtained using the wavelet transformation gave an effect result over the full spectrum. Lou and Loparo (2003) carried out experiments using the wavelet transformation and neuro-fuzzy diagnostic classifier with load variation tests. They concluded that the

results could reliably separate different fault conditions under the presence of load variation.

2.4.7 High Frequency Resonance Technique (HFRT)

Randal (2007) reported that the HFRT is effective in applications on bearings, especially with the random slip experienced in bearings, although small, gives a fundamental change in the character of the signal and is the reason why envelope analysis cannot extract diagnostic information from frequency analyses of the raw signal. It also allows bearing signals to be separated from the gear signals with which are often mixed.

2.4.8 Time-Frequency and Time-Scale Methods

Li, Mo-Yuen & Yodyium (2000) presented an approach for diagnosing rolling element bearing faults effectively using neural networks and time-frequency domain vibration analysis. The rolling element bearing fault may affect the vibration for a short period of time within a cycle and therefore time-frequency techniques, which measure the variation of spectral features, can be used to locate the fault. Defects such as bearing installation, wear, and cavities can be detected by spectrum analysis of the high frequency vibration envelope but special signal processing and frequency band must be selected.

2.4.9 Short Time Fourier Transform (STFT)

The STFT provides information on the time and frequency of a vibration signal and is constructed by shifting a window function in time over the whole signal. Consecutive overlapping transforms are performed to give a description of the spectrum evolution, which are arranged chronologically to construct the time-frequency distribution of the signal. The distribution has good time resolution but poor frequency resolution.

2.4.10 Wigner-Ville Distributions (WVD)

The WVD was developed to improve the time-frequency resolution of the short time fourier transform, and the distribution is based on a manipulation of the power spectral density (PSD), which is a fourier transform of an autocorrelation.

2.4.11 Continuous Wavelet Transform (CWT)

A disadvantage of the STFT is that the time resolution remains constant once the window length and shape have been chosen, and a more flexible approach is required where the window size can be varied to enhance either the time or the frequency resolution. A wavelet is a waveform of limited duration with an average value of zero, and performs a decomposition of the vibration signal into a weighted set of scaled wavelet functions. The flexible scheme of time and frequency localisation makes the wavelet transform attractive for the analysis of signals involving discontinuities and transients. The frequency content of the wavelet signal is altered through stretching or compressing, and the action is referred to as scaling, which is inversely proportional to the frequency content of the signal. The wavelet is shifted along the vibration signal at various frequency scales to determine the correlation between the wavelet and the particular section of the signal. Bearing damage can be detected at a specific time instant by selecting a wavelet that correlates well with the time waveform caused by a particular defect. The success of wavelet analysis is based on the selection of the correct wavelet and the interpretation of the patterns, which it forms in the correlation map.

According to Paya, Esat and Badi (1997), wavelet transforms are well known for their capacity to treat transient signals while Wigner-Ville distributions are more suitable to non-transient signals. The results obtained in this work showed that wavelet transforms are an excellent technique to use to pre-process vibration data and to train a network, because it converges much faster compared to the same data pre-processed by FFT. The reason for this is that wavelet transforms are capable of analysing transients, which simplifies fault identification resulting in precise information being presented to the neural network. They concluded that spectral analysis techniques are not reliable and efficient enough when the fault advancement is small or when multiple faults are present and that the combination of wavelet transform with an artificial neural network provided a useful tool for intelligent diagnostics of faults in rotating machinery.

Lou *et al.* (2002) applied a wavelet-based technique for rolling element bearing diagnostics and found that inner race and ball faults could be identified relatively easily from FFT data under normal conditions. The author observed that non-stationary or transient characteristics like drift, trends, abrupt changes and the beginning and end of events required a higher frequency analysis method.

Azovtsev *et al*. (1996) showed that the shock pulse method immediately indicated change in the recorded values if the applied load in the bearing increased.

2.5 THE FREQUENCY BAND OF SHOCK PULSE MONITORING

Neville (1979) found that shock- pulses in a bearing generated very high frequency vibrations within the structure of the machine, this high frequency vibration caused no movement of the machine, so the machine as a whole did not move. Therefore, conventional vibration methods have little or no effect on vibrations monitoring in the high frequency levels. This thesis focused on the higher frequency vibration band in the spectrum for bearings, and that is the frequency of 10kHz to 50kHz. Sohoel (1994) proved that mechanical shocks appear in the high frequency vibration spectrum from 10-50kHz and can be monitored by various techniques, such as shock pulse monitoring, spike energy and high frequency resonance.

Barkov et al. (1997) found that defects in rolling element bearings first influence the properties of friction forces in the bearing. These friction forces could only be detected by high frequency vibration analysis methods. The shock pulses that appear in bearings when rolling elements come in contact with defect surfaces can also be seen as friction forces and that is why the SPM technique, which measures vibrations at high frequencies, can be used effectively. The author noted that only when the defects become severe would low frequency analysis techniques be effective.

Liu, Chen & Zhang (1991) found that the shock pulse monitoring was very successful in bearing applications because scuffing, pitting and spalling of bearings all generate signals above 20kHz, which was outside the frequency range of other machine defects. They found that a raceway with a poor surface finish gave rise to increased friction forces in the bearing. This increase of friction forces within a bearing intern gave rise to increased levels of sound pressure and intensity. This could be heard with the use of ultrasonic equipment. Once the surface deteriorated, further defects appeared in the bearings, and transient vibrations were generated. These defects on the rolling surfaces caused mechanical impact also called mechanical shocks or shock pulses. These shocks emitted elastic waves that travel at the speed of sound through the bearing casing and bearing housing at 292 km/hr and are transient in nature, the signal damps out quickly as they pass through the carbon molecules in the bearing housing.

Barthel (1977) mentioned that a bearing can reach an advanced stage of damage before the fundamental bearing vibrations rises above the background vibration noise levels. High frequency shock pulse are therefore useful in identify failure earlier in order to save the high cost of breakdowns.

Kuhnell (1985); Barthel (1977); Brown (1977); Butler (1973) and (Morando 1988) carried out tests with the shock pulse monitoring technique and found that it was very effective in identifying bearing damage.

2.6 SHOCK PULSE MONITORING APPLIED TO VARIABLE SPEED AND LOAD CONDITIONS

Sohoel (1971) experimented with the shock pulses by considering the physical nature of the elastic shock waves that radiate from an impact point and by using the Heinrich Hertz equation for elastic impact, he calculate the impact contact force-time function and concluded that an accelerometer with a resonant frequency in the range of 25 to 30kHz will respond proportionally to the impact

velocity. He also concluded that the shock pulse amplitude exhibited a quadratic dependence on the impact velocity.

Boto (1971) developed a theoretical model to prove Sohoel's (1971) findings with respect to a rolling element bearing. The theoretical model was based on the depth of the cavity, the speed of rotation, the dimensions of the bearing and the material constant. With this model he proved that for a certain bearing the shock pulse value generated was proportional to the depth of cavity through which the roller passed and the speed of rotation.

Sohoel (1984) performed further tests on a rolling element bearing and found that shock pulses would radiate from the impact point in a half spherical way. He stated that a piezoelectric transducer with a well-defined mechanical resonance frequency of 32kHz positioned in the direction of loaded region will best provide effective results. Sohoel (1994) experimented with changing speed to determine how the dBsv (decibel shock value) would be affected. He revered to the dBsv as the largest maximum shock value. He also concluded that all new bearings display a certain amount of shock and this he referred to as the initial decibel value (dBi). Subtracting this value from the dBsv value, a new decibel normalised value (dBn) was obtained. The dBn value is not affected by speed and can be used to calculate the shock value, see Section 3.4. Daabin and Wong (1990) also experimented with the bearing speed and they discovered that the peak acceleration varies as the square of the shock velocity. Sohoel (1994) states that in the laboratory result it was proven that a doubling of the bearing's rotational speed will increase the amplitude of recorded transients four times, and that the impact velocities within the bearing follow any variation in the rolling velocity proportionally. Consequently, the accelerometer will output transient amplitudes that vary proportionally with the square of any variation in rpm.

Barkov *et al.* (1997) observed that incipient bearing defects could be analysed by shock pulse and friction forces, but friction forces could be monitored more effectively with friction force amplitude modulation in low- and high-speed

machines. With low speeds, the number of shocks was much higher than in high speeds because the lubrication film thickness with low speed was thinner, creating more shocks. With the enveloping method, this could create problems in identifying the severity of shocks because of overlapping and integration of shock pulses. According to Barkov *et al*. (1997), who carried out a study in high frequency excitation caused by shock pulses in non-linear systems, with enveloping analysis and modulating the intervals between shock pulses, the technique is reliable only if the bearing has damage in one of the rotating components.

Excessive vibrations due to the harsh operating condition of the dragline induce many spikes at the low frequency band, complicating the analysis of the bearing vibration even further, and therefore, the shock pulse technique that measures in the high frequency will be more effective. Monitoring in the high frequency also has the advantage that bearing failures are picked up at the incipient stage of damage.

When bearings first begin to wear, they begin to exit the natural frequency of their components. These components are the rolling elements, bearing race and cage. One set of the natural frequencies is concentrated in the region of 1kHz to 10kHz and the other in the frequency region of 20kHz to 100kHz. In the upper frequency, the frequency is referred to as ultrasonic. It is in this region that the shock pulse monitoring method is applied.
Thus traditional vibration readings are applied in the lower frequency region and shock pulse monitoring is in the higher frequency region, were pulses are generated due to impacts caused by protrusions or cavities

Each bearing has a free structural resonance and these may change when the components are assembled and loaded in the presence of lubrication. These resonances will also change with external load and speed changes.

2.7 TRANSDUCERS USED IN HIGH FREQUENCY VIBRATION MONITORING.

To select a transducer for mechanical shock analysis, it is required to know the frequency at which the mechanical shocks take place. It has been identified above that the mechanical shocks generate elastic waves that are of transient nature and which oscillate at a frequency of 30-50kHz.

Transducers are divided into three categories, displacement transducers, velocity transducers and accelerometers. Displacement transducers are designed for a frequency range of 0-1000Hz. A velocity transducer is designed for a frequency range of 8-1500Hz, and therefore, can measure over a wide frequency range. A velocity transducer typically will be applied in applications where the exact defect frequency is not known. An accelerometer is designed for the high frequency oscillations and various accelerometers work in the 1kHz to 50Khz range. They are normally much lighter than any other type of transducers to allow for sensitivity in the high resolution vibrations. The accelerometers are categorised in the following three types: shear type, compression type and flexural type. The compression type is categorised with upright, inverted and isolated. The accelerometers design is completely different from any other transducer. Normal displacement and velocity transducers constitute of a mass with a spring system, and sometimes a fluid system. The accelerometers can have seismic mass or piezoelectric crystals in them. The seismic mass accelerometer is normally only used in seismic applications. The piezoelectric accelerometer is a self-generating device with no moving parts and a high sensitivity to mass ratio. The piezoelectric crystal response to the high frequency is very sensitive and thus makes it effective in the 1kHz to 50kHz range.

To measure mechanical shock pulse-based measurement, an accelerometer is used for measuring. The accelerometer gives preference to high frequency vibrations. Sohoel (1994) found that an accelerometer, with a resonance frequency around 32 KHz, will give optimal sensitivity to the elastic wave front.

This is also above the normal vibration frequencies of common machine elements. The TRA22 transducer, which consists of a piezo-electrical element, senses the shocks, which are generated by the transient vibrations in a bearing. Bearing sizes and speeds are pre-programmed into the memory of the instrument by the suppliers.

Smith (1993) carried out test with various transducers on slow to medium speeds using bearings with asperity-point contacts. These shocks take place at high frequencies and in the experiments; he concludes that high frequency shocks are best analysed with an accelerometer.

Thorsen & Dalva (1998) state that if piezoelectric transducers were connected to defective bearing, shock waves were generated. A crack in the rotating race created shock impulses that varied in intensity with changes in the load. A crack in the stationary race caused pulses, the intensity of which was independent of the bearing load.

2.8 CONCLUSION

The literature on research work in the field of shock pulse monitoring was very limited and only focused on constant speed applications. Constant speed applications have been researched and well documented but literature on variable speed and variable load applications still have many areas of research possibilities.

The first article referring to Shock pulse monitoring was in 1966, and the technique was only patented in 1971. The next article documented was by Sohoel (1994) and only in the late nineteenth century was their research articles published on shock pulse methods.

Variables speed motor drive applications have been there for over a century but were used in limited applications. Only in the last quarter of the century has

variable speed applications taken over the market. Variable speed condition monitoring articles were found on various other condition monitoring applications.

Sufficient literature could not be found to formulate and structure a research modelling method to support a proper thesis outline and therefor the findings of the research had to rely on empirical testing methods to obtain results.

CHAPTER 3: EXPERIMENTAL DESIGN AND PROCEDURES

3.1 INTRODUCTION

A test rig was built on which shock pulses could be generated and related data collected on a bearing. The test rig was designed to allow the bearing to run at variable speed increments with a number of acceleration periods. The loading on the bearing could also be altered, and a constant drip feed lubrication method applied to ensure effective lubrication under all operating conditions. The temperature of the bearing was maintaned at a constant value of 28 degrees by a hot air supply blown over it. The speed of the test rig was monitored by a tachometer. Tests were performed on bearings with induced 0.1mm and 0.2mm defects on the bearing outer races and the arising shock values were recorded using the shock pulse monitoring method.

The diagram in Figure 3.1, illustrates the outline of the dissertation and methodology. The bearing test piece provided the shock value data that woulld be diagnosed. The measured signal was analysed, diagnosed, prognosed and results generated.

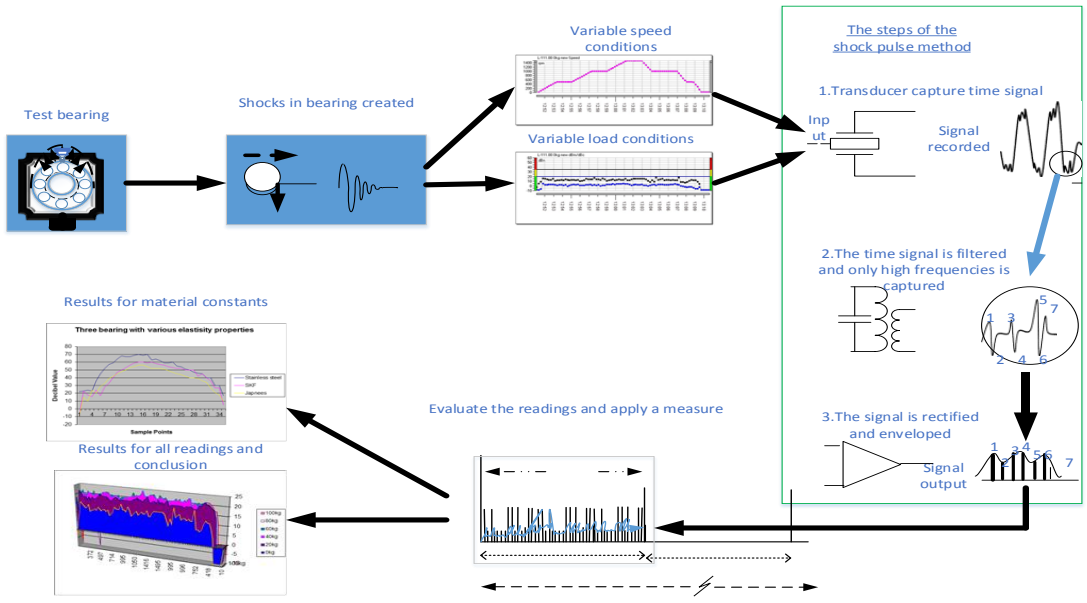

Figure 3.1 Order of experimental tests.

3.2 THE GEOMETRY OF THE BEARING AND THE ORIGIN OF SHOCK PULSES

Bearings can attain their life cycles if operated under design specifications and ideal conditions. If the operating conditions are not ideal, or the loading on raceway is higher than the design specifications, imperfections will develop in the raceway. When a rolling bearing component comes in contact with such an imperfection a shock pulse occurs in the bearing, giving rise to transient vibrations that dampen out quickly. The theoretical model sown in Figure 3.2 illustrates an over-exaggerated imperfection on a stationary outer raceway. The figure shows how the spherical roller element hits the imperfection or cavity, and creates a shock pulse. The impact is modelled for a spherical rolling element rotating about point *A* which impacts point *B* at right angles to line *AB.* To calculate the shock pulse value induced on impact, the theoretical model of Boto (1971) was applied in the analyses of shock pulses on the test bearings.

In Boto's (1971) article he indicated that the electric voltage (*E*) generated in an accelerometer is expressed by Equation 3.1, thus

$$E = V_S^{\,2} \times Mc \qquad (3.1)$$

Calculating the impact velocity Vs at point B, which causes the shock pulse.

E - Electric voltage

V_s - Impact velocity

V_w - Tangential velocity

$\mathbf{n}_i$ - Shaft speed

n - Ball rotational speed

D_B - spherical roller diameter

D_i - Inner race diameter

V - Peripheral velocity

y - Ball depth in cavity

x - Cord *AB*

M_c - Material constant

y_i = D_B - y

The geometry of Figure 3.2 (Boto 1971) will be used to calculate the impact velocity (Vs) of the spherical roller entering the cavity at point *A*, considering rotation about point *A*, and determining the velocity Vs at point of impact, B.

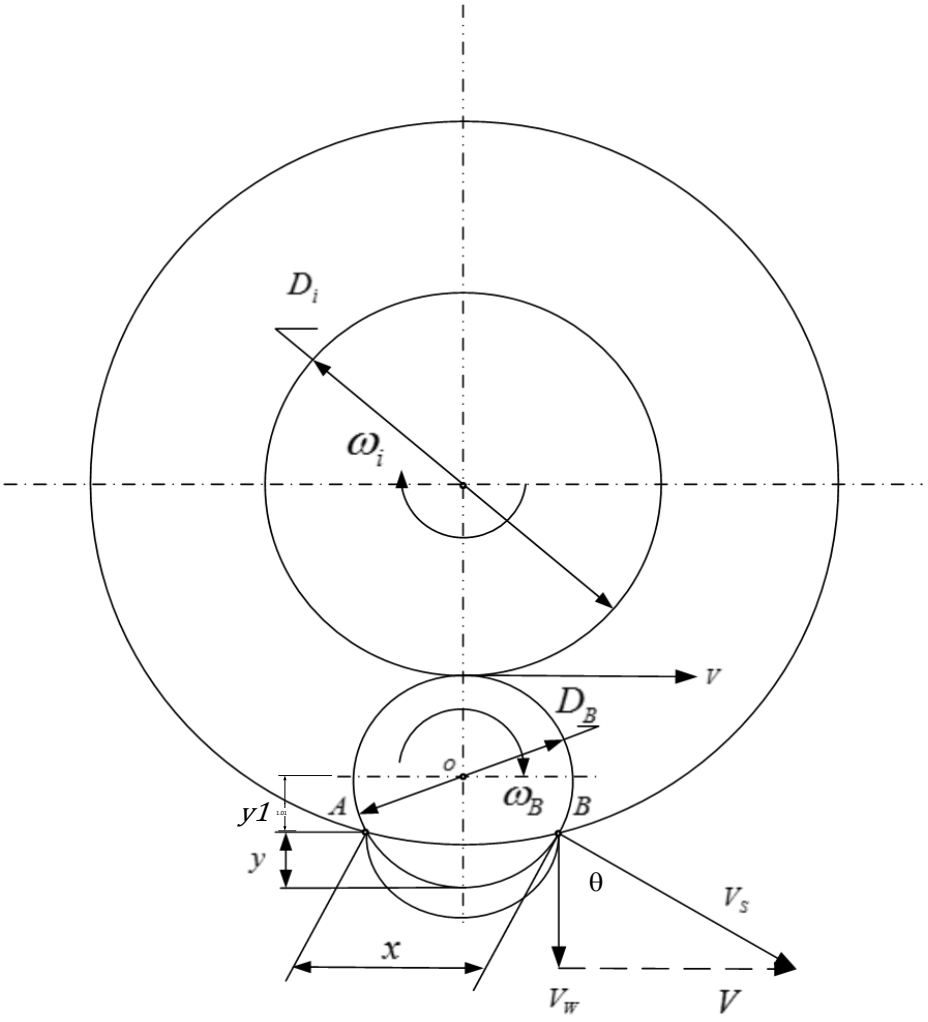

Figure 3.2 Geometry of a roller ball hitting a cavity and velocity vector diagram.

Before determining the radial velocity Vs at the point of impact *B,* the peripheral velocity $V,$ can be obtained by using the following analytical relationships:

$$V = \omega_i \frac{D_i}{2} \tag{3.2}$$

$$\omega_i = 2\pi n_i \tag{3.3}$$

Substituting (3.3) into (3.2)

$$V = 2\pi n_i \frac{D_i}{2}$$

$$V = \pi n_i D_i \tag{3.4}$$

The peripheral velocity can also be determined from the tangential velocity Vs on the point of impact by using the relative motion equation as follows.

Considering the geometry of Figure 3.2, the relative motion equation is,

$$\frac{V_w}{x} = \frac{V}{D_B} \tag{3.5}$$

Sine the angle between Vs and $Vw \times \cos\theta$ is very small, the $\cos\theta \cong 1$ and therefore

$$V_S = V_W \tag{3.6}$$

Substituting (3.6) in (3.5)

$$\frac{V_s}{x} = \frac{V}{D_B} \tag{3.7}$$

Substituting (3.4) in (3.7)

$$V_s = \frac{x\pi n_i \times D_i}{D_B} \tag{3.8}$$

Before any radial velocity Vs can be determined the radius x around the pivot point *A* need to be evaluated.

Applying Pythagoras rule to the triangle ABC,

$$\left(\frac{\mathrm{D_B}}{2}\right)^2 = \left(\frac{x}{2}\right)^2 + {y_1}^2 \tag{3.9}$$

$${y_1}^2 = \left(\frac{D_B}{2} - y\right)^2 \tag{3.10}$$

Substituting (3.10) in (3.9)

$$\left(\frac{D_B}{2}\right)^2 = \left(\frac{x}{2}\right)^2 + \left(\frac{D_B}{2} - y\right)^2$$

Factorise and simplify

$$\frac{{D_B}^2}{4} = \frac{x^2}{4} + \frac{{D_B}^2}{4} - \left(\frac{2D_B y}{2}\right) + y^2$$

By simplifying

$$\therefore y(D_B - y) = \frac{x^2}{4} \tag{3.11}$$

Since $(D_B - y) \Leftrightarrow D_B$

Then $x^2 = 4yD_B$ (3.12)

Substituting (3.12) in (3.8)

$$Vs = \left(\sqrt{4yD_B}\right) \times \frac{\pi n_i D_i}{D_B} \quad (3.13)$$

Square (3.13)

$$Vs^2 = \left(4yD_B\right) \times \frac{\pi^2 n_i{}^2 D_i{}^2}{D_B{}^2}$$

By simplifying

$$Vs^2 = \left(4\pi^2\right) \times n_i{}^2 \times \frac{D_i{}^2}{D_B} \times y \quad (3.14)$$

Substituting (3.14) in (3.1)

$$\mathrm{E} = \left(n_i{}^2 \frac{D_i{}^2}{D_B} y \right) \times .Mc \quad (3.15)$$

This formula quantifies the expected electrical voltage (E) output at the transducer. The formula indicates that the expected output voltage generated is depended on the square of the speed and bearing diameter.

3.2 CAPTURING THE EXPERIMENTAL SHOCK VALUE AND PROCESSING THE DATA

In Section 3.1, the origin of the shock pulse was explained and how the shock pulse value and the expected transducer voltage was determined. In Section 3.2, the transient shock value is investigated. Figure 3.2 shows how a spherical roller ball bearing impacts a cavity in the bearing outer race. At the moment of impact, a transient shock wave spreads through the bearing housing. The shock wave travels through the bearing housing and strikes the shock pulse transducer causing the oscillation of the piezoelectric element of the transducer as shown in Figure 3.3. An electric current is induced and fed into the charge amplifier, which converts the signal to a potential voltage output signal (E). The voltage output signal then is converted to a decibel value as explained in Section 3.2.1. The decibel value is captured with the Lenova T30 instrument and the instrument processes the signal. The data from the instrument is downloaded onto the SPM software. The dB amplitude of the transient shock value represents the condition of the bearing and is referred to as the decibel shock value (dBsv).

After impact occurred, both the bearing housing and the roller start to vibrate, and with a frequency of vibration that is a function of the mass and the shape of the components of the bearing, (Morando 1996). In Figure 3.4, the second phase of the impact is shown. This is the vibration phase. There oscillating waves are propagated and captured using traditional vibration analyses. With every impact of the spherical roller striking the cavity, a series of pulses are created in the vibration signal, and Figure 3.5 represents the signal.

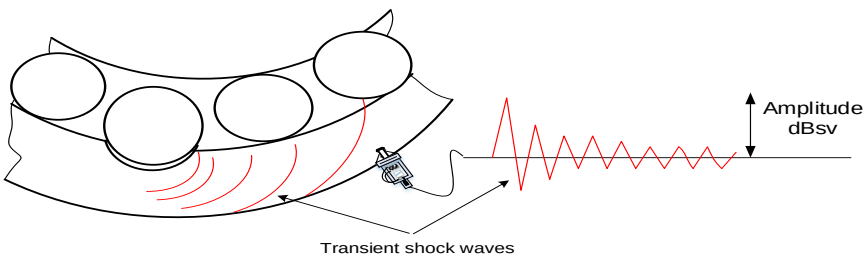

Figure 3.3 Transient shock induced in bearing housing.

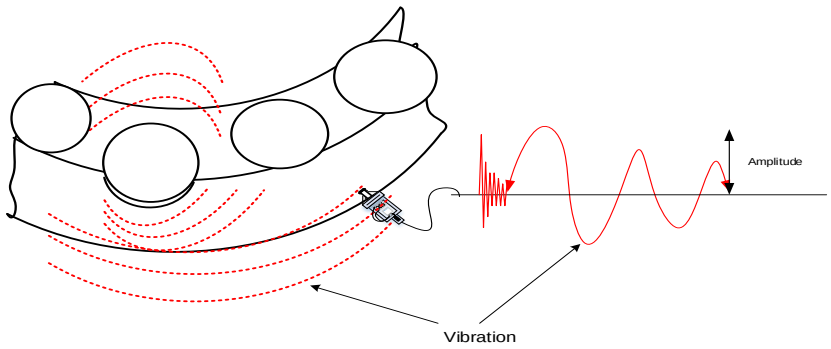

Figure 3.4 Vibration induced on both bearing housing and roller

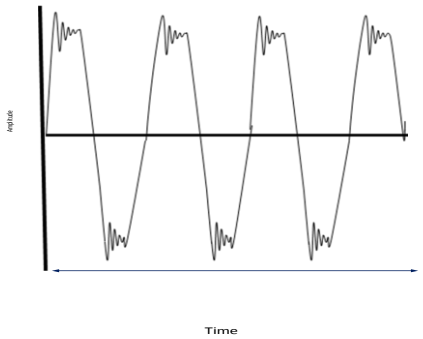

Figure 3.5 Low frequency vibration signal with high frequency shock pulse appearing on the crest of the sine wave.

3.2.1 Processing the shock value recorded

Figure 3.6 is a circuit diagram indicating how the shock pulse value is processed; this diagram is adapted from Heron (1985). The shock pulse signal (dBsv) is captured by a unique shock pulse transducer, which generates a large amplitude oscillation to the weak shock pulse captured. The reason for this is the transducer is excited at its resonance frequency of 32 kHz. The combined signal then passes through a high band pass filter signal that filters out low frequency signals, and the signals above 32kHz pass through. This means that all shock pulses from other sources are isolated. After the filtering process, the transient signal passes through a signal rectifier. All the negative signals are converted to positive signals. The signal is then amplified and passed through a low pass filter and thereafter enveloping is applied. The signal is then converted into an analogue electric pulse. The enveloped signal is referred to

as a pulse train, and is illustrated in Figure 3.7. Two values are read from this enveloped pulse train, the largest peak value is called the decibel shock value (dBsv), and the smallest peak value is called the decibel carpet value (dBc).

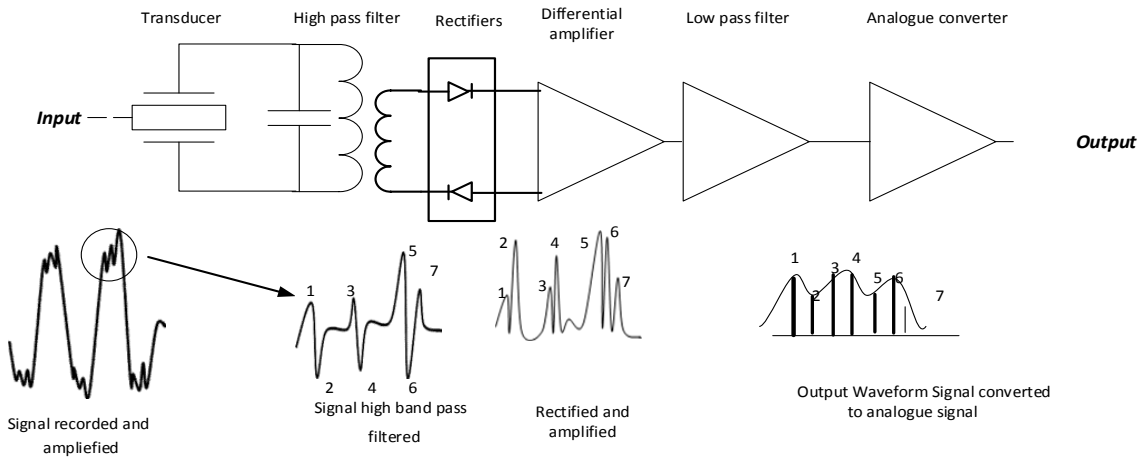

Figure 3.6 Shock pulse signal processing.

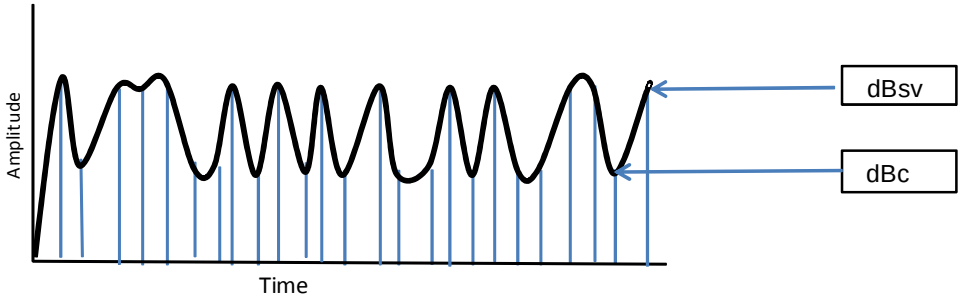

Figure 3.7 Enveloped pulse train representing the dBsv and dBc values as displayed in the time waveform.

From this pulse train there are one second high frequency samples captured. These high frequency one second samples gets divided into many five millisecond time windows; each five millisecond window has 200 sampled readings. Of the 200 sampled readings, the maximum and minimum values are selected from each five millisecond time window. See Figure 3.8. The maximum peak values are the dBsv and the minimum peak value are the dBc values.

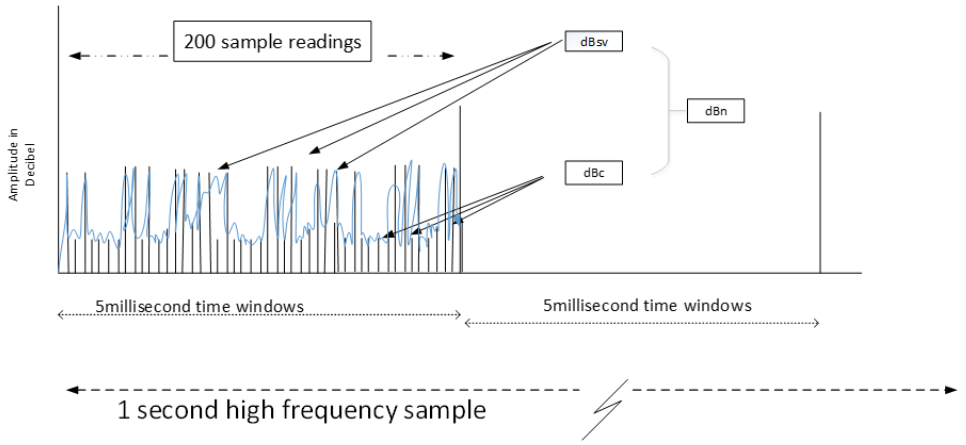

Figure 3.8 Sampling the shock values

The voltage (E) generated in an accelerometer is equal to the impact velocity (V_S^2) multipied by the material constant (M_c). The voltage E is related directly to the value of dBsv. dBsv represents the damage in the bearing surfaces and is an effective bearing condition monitoring parameter that can be used to identify initial stages of bearing failure. This can be applied effectively under constant speed conditions. In a variable speed condition, the impact velocity is constantly changing, and because dBsv is dependent on impact velocity, it will continuously change. To trend the condition of the bearing under continuously changing operating parameters is difficult.

In order to overcome this trending problem, a new value that was presented by Sohoel (1994) is taken into consideration. The bearing internal shaft diameter and the speed of rotation are used in a formula to determine a value referred to as initial decibel value (dBi). This value represents a shock value for a new bearing.

dBi = 20 * (log N) + log(shaft diameter)- log(2150) (3.16)

where N stands for the number of revolutions per minute.

If the dBi value is subtracted from the dBsv value, a normalised value dBn is obtained for the bearing. The normalised value can then be plotted and a trend can be drawn of the condition of the bearing monitored. Li *et al*. (2000) and Bloch (2000) give the following relationship between dBn, dBsv and dBi:

$$dBn = dBsv - dBi \qquad (3.17)$$

The dBn value represents the difference in decibel between a new and used bearing. It can be used to trend the change in bearing damage, irrespective of the speed. Because the speed is a common denominator in both formulae, the values represent the condition of a bearing.

To carry out the experiment the variable speed was captured by a tacho meter and analysed in the SPM instrument. Before every SPM reading was captured, the shaft speed was captured and the dBi value was determined so that the dBsv value could be recorded. The (dBc) value represents the roughness and lubrication quality of the bearing raceway Li *et al*. (2000) and this is discussed in Section 3.3.6.

3.3 TEST RIG DESIGN

The test rig was assembled as in the schematic layout shown in Figure 3.9.A. A three dimensional representation of the actual test rig design is displayed in Figure 3.9.B

A variable speed control panel controlled the variable speed and load condition. A photo of the actual test rig design is displayed in Figure 3.10

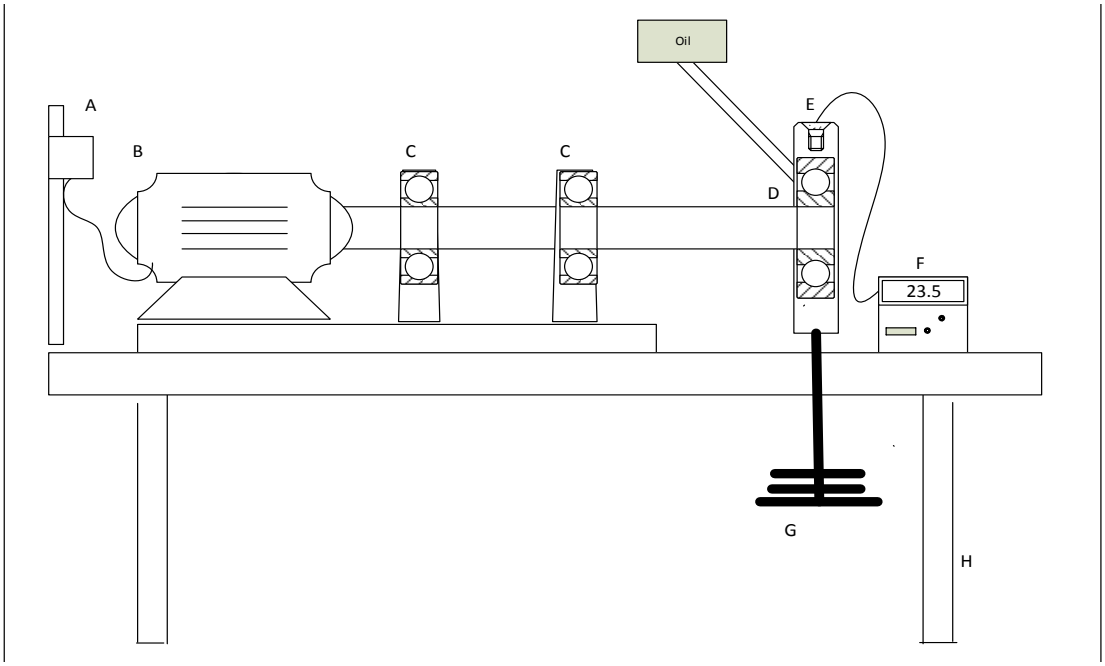

Figure 3.9A Test rig

A – PLC control unit, B – Motor, C –Support bearings

D – Test bearing, E- Transducer, F- Recording instrument, G – Shaft loading device, H – Test bench

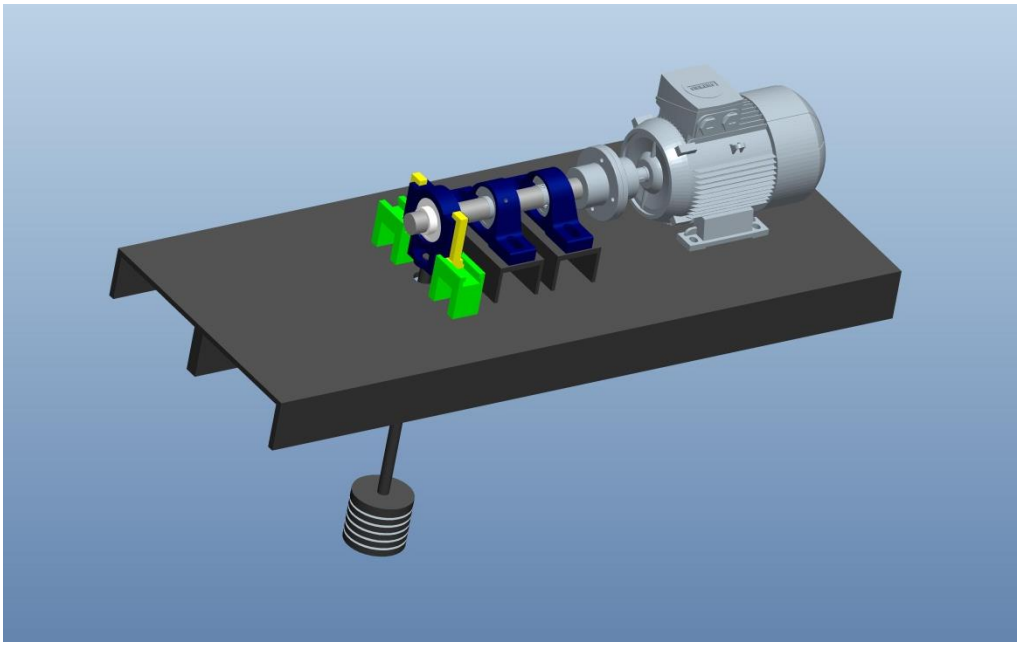

Figure 3.9B Three-dimensional drawing of test rig

Figure 3.10 Photo of test rig

3.3.1 Variable speed drive

The variable speed motor used, was a 2.2 kW AC motor controlled by the programmable logic controller (PLC) as seen in Figure 3.10. The PLC was programmed to drive the motor from 0rpm up to 1500rpm, and down to 0rpm. The controller also stepped the motor speed by 200rpm from 0rpm to 1500rpm, and to perform various acceleration and deceleration running cycles.

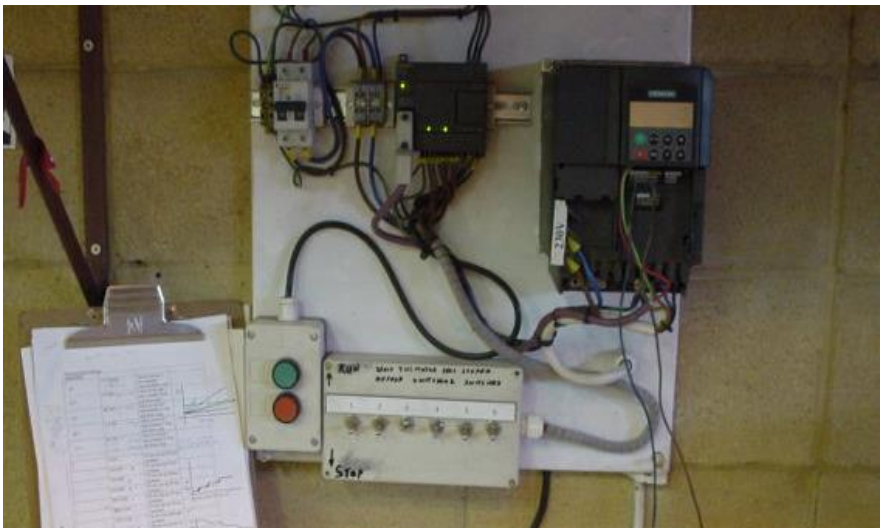

Figure 3.11 Programmable logic controller (PLC) used for the experiments

3.3.2 Variable load

To carry out tests under variable load conditions, various dead weight loads were hung from the casing in which the test bearing was situated as shown in figure 3.9. This loading design was selected because it provided the option of changing the loading while the speed was varied. These loads were applied by suspending them on a support that was attached to the bearing housing. The static load that the bearing is designed for is 1.5kN as stipulated in the manufacturer's data sheet shown in Appendix 6. The intention of this transverse loading was not to destroy the bearing, but to obtain shock loads under variable speeds and different transverse loads. The maximum dead weight load applied was therefore limited to 80kg, giving a total of 800 Newtons.

3.3.3 Critical positioning of test bearing and sensor

The bearing and holding casing was selected to allow easy removal of the bearing after each test. The transducer was fitted on top and the dead weight was suspended at the bottom as shown in Figure 3.12. With this type of set-up, the applied transverse load acted directly onto the damaged area on the bearing outer race, allowing for maximum shock pulses to occur. According to Barkov (1998), vibration recordings should always be recorded in the load zone of a bearing, or as close as possible to the load zone. Therefore, the transducer was fitted directly above the load zone of the bearing, allowing for effective recording of the shock pulses.

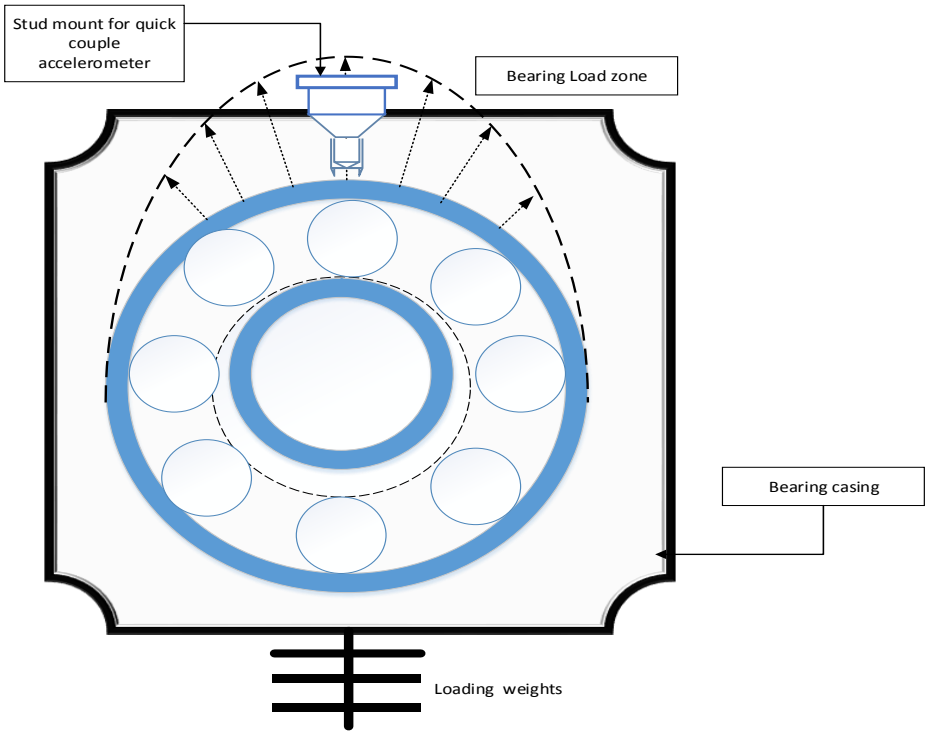

Figure 3.12 Bearing holder with a quick couple connector fitted in the load zone.

3.3.4 Accelerometer

The accelerometer is the most important link between the signal received from the bearing and the instrument recording the signal. The accelerometer is the only transducer that can detect pressure wave vibrations and is displayed in the time domain. Recording the desired signal requires the correct selection of an accelerometer type and with correct specification. For the purpose of this research, the SPM shock pulse accelerometer was used in conjunction with the shock pulse instrument, and Code Master Pro software. A compression accelerometer type with a piezoelectric crystal was used, as seen in Figure 3.13. A piezoelectric crystal contains molecules with asymmetrical charge distributions, and when forces are applied to the crystal, positive and negative charges are generated that induce an electric current. The crystal is selected so that only shock pulse occurring at 32kHz will induce a force in the crystal (Sohoel 1971).

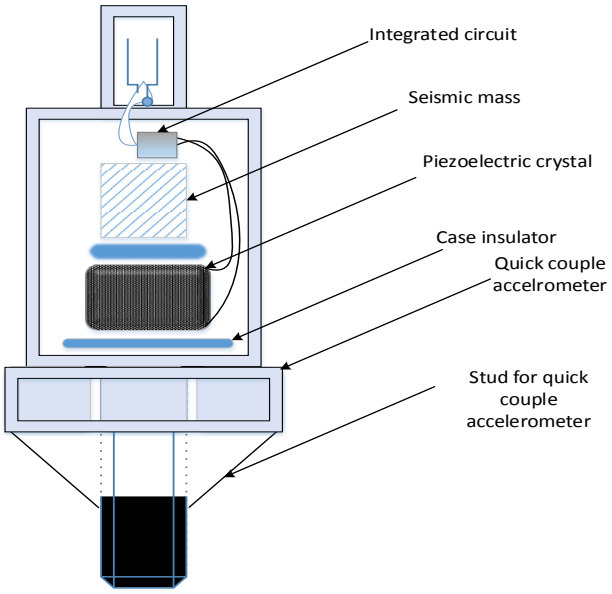

Figure 3.13 Accelerometer with piezoelectric crystals

The mounting of the accelerometer is very important and therefore the accelerometer was mounted on a stud as seen in figure 3.12. Stud mount techniques are the best method for obtaining effective vibration signals from a machine (Boto 1971).The accelerometer was installed according to SPM specifications, which emphases that a hole of 8 mm is drilled, taped and counter sunken. This counter sunk side gives a good bond between surfaces to ensure that transient shock values are transferred effectively (Boto 1971).

3.3.5 Bearings

Engja, Rasmussen & Lippe (1977) carried out some test on mechanical impedance due to flexible mountings. They proved that the stiffness of a bearing structure is crucial in experimental work and therefore, the test rig was designed with a 30 mm diameter shaft that was supported by two roller bearings in pillar blocks mounted onto a 8 mm channel iron base plate, as indicated in Figures 3.9 A and B.

A test bearing was mounted on the non-drive end of the shaft and was supported between two guides. The bearing selected was a spherical roller ball Y-bearing series YAR 206 (TU30) (see data sheet Appendix 6). This bearing

was selected because shock pulse on a damage race way of a spherical roller bearing is more prominent than on a cylindrical roller bearing, according to Barkov *et al.* (1997). Spherical roller bearings give a higher shock value than a cylindrical roller bearing because of the point load on the contact face of the bearing. The TU30 bearing holder design was selected to allow for a load to be mounted on the bottom of the bearing (see Appendix 6 for bearing manufacture specification). On this bearing, various tests of speed variation and load variation were performed, as stated in Section 3.4. Two test bearings were used with similar induced failure on the outer race, as seen in Figure 3.14. See Appendix 7 for more details on failure-induced defects on bearings.

Figure 3.14 Test bearings

3.3.6 Lubrication method

Following research by Shawki (1979) and Anon (1984), the bearing was lubricated with a drip feed system by an oil container that was mounted on top of the bearing. A restricted feeder pipe leading into the race of the bearing allowed the lubrication to drip onto the bearing housing and pass through the bearing without restricting it. This provided a constant and controlled lubricant. The dBc value was recorded during the test to ensure that the lubrication condition remained constant during all the tests, (Sohoel 1984). The lubrication that was used for the experimental work was a SAE 40 oil, with a viscosity of 95 (see Appendix 6 for lubrication specifications).

3.3.7 Temperature control during testing

For the duration of the tests, a fan heater was used to blow hot air at 30 degrees Celsius over the bearing under test as seen in Figure 3.15. This was done to ensure that the clearances in the bearing remained constant during the tests. The temperature was measured at the beginning and at the end of each test to ensure stable conditions.

Figure 3.15 Fan heater displayed in background blowing hot air over the test bearing

3.4 EXPERIMENTAL TESTS PERFORMED

There were five different tests performed and the experimental data details are given in Sections 3.4.1 to 3.4.5.

3.4.1 Variable speed test focused on dBsv and dBn values

In this experiment, the effect of variable speed on the dBsv and dBn shock values, and whether the condition of the bearing could be monitored under these conditions, was investigated. To capture data under variable speed conditions, a tacho meter was used to record the speed of rotation. Before every reading was captured, the shaft speed was captured first, and the dBi value was calculated so that the dBsv and dBn values could be recorded.

3.4.2 Variable speed test focused on acceleration.

In this experiment, the effect of variable speed on the shock value, and whether the condition of the bearing could be monitored under these conditions of acceleration was investigated. Four different readings were captured, each with different acceleration periods.

3.4.3 Variable speed test focused on deceleration.

In this experiment, the effect of variable speed on the shock value, and whether the condition of the bearing could be monitored under these load conditions of deceleration was investigated. Five different readings were captured, each with different deceleration periods.

3.4.4 Variable load test

In this experiment, the speed was kept constant and the effects of varying the transverse load on the bearing and whether the condition of the bearing could be monitored under these conditions were investigated. Four different readings were captured, each with different applied loads.

3.4.5 Variable speed and load conditions

In this section, the effects of variable speed and variable load on the bearing, and whether the condition of the bearing could be monitored under these speed load conditions was investigated. Two test were performed, one with a 1 mm defect on the outer race of the bearing and one with a 2 mm defect on outer race of the bearing.

3.4.4 Presentation of measured data

From each experiments performed, the results were captured and presented graphically in each section. The measured data sheets of the experiments are presented in Appendix 1 to 5. Each test was performed at various bearing operating conditions. The graphs are analysed and conclusions presented in Chapter 4.

3.4.5 Delimitations in capturing of data

Certain delimitations exist in the capturing of the shock pulses at low speeds. Barkov *et al*. (1997) and Smith (1993) both concluded in their articles that on slow rotating bearings it is very difficult to measure the shock pulse values. They noted that the speed of a bearing should be above 200rpm in order to obtain an effective result. It is due to these findings that shock pulse values below the speed of 200rpm will not be considered in the analyses.

3.4.6 Graphical representation of data captured

Shock pulse values are influenced by factors such as bearing size, rpm, signal damping and lubrication. Two parameters that are used to determine bearing condition are the carpet value dBc and the maximum dBm value. The carpet value indicates the lubrication condition. A high dBc value can be caused by a number of lubrication conditions such as insufficient lubrication, lubrication contamination and improper bearing load. (Barkov et al. 1997)

A high dBm value indicates damaged bearing elements. A high maximum dBm value is generated by the bearing elements hitting a defect within the bearing. The dBm values will always be greater than the dBc values. The dBm and dBc values will increase in amplitude by roughly the same amount if the lubrication breaks down. (Barkov et al. 1997) If bearing defects are present then the dBm values will increase or trend upward faster than dBc values, and the separation between the two will increase. (Sohoel 1984).

In Figure 3.16 the low dBm and the high dBm values recorded are presented in three color zones as presented by the SPM manufactures specification. The green color indicates that the bearing is in a good condition and the value ranges up to 20dB. The yellow color indicates a bearing entering an alarm value and ranges between 20dB to 35dB. The red color indicates a damaged bearing and the value ranges between 35dB to 60dB.

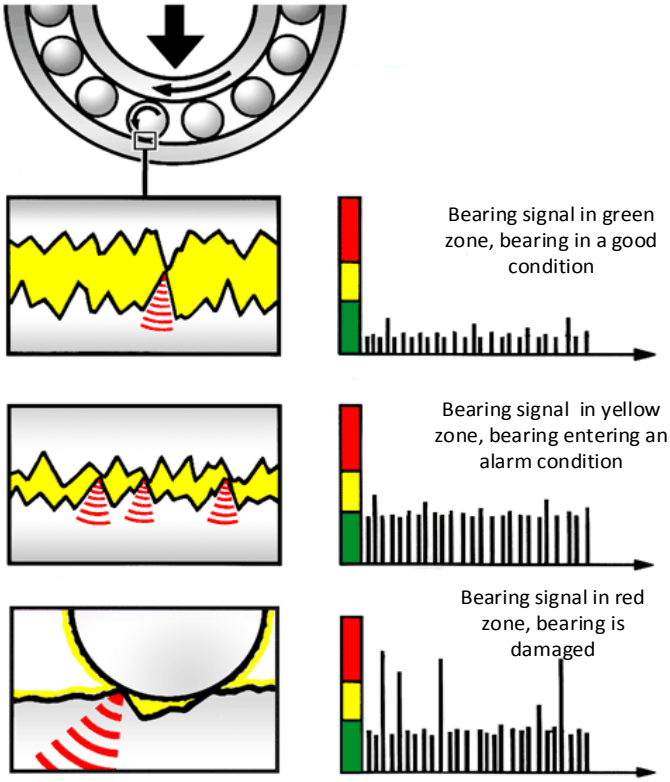

Figure 3.16 Three SPM color zone of good, alert and bad bearing conditions (SPM specification, August 1994)

CHAPTER 4: EXPERIMENTAL RESULTS, ANALYSIS AND DISCUSSION

4.1 INTRODUCTION

In this chapter, experimental results for various operating conditions are presented. In Section 4.2, the purpose of using the dBm value rather than using the dBsv as derived in Sohoel's work of 1966 is discussed. In Section 4.3, the dBm values recorded during various acceleration intervals, and in Section 4.4, the dBm values recorded during various deceleration intervals are reported. In Section 4.5, the speed was kept constant and the load varied while the dBm value was recorded. In Section 4.6.1, there were various tests performed at various speeds and various loads on a bearing with a 0.1mm defects on the bearing outer race. In Section 4.6.2, there were various tests performed at various speeds and various loads on a bearing with a 0.2mm defect on the bearing outer race. The data captured for the experimental graphs in Section 4 are all presented in the Appendix 1 to 5. At the end of each set of experiments, there are discussions.

4.2 DBSV AND DBM VALUES FOR VARIABLE SPEED AND A FIXED LOAD

In this section, one test was performed under variable speed conditions on a bearing with an outer race defect as stated in chapter 3, section 3.3.5. The decibel (dB) values were captured by the accelerometer and the relate speed was captured by a tacho meter. The speed was varied between 0 rpm and 1500 rpm and a fixed load of 60 kg was placed on the bearing. The experimental results are displayed in Figure 4.1. The shock pulses are displayed in decibel shock value (dBsv) representing the actual condition of the bearing. As the speed increases the dBsv value increases proportionally with the rotational speed of the bearing (Bloch, 2000). The dBsv, which reflects the damage in the bearing, is irregular. The value was observed to fluctuate between 20dB and 38dB. A value of 20dB represents insignificant damage and a value of 38dB

represents an early warning damage on bearing (Brown 1971). The result as displayed in Figure 4.1 proved that the dBsv value could not predict the condition of the bearing while the speed was varying.

To overcome the problem of the dBsv changing in value as the speed changes the bearing shaft size and the speed of the shaft was taken to calculate the dBi value using equation 3.16 for every speed interval. The dBm value was calculated according to the equation 3.17, and plotted. The results are displayed in Figure 4.1 and in Appendix 1.

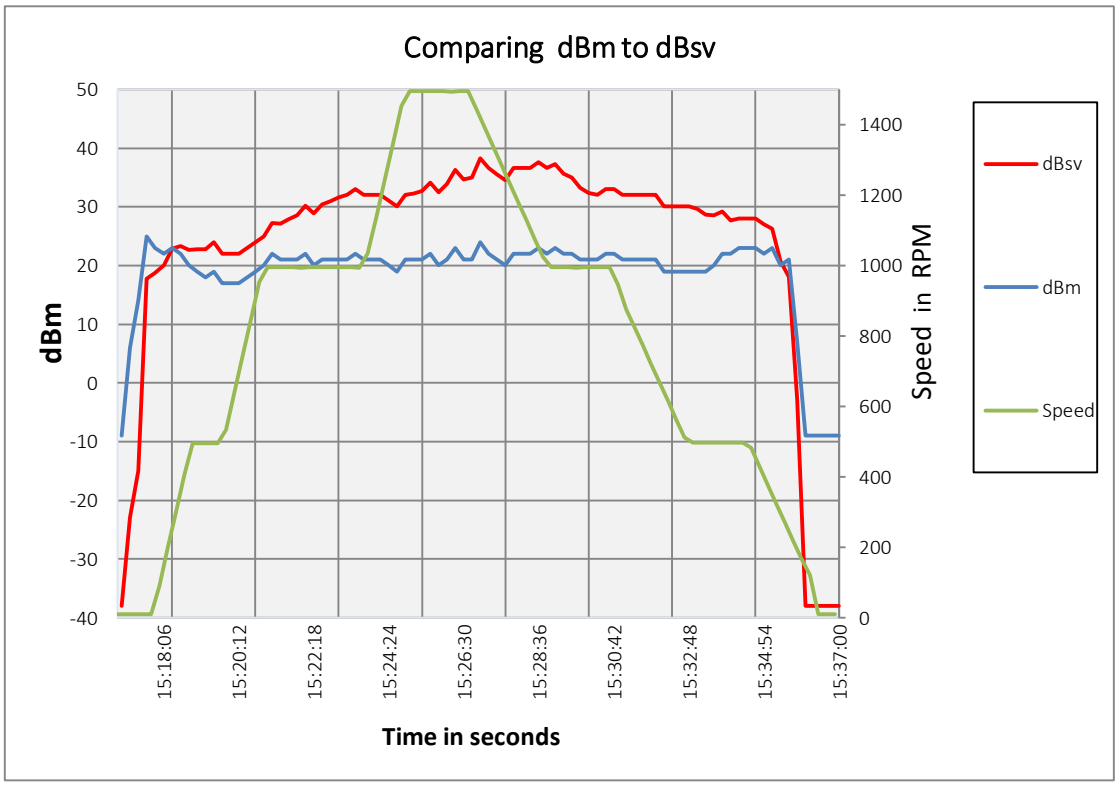

Figure 4.1 Relationship between dBsv and dBm

The dBm value stays fairly constant with varying speed. The value fluctuated between 19dB and 23dB.

The results in Figure 4.1 indicate that the dBsv value could not be used under variable speed because the value fluctuated by 18dB. A fluctuation of 18dB would cause the state of the bearing to fluctuate between good and bad conditions, as stated in Section 3.4.5. The dBm value gave a fairly constant

value, allowing the condition of the bearing to be monitored while the speed was varying. To ensure that the dBm stayed constant under all variable and erratic speed conditions, more tests were performed in Section 4.3 with various acceleration periods and in Section 4.4 with various deceleration periods. In the experimental results that follow, only the dBm normalised values were calculated.

4.3 RESULTS FOR A VARIABLE SPEED, WITH A FOCUS ON ACCELERATION INTERVALS

In this experiment, four tests were performed for various acceleration intervals on a bearing with an outer race defect as discussed in Chapter 3 Section 3.3.5. The dBm values were recorded while the speed was increased from 0 rpm to 1500 rpm in various time intervals. This was done to determine how the dBm value would be affected during acceleration periods. The tests were carried out under controlled conditions as discussed in Chapter 3, Section 3.3. In each test, there are three graphs displayed. The bottom graph in pink displays the speed of rotation of the bearing, the blue graph displays dBc values and the black graph displays the dBm. Each reading was taken at a respective speed as indicated in the bottom speed graph.

4.3.1 Test one

In this experiment, the speed was increased from 0 rpm to 1500 rpm in a one-minute interval. From Figure 4.2 the dBm value stabilised at 21dBm once the 200 rpm point was reached, and remained fairly constant for the duration of the tests.

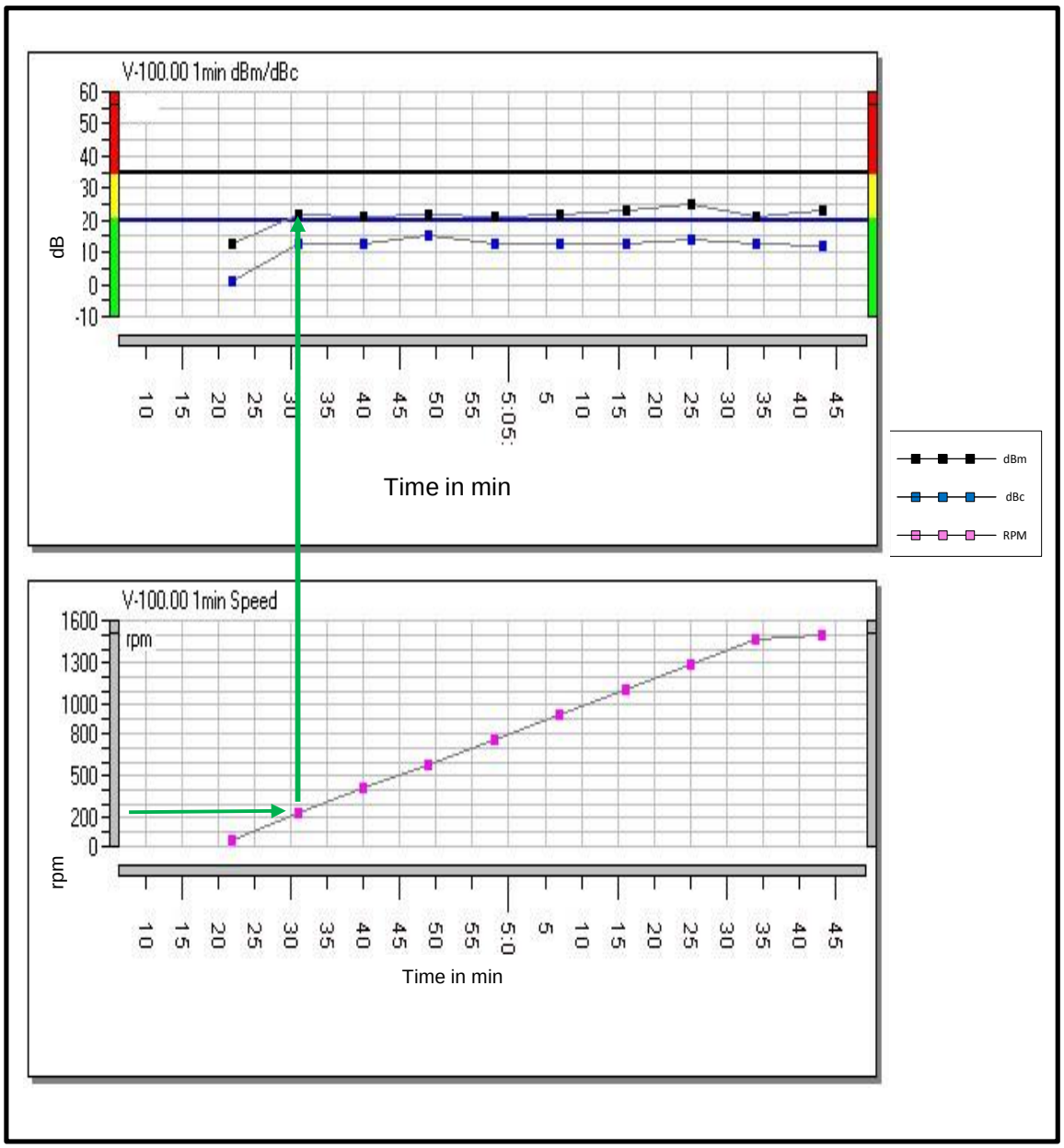

Figure 4.2 dBm values for a 1min acceleration period

4.3.2 Test two

In this experiment, the speed was increased from 0 rpm to 1500 rpm in a three-minute interval. In Figure 4.3 the dBm value stabilised at 21dBm once the 200 rpm point was reached, and remained fairly constant for the duration of the tests.

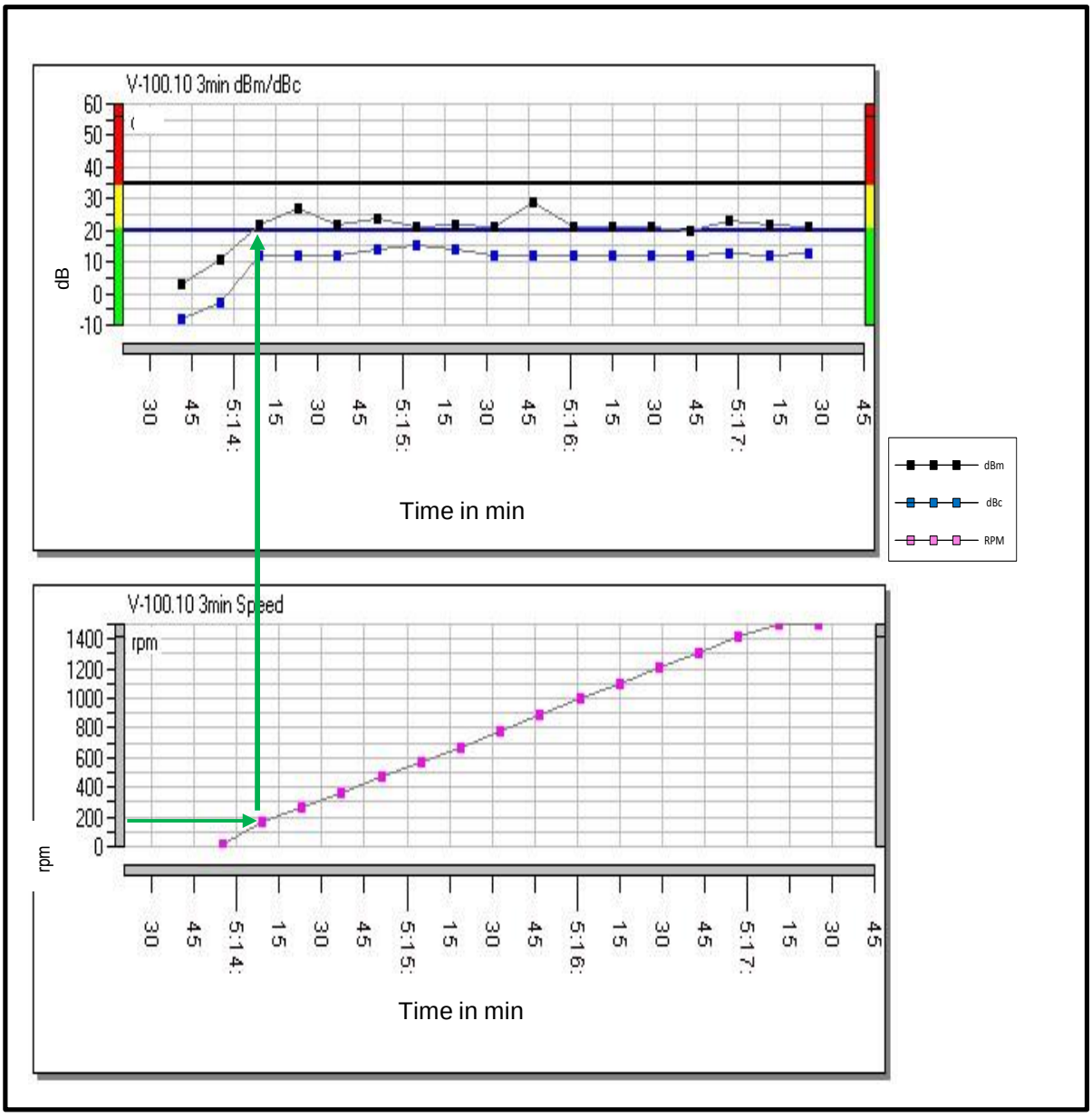

Figure 4.3 dBm values for a 3min acceleration period

4.3.3 Test three

In this experiment, the speed was increased from 0 rpm to 1500 rpm in a six-minute interval. In Figure 4.4 the dBm value stabilised at 21 dBm once the 200 rpm point was reached, and remained fairly constant for the duration of the tests.

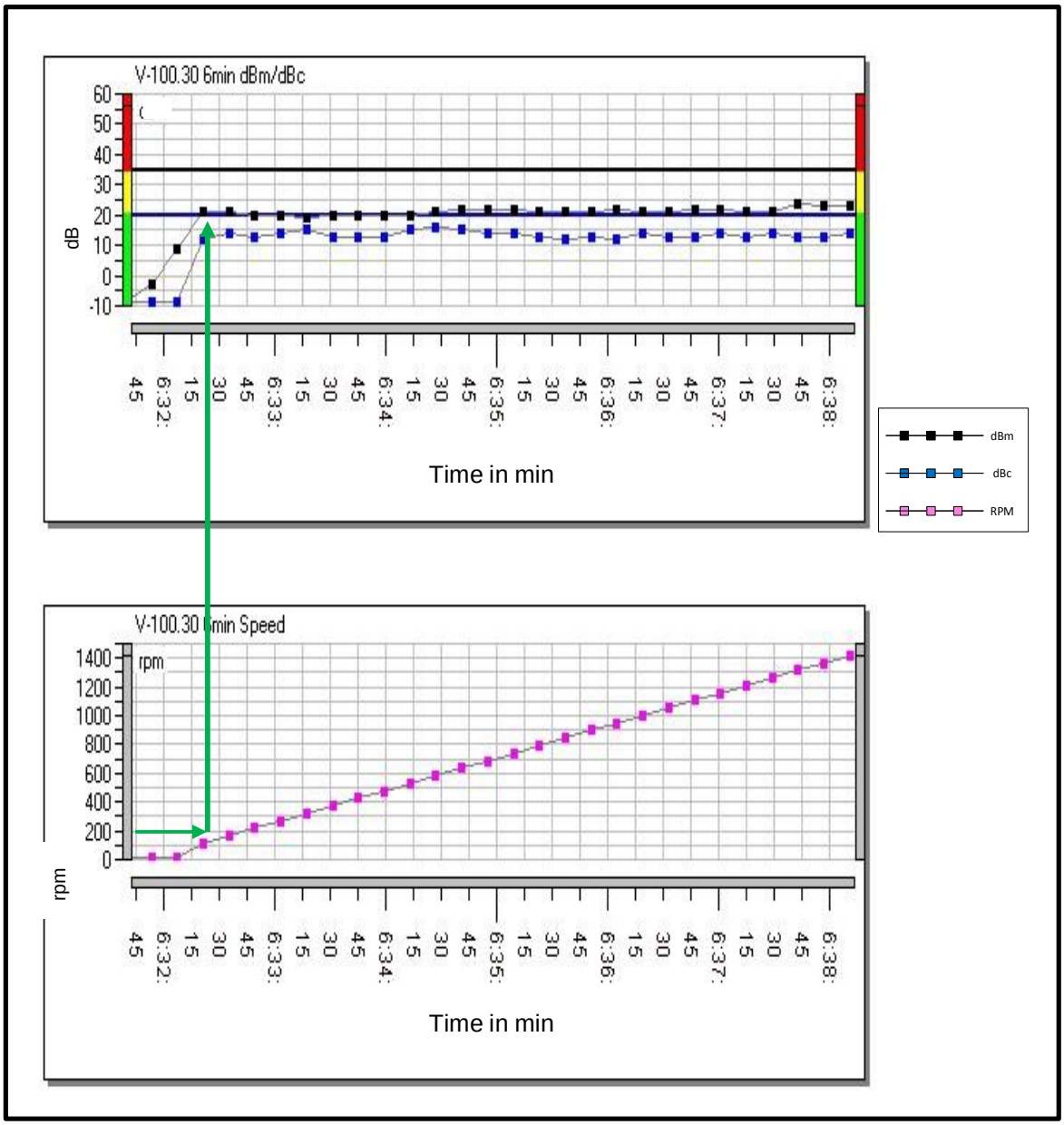

Figure 4.4 dBm values for a 6min acceleration period

4.3.4 Test four

In this experiment, the speed was accelerated from 0rpm to 1500 rpm in a nine-minute interval. In Figure 4.5 the dBm value stabilised at 19 dBm once the 200 rpm point was reached, and remained fairly constant for the duration of the tests.

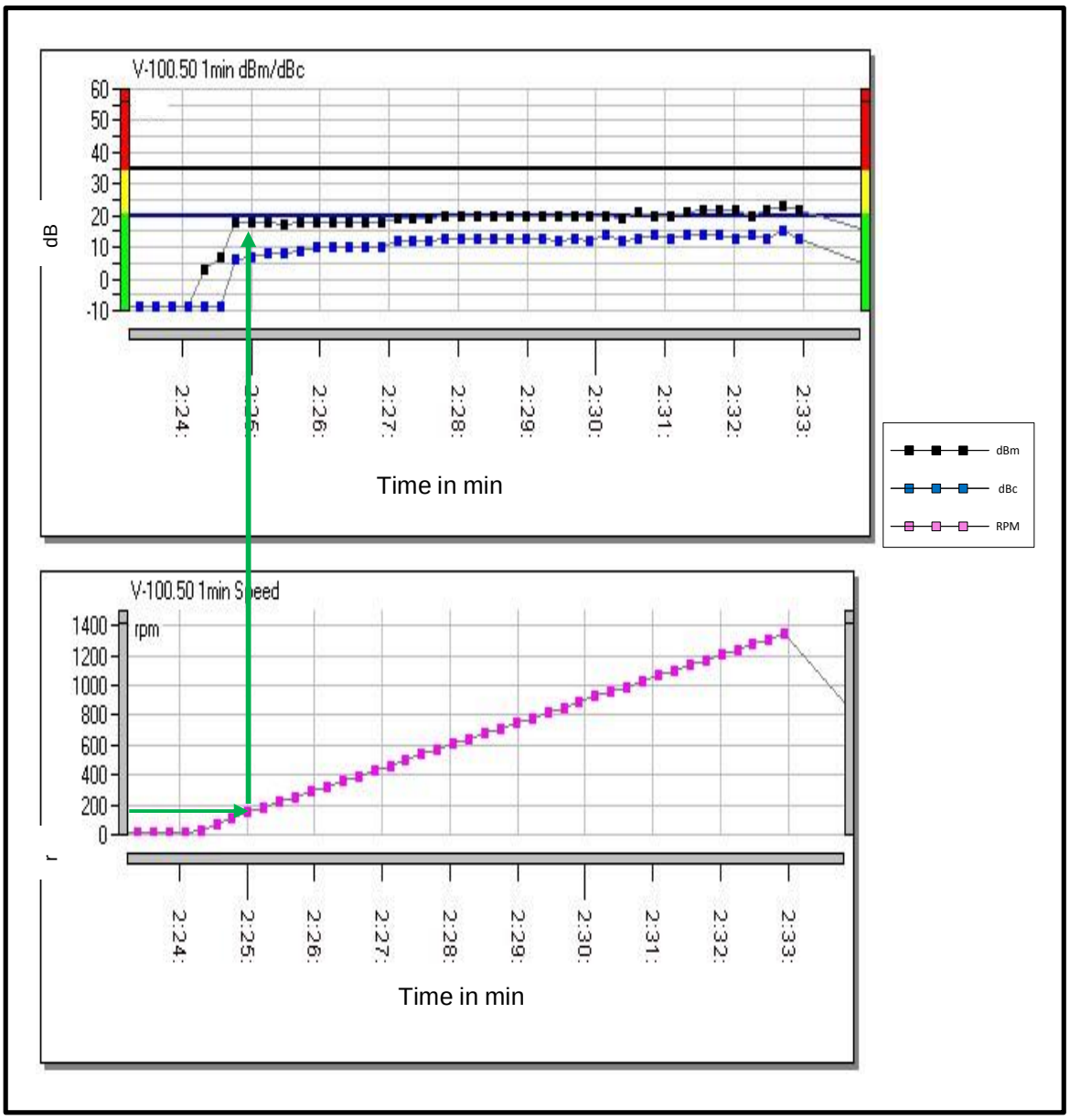

Figure 4.5 dBm values for a 9min acceleration period

4.3.5 Discussion of results for Section 4.3.1 to Section 4.3.4

The graph in Figure 4.6 represents a combination of the above four experiments as displayed in Figures 4.2 to 4.5. The dBm value fluctuated erratically at the start of the experiment, but once the 200 rpm speed was reached it stabilised at about 21 dBm. The green arrow in Figures 4.2 to 4.5 indicated this point of stabilisation. This dBm fluctuation before the 200 rpm speed was reached can be as a result of the low dynamic forces in the bearing during start-up. Once the dynamic forces increase, the lubrication moves into the hydrostatic mode, the rolling elements in the bearing become static, and the erratic results stabilise (Harris 1995:32:23).

The dBm value shows a total of 4 dBm fluctuation from the combined results of all the four experiments. This was constant from the 200 rpm speed range to the 1500 rpm speed range. The change in dBm over the wide range of speed fluctuation is 4 dBm. This is minimal and therefore it can be concluded that irrespective of the roller bearing speed and acceleration period, the dBm value stays constant under variable speed applications.

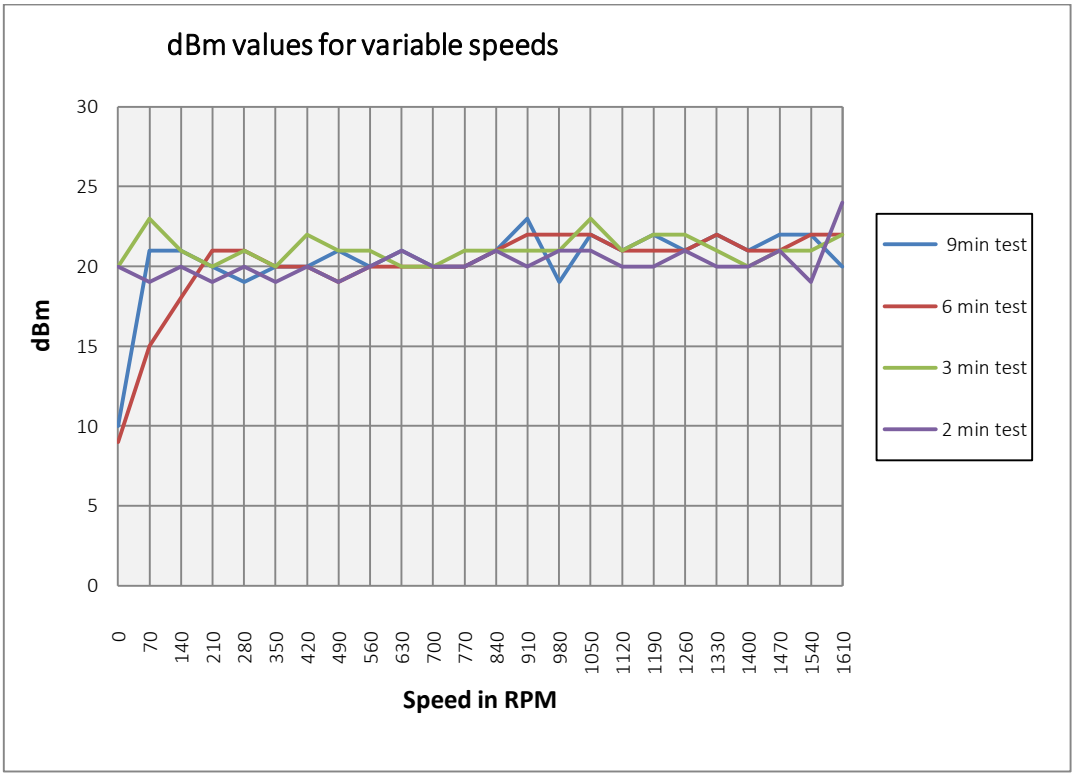

Figure 4.6 dBm values for various acceleration periods

4.4 VARIABLE SPEED DURING DECELERATION

In this experiment, five tests were performed under variable speed conditions on a bearing with an outer race defect as discussed in Chapter 3, Section 3.3.5. The dBm values were recorded while the speed was alternated to determine how the dBm value would be affected during deceleration periods. The tests were carried out under controlled conditions as discussed in Chapter 3, Section 3.3. In each test, there are three graphs displayed as shown in Figures 4.7 to 4.11. The bottom graph in pink displays the speed of rotation of the bearing, the blue graph displays dBc values and the black graph displays the dBm. Each

reading was taken at a respective speed as indicated in the bottom speed graph.

4.4.1 Test one

In this experiment, the speed was alternated between 100 rpm and 600rpm. In Figure 4.7, the dBm value only fluctuated slightly during the deceleration period.

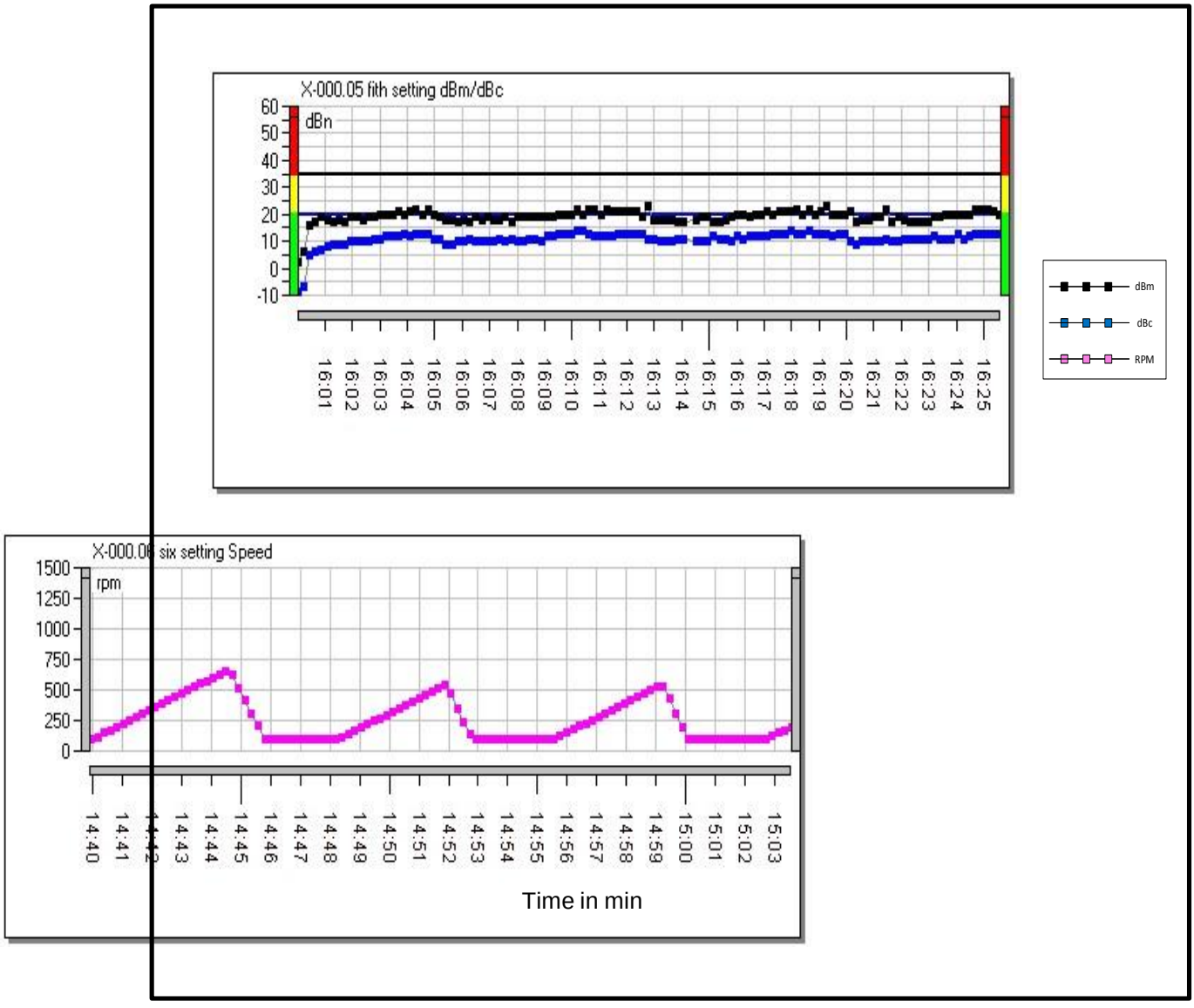

Figure 4.7 dBm values during a 600 rpm deceleration period

4.4.2 Test two

In this experiment, the speed alternated between 100 rpm and 700 rpm. In Figure 4.8, the dBm value fluctuated quite erratically during the deceleration period.

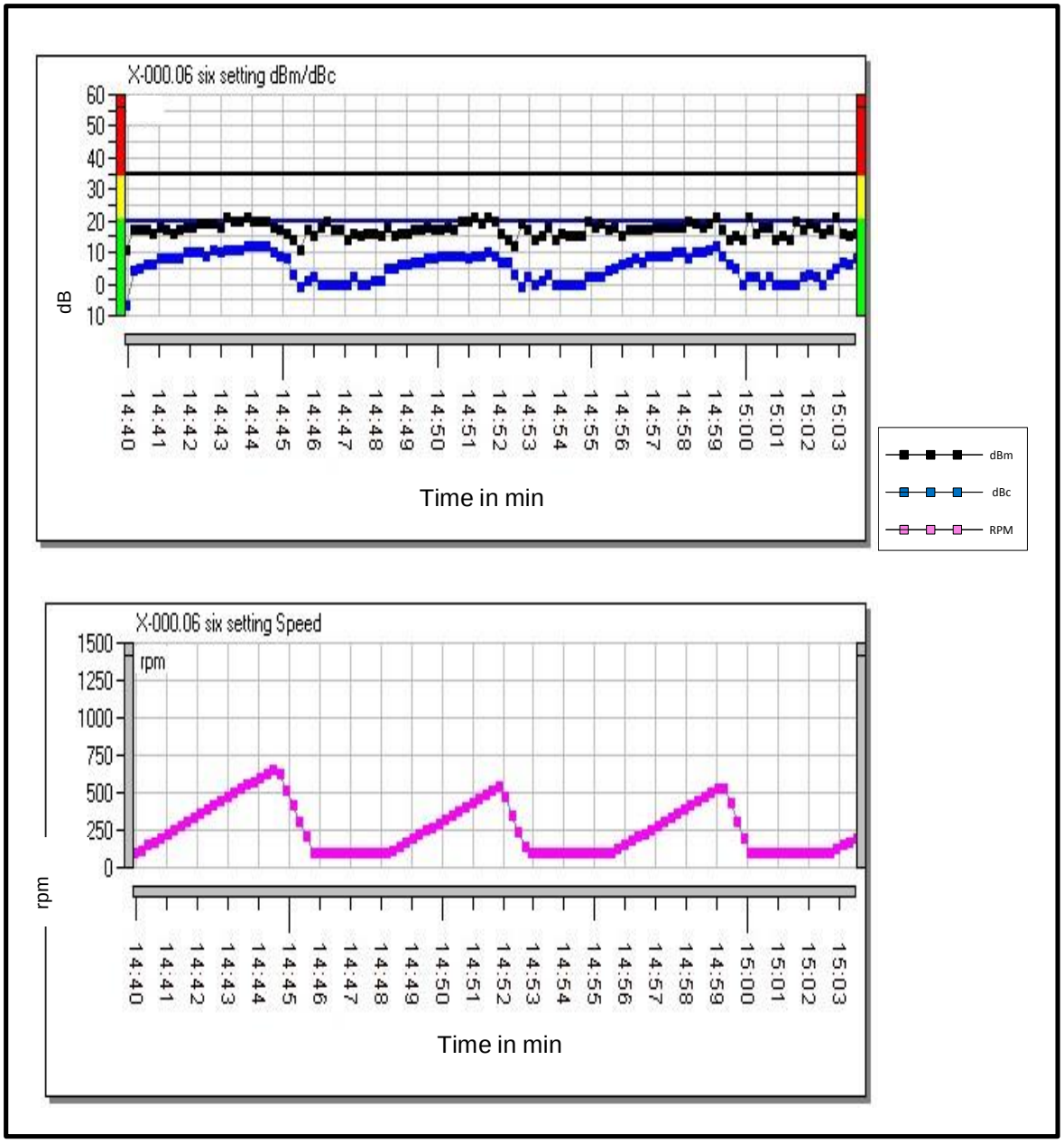

Figure 4.8 dBm values during a 700 rpm deceleration period

4.4.3 Test three

In this experiment, the speed alternated between 0 rpm and 1200 rpm. In Figure 4.9, the dBm value fluctuated erratically during the deceleration period.

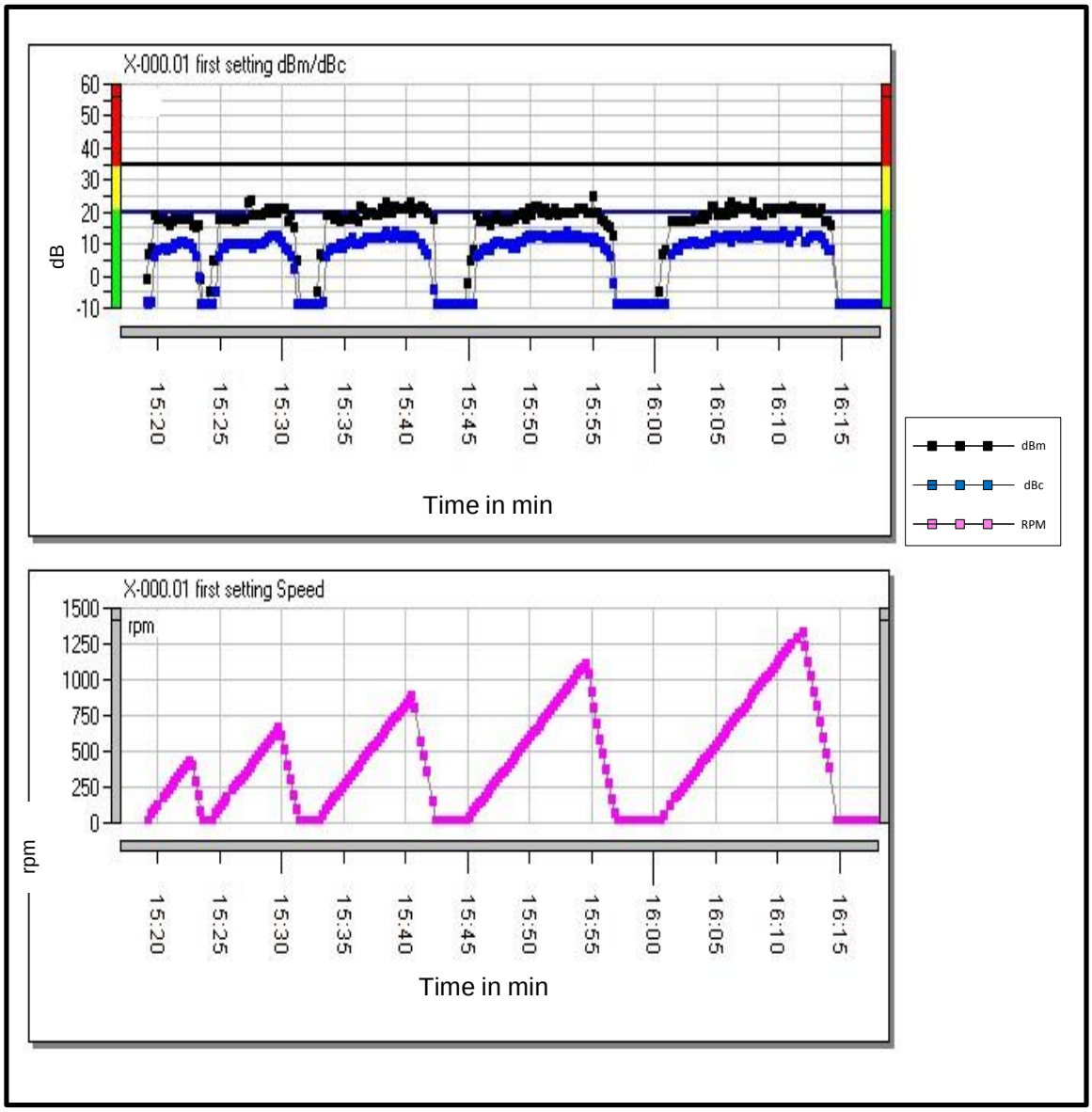

Figure 4.9 dBm values during a 1200 rpm deceleration period

4.4.4 Test four

In this experiment, the speed ranged from 0 rpm to 1400 rpm and was stepped down in 250 rpm decrements. In Figure 4.10, the dBm value remained fairly

constant between 15 dBm and 20 dBm for the duration of the tests. Once the speed went below 200 rpm, no values could be recorded.

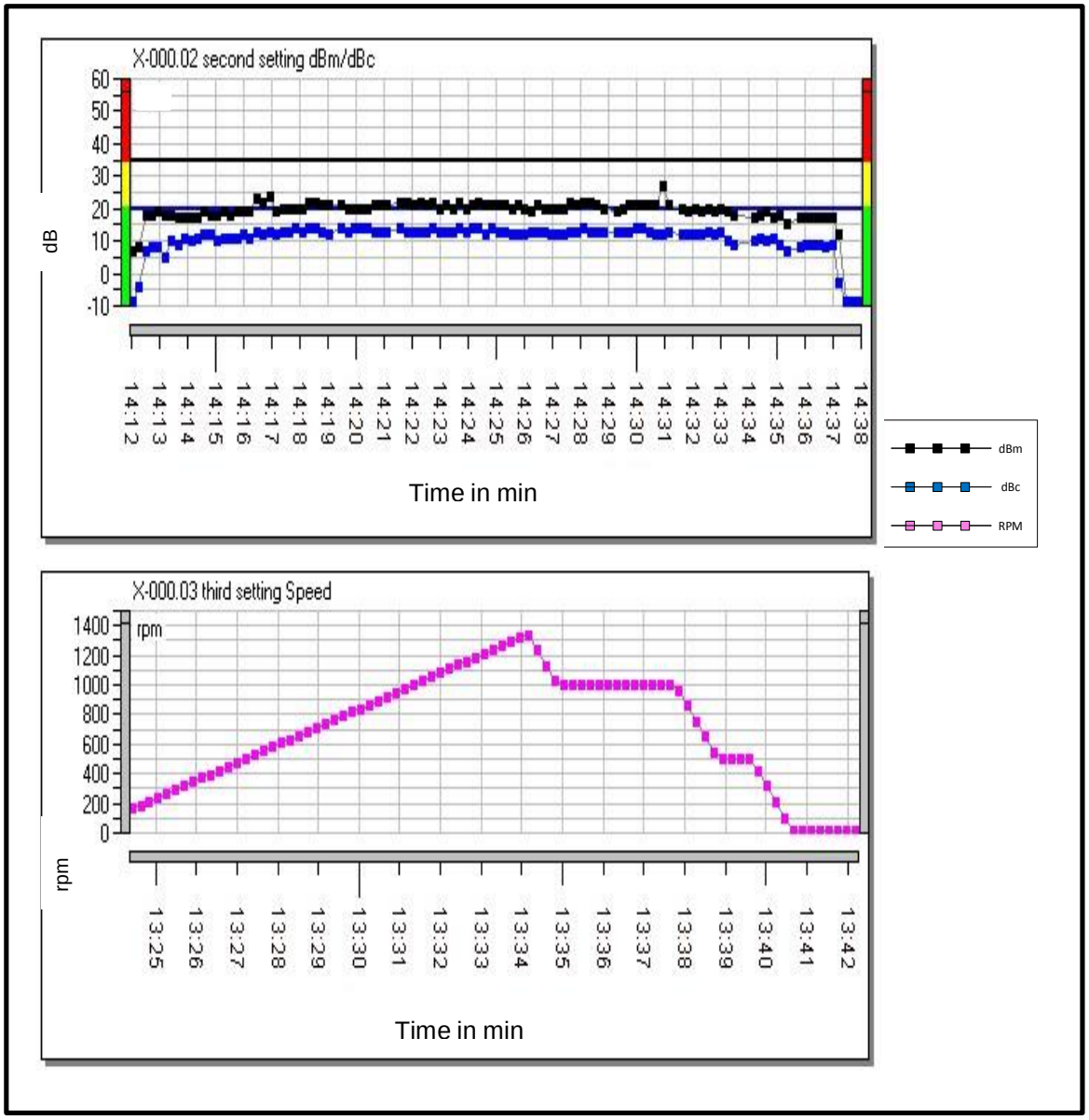

Figure 4.10 dBm values in 200 rpm decelerating decrements

4.4.5 Test five

In this experiment, the speed range was 0 rpm to 1400 rpm and was stepped down in 450 rpm decrements. In Figure 4.11, the dBm value remained fairly constant between 15 dBm and 22 dBm for the duration of the tests. Once the speed went below 200 rpm, no values could be recorded.

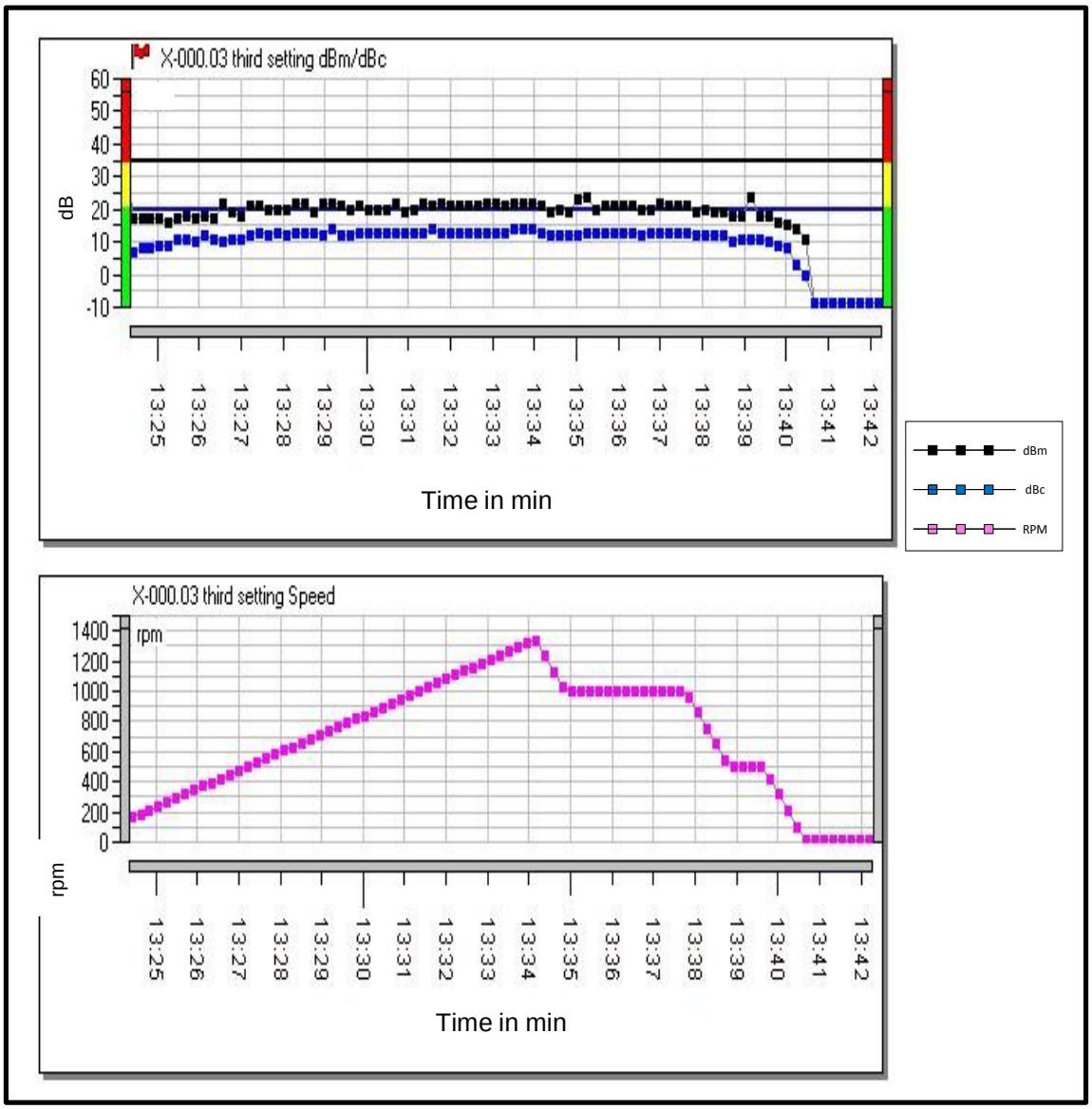

Figure 4.11 dBm values in 450 rpm decelerating decrements

4.4.6 Discussion of results for Section 4.4.1 to Section 4.4.5

From the graphs in Figure 4.7 and 4.8, it was observed that for deceleration period, the shock values was erratic. For the graphs in Figures 4.9 and 4.11 it was observed that for the gradual deceleration period until 0 rpm showed consistent shock values with a slight drop in the dBm value as the speed reduced. Initially, the dBm dropped by 5 dBm as the speed decelerated, and only once the speed reached about 200 rpm the dBm value dropped erratically.

From the graphs in Figures 4.7 and 4.8, the erratic change in the shock value (dBm) during the deceleration period can be explained by the phenomena of

erratic dynamic forces in the bearing rolling elements. A second phenomenon that occurs is that the lubrication loses its hydrostatic force as the speed reduces and metal-to-metal contact occurs in the bearing and the dBm value increases.

From the graphs in Figures 4.9 and 4.11, the change in dBm over the wide range of deceleration is much less than during the erratic deceleration periods.

4.4.7 Conclusion for acceleration and deceleration experiments.

From the experiments performed in Section 4.3, it could be concluded that, irrespective of the speed of rotation of the bearing and the various time periods during which the acceleration was altering, the dBm value could be used effectively to record the condition of the bearing once the 200 rpm speed had been exceeded. Only once the 200 rpm speed was achieved, was there enough dynamic force within the bearing to generate a shock pulse that was evident. Thus, it was concluded that the dBm value could be used to trend the condition of a bearing operating at variable speed and constant load during any length of acceleration period.

From the experiments performed in Section 4.4, it was concluded that the dBm value for all four tests presented similar results during deceleration. During the deceleration stage, it was found that the dBm shows a tendency to fluctuate significantly as the bearing decelerates. This could be as a result of a more erratic thrust load on the bearing, and that the bearing components have more play, and thus, irregular shocks took place.

4.5 CONSTANT SPEED WITH VARYING LOAD

In this section, the effect of variable load on the dBm value and a possibility to monitor the condition of a bearing while the load was varied were investigated. Four experimental tests were performed with various loads applied to the test bearing with 0.1 mm defect on the bearing outer race. These experiments were aimed at determining how the shock pulse values would be affected when the load was increased. The tests were carried out under controlled conditions as

discussed in Chapter 3. The speed was maintained at 900 rpm while the load was varied from no load to a maximum of 80 kg. The experimental tests are represented in Section 4.5.1 to 4.5.4.

In these experiments, the lubricant was removed from the bearing to obtain maximum high stress loading on the bearing surface. The bearing speed was kept at 900 rpm to limit heat due to friction. The purpose of running the bearing with no oil was to obtain maximum dBm shock values.

4.5.1 Test one

In this test, the speed was kept at 900 rpm and no load was applied to the bearing. An average of 35 dBm value was recorded and is presented in Figure 4.12. The lubrication was removed from the bearing, and therefore, the dBc value was 20, indicating oil starvation.

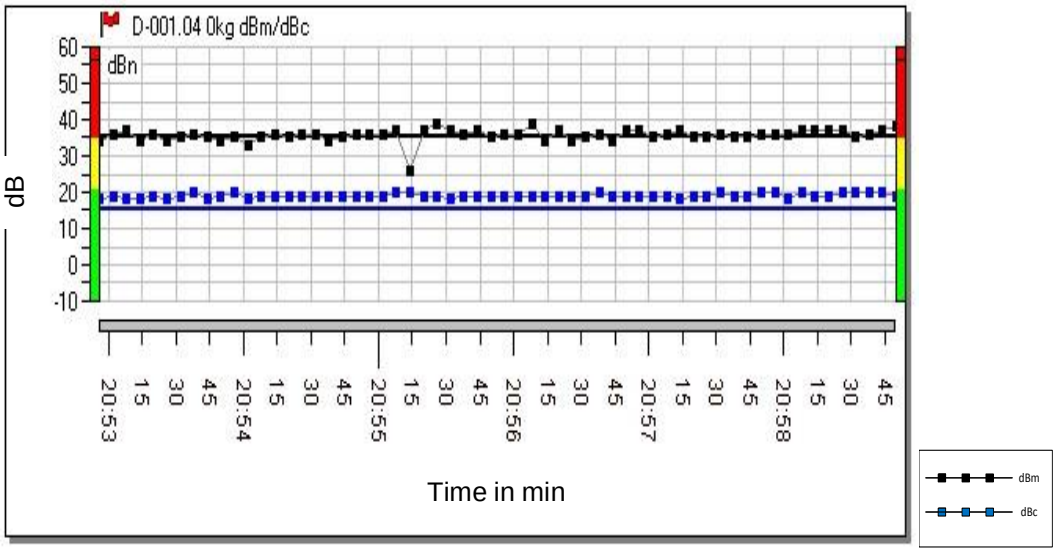

Figure 4.12 dBm values with no load

4.5.2 Test two

In this test, the speed was kept at 900 rpm and a 20 kg load was applied to the bearing. A 40 dBm value was recorded and is presented in Figure 4.13.

The lubrication was removed from the bearing, and therefore, the dBc value was 20, indicating oil starvation.

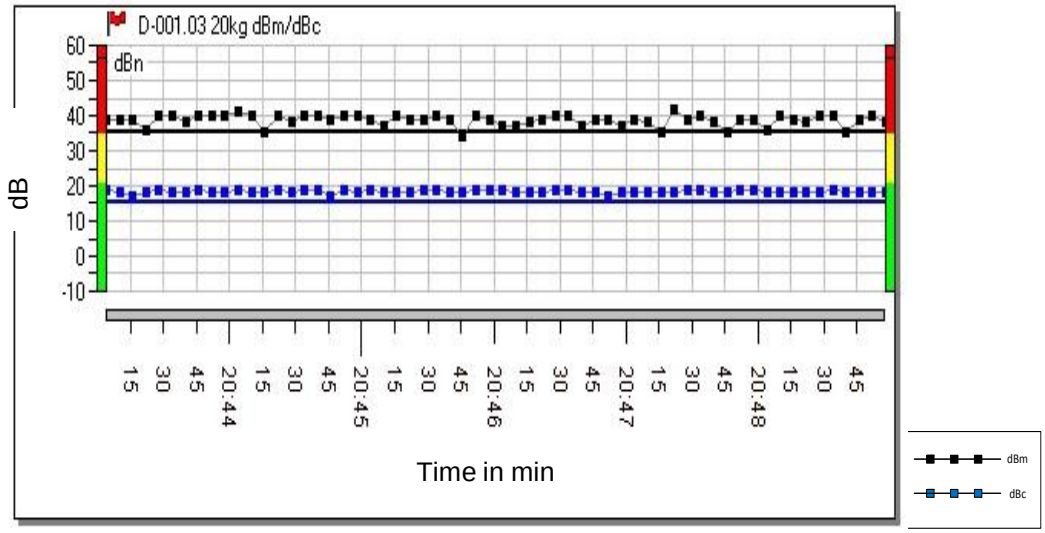

Figure 4.13 dBm values with applied load of 20 kg

4.5.3 Test three

In this test, the speed was kept at 900 rpm and a 50 kg load was applied to the bearing. A 45 dBm value was recorded, and is presented in Figure 4.14.

The lubrication was removed from the bearing, and therefore, the dBc value was 20, indicating oil starvation.

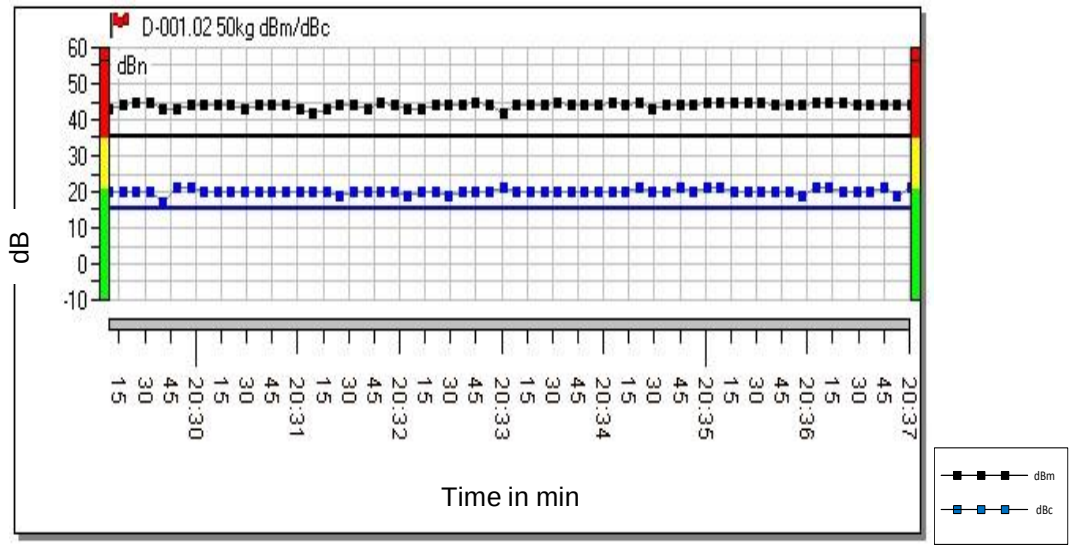

Figure 4.14 dBm values with applied load of 50 kg

4.5.4 Test four

In this test, the speed was kept at 900 rpm and a 80 kg load was applied to the bearing. An average of 47 dBm value was recorded and is presented in Figure 4.15. The lubrication was removed from the bearing, and therefore, the dBc value was 20, indicating oil starvation.

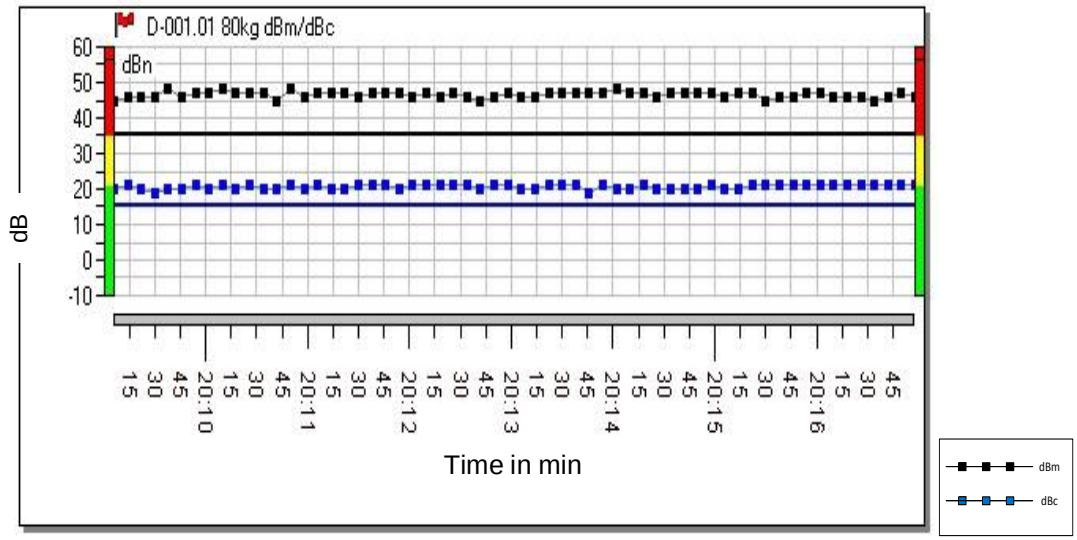

Figure 4.15 dBm values with applied load of 80 kg

4.5.5 Discussion of results presented in Section 4.5.1 to Section 4.5.4

The graph in Figure 4.16 below represents a combination of the dBm values for the above four experiments as displayed in Figures 4.12 to 4.15. In Figure 4.16, it was evident that an increase in load resulted in an increase in dBm value. The dBm increase was only 6 dBm. This dBm increase is very small compared to a mass variation of 80 kg or 800 Newton. The change in the dBm value is significantly small.

Evidence of the lubrication that was removed could be seen by the increase in the dBc value on the bottom line graph in Figures 4.12 to 4.15. The value for no lubrication was 20 dBc compared to a lubricated bearing with a dBc of 10. With the lubrication removed, the dBm value showed a remarkable increase in value. This was clearly evident in all the dBm values for each graph.

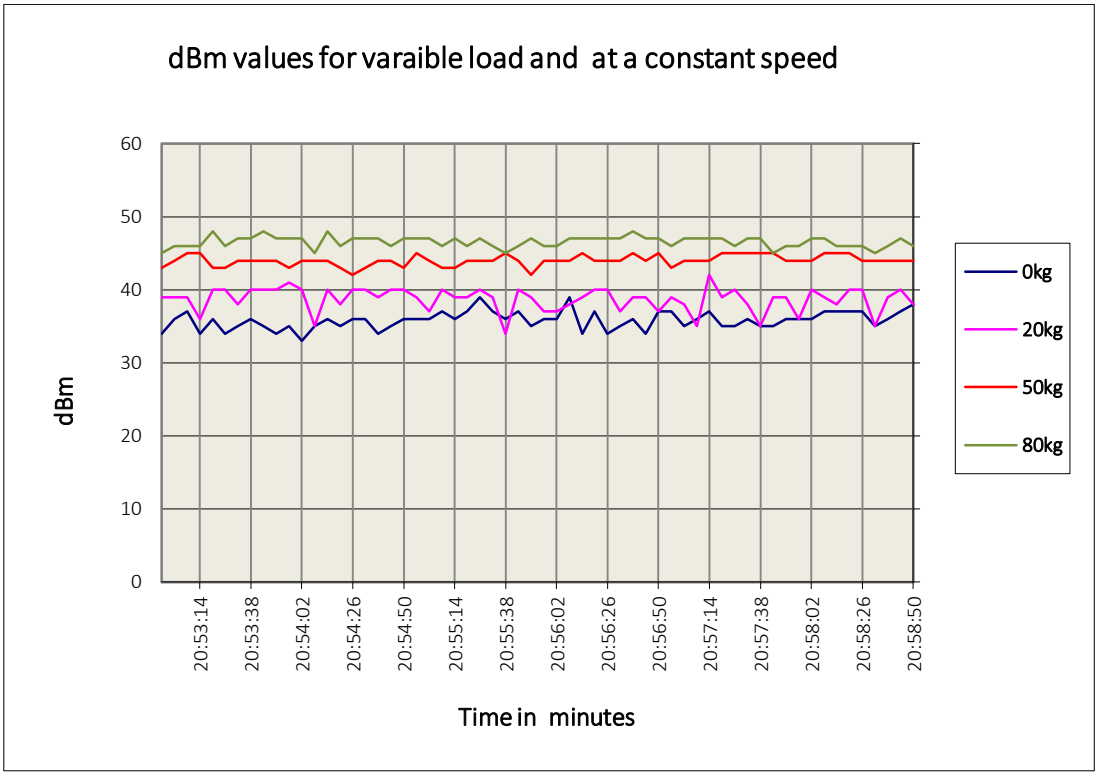

Figure 4.16 Combined dBm values for various applied loads at constant speed

4.5.6 Conclusion

When a load was applied to the bearing, the dBm value increased. The increase was insignificant, with respect to the total load increase of 80 kg or 800 N. For small load changes of 20 kg or 200 N, the dBm value was hardly noticeable. Therefore, it was recommended that when recording the shock value, it should be performed only during periods that the load on the machine is constant.

In Figure 4.16, it can be noticed that with no load or very light loads of 20 kg, the dBm readings fluctuated considerably. This is due to more freedom in bearing movement experienced with light loads. Therefore, the dBm value had more fluctuating values. With heavier loads of 50 kg and 80 kg, a more constant dBm value was obtained than with light loads. Thus, it can be concluded that in heavier loads there is more load on the bearing, allowing for less movement in the bearing and resulting in a more constant reading. In conclusion, it could be noted that during recording, one should consider recording the dBm value only once the machine attains full speed and full load.

4.6 RESULTS FOR VARIABLE SPEED AND VARIABLE LOAD

In Section 4.5, it was observed that a varying load of 30 kg had little effect on the shock value. In Section 4.3, it was noted that when the speed varies, the shock value could be effectively recorded using the dBm value. In this section the effect of varying load and variable speed on the shock value, was investigated simultaneously. Two tests were performed, one on a 0.1 mm pin hole damaged bearing and the other on a 0.2 mm pin hole damaged bearing.

4.6.1 Experimental results for a bearing with 0.1 mm defect

In this experiment, six tests on a bearing with 0.1mm defect were performed. With the start of each new test the applied load were increased by 20 kg. The first test started at 0 kg and the last test ended with an applied load of 100 kg. During each test the motor speed was increased from 0 rpm to 1500 rpm and back to 0 rpm. During each test the dBm values was recorded. This was done to determine whether the dBm value would stay constant, irrespective of the speed and load changes. The tests were carried out under controlled conditions as discussed in Chapter 3. In each test, there are three graphs displayed, as given in Figures 4.17 to 4.22. The bottom graph in pink displays the speed of rotation of the bearing, the blue graph displays dBc values and the black graph displays the dBm. Each reading was taken at a respective speed as indicated in the bottom speed graph.

4.6.1.1 Test One

In this experiment, there was no load applied and the speed was varied between 0 rpm and 1500 rpm. In Figure 4.17, the dBm value stabilised at 200 rpm and remained constant for the duration of the acceleration test. An average dBm of 13 was calculated from the test data as seen in Appendix 3. The dBm value fluctuated in the deceleration stage. This fluctuation in the dBm value was caused by the changing thrust loads in the bearing during deceleration. The dBc value was five and very stable, which indicated a well-lubricated bearing.

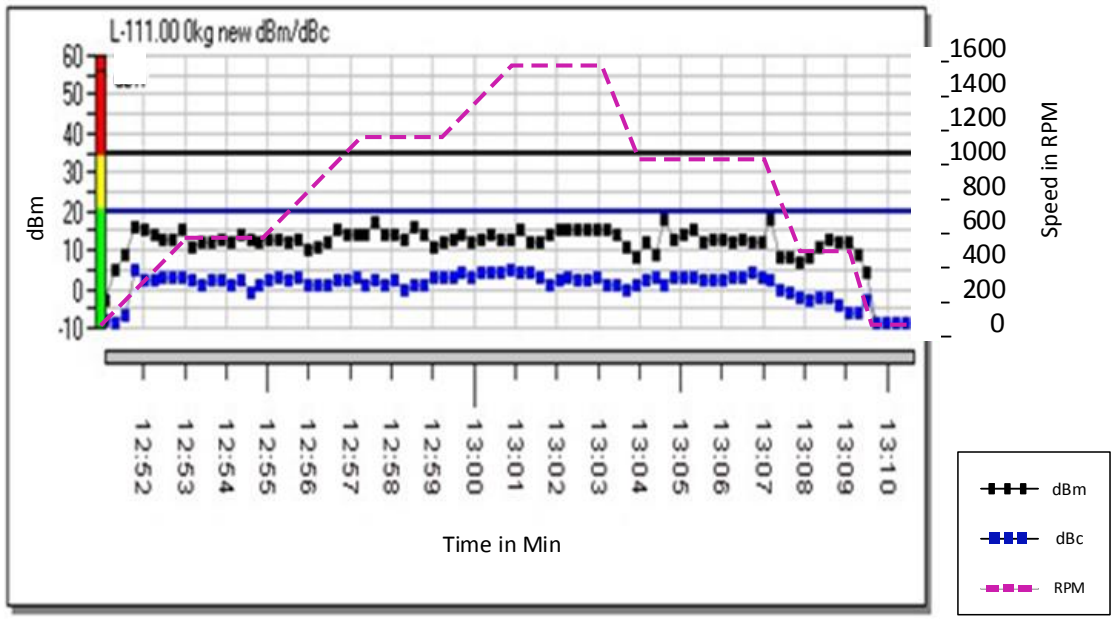

Figure. 4.17 dBm values with no load and speed variation

4.6.1.2 Test Two

In this experiment, the load was kept at 20 kg and the speed was varied between 0 rpm and 1500 rpm. In Figure 4.18, the dBm value stabilised at 200 rpm and remained constant for the duration of the test. An average dBm of 20 was recorded for the duration of the test. The dBc value was five and very stable, which indicated a well-lubricated bearing.

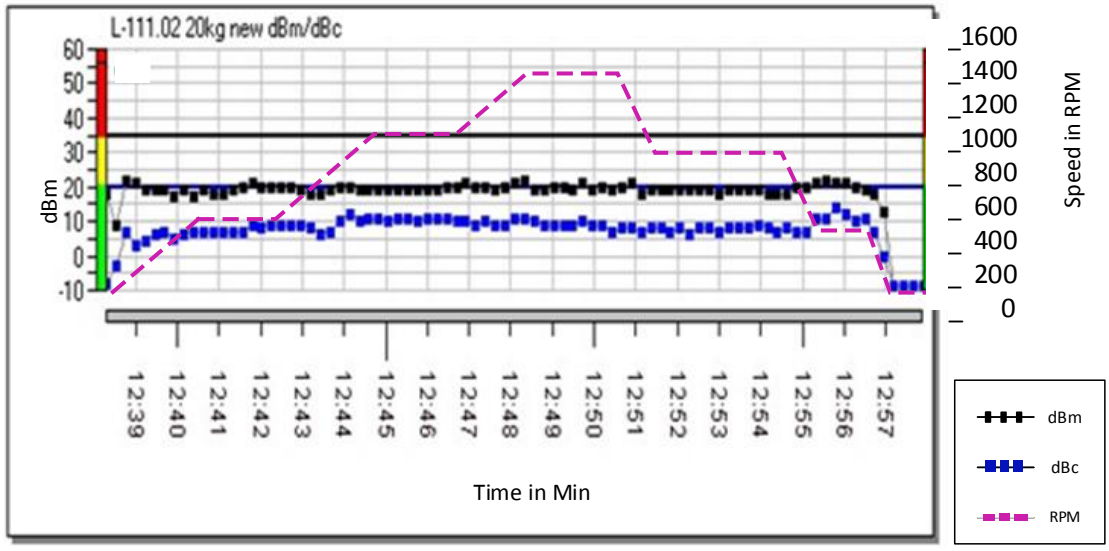

Figure 4.18 dBm values with 20 kg load and speed variation

4.6.1.3 Test three

In this experiment, the load was kept at 40 kg and the speed was varied between 0rpm and 1500rpm. In Figure 4.19, the dBm value stabilised at 200 rpm and remained constant for the duration of the test. An average dBm of 20 was recorded for the duration of the test. The dBc value was five and very stable, which indicated a well-lubricated bearing.

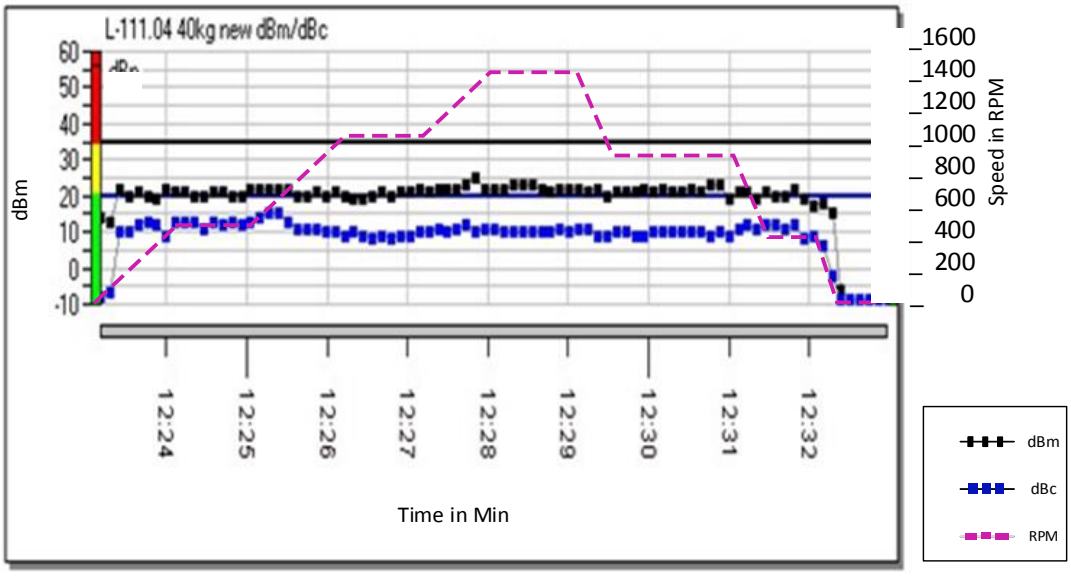

Figure 4.19 dBm values with 40 kg load and speed variation

4.6.1.4 Test Four

In this experiment, the load was kept at 60 kg and the speed was varied between 0 rpm and 1500 rpm. In Figure 4.20, the dBm value stabilised at 200 rpm and remained constant for the duration of the test. An average dBm of 20 was recorded for the duration of the test. The dBc value was eight and very stable, which indicated a well-lubricated bearing.

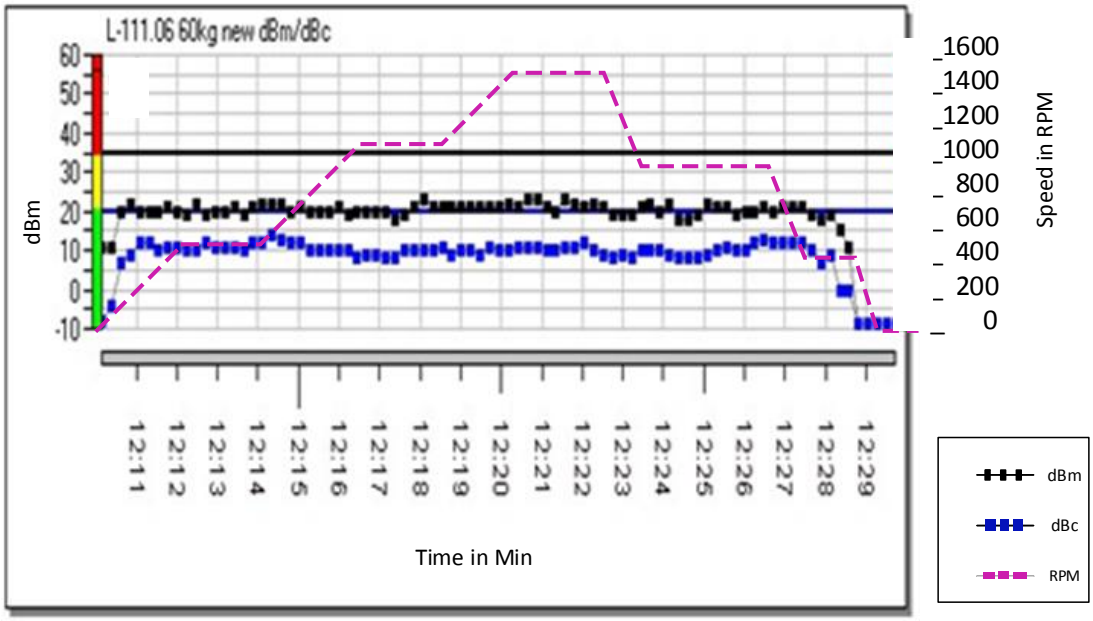

Figure 4.20 dBm values with 60 kg load and speed variation

4.6.1.5 Test five

In this experiment, the load was kept at 80 kg and the speed was varied between 0 rpm and 1500 rpm. In Figure 4.21, the dBm value stabilised at 200 rpm and remained constant for the duration of the test. An average dBm of 20 was recorded for the duration of the test. The dBc value was 10 and stable, which indicated a well-lubricated bearing.

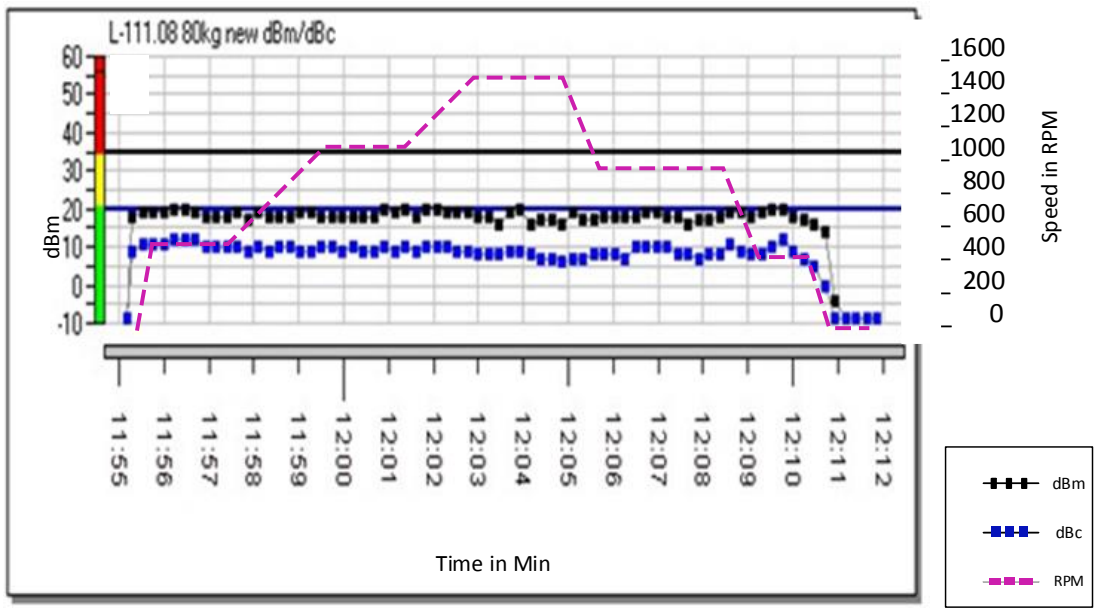

Figure 4.21 dBm values with 80 kg load and speed variation

4.6.1.6 Test six

In this experiment, the load was kept at 100 kg and the speed was varied between 0 rpm and 1500 rpm. In Figure 4.22, the dBm value stabilised at 200 rpm and remained constant for the duration of the test. An average dBm of 20 was recorded for the duration of the test. The dBc value was 10 and stable, which indicated a well-lubricated bearing.

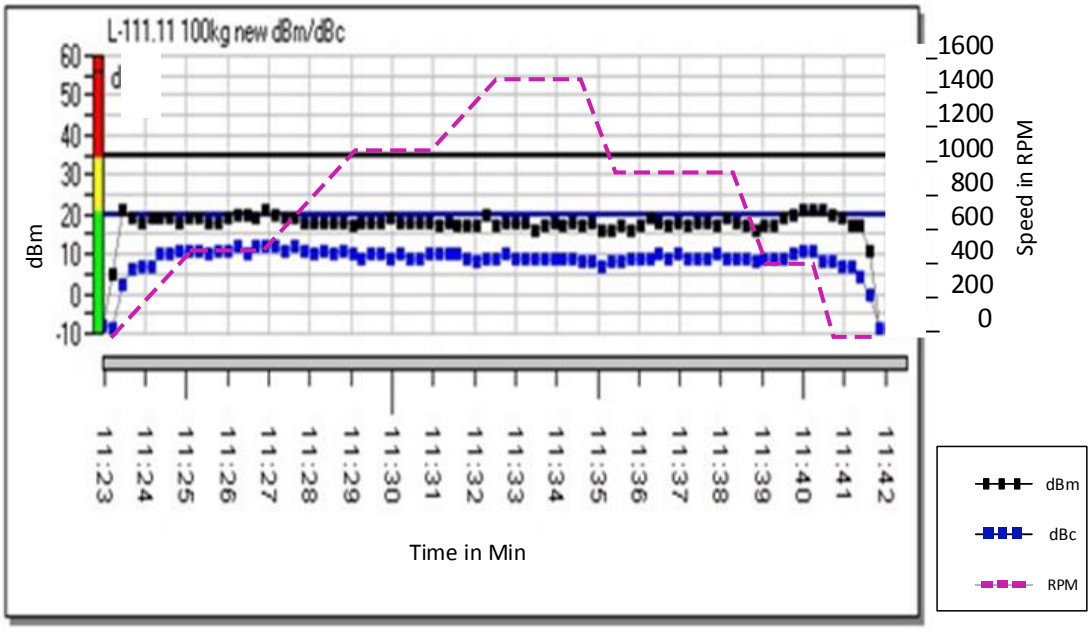

Figure 4.22 dBm values with 100 kg load and speed variation

4.6.1.7 Discussion of results in Section 4.6.1.1 to Section 4.6.1.6

The graph in Figure 4.23 below represents a combination of the above six graphs as displayed in Figures 4.17 to 4.22. In Figure 4.23, test one with no load condition gave values that were not similar to the other test performed. The load change from zero to 20 kg in test two, resulted in a change of 7 dBm. The load change from 20 kg in test two to 100 kg in test six, resulted in a change of 3 dBm. A dBm with a difference of 3 dBm is very small for a load change of 80 kg. The dBm severity rating only changes from a potential fault in a bearing to an actual fault in a bearing once there is a change 15 dBm. See specifications in Section 3. Any fluctuation below that can still render a bearing in an acceptable condition. This indicates that the normalised shock pulse value of a bearing under load can undergo load changes while recording the normalised shock value. The dBc values in Figures 4.17 to Figure 4.22 represent the condition of the bearing roller surface, and this value was used as a control method to ensure that the lubrication was constant at all times.

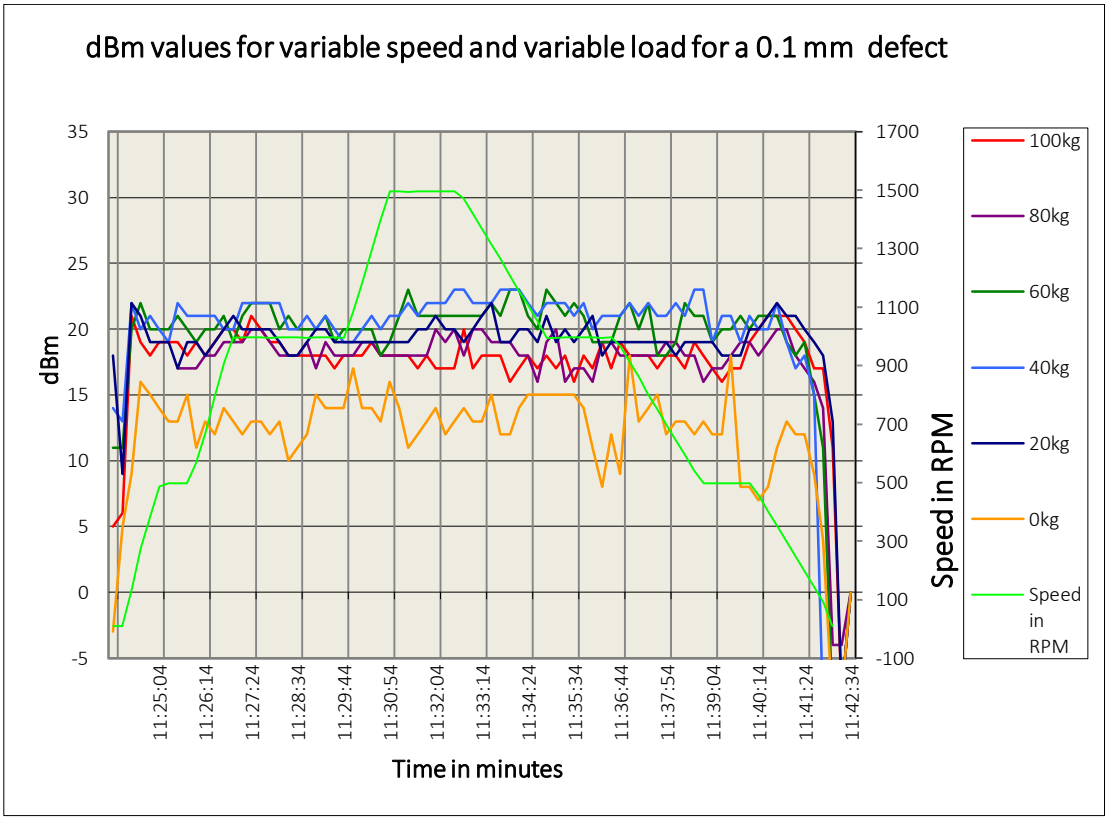

Fig 4.23 dBm values for variable speed and variable load conditions

4.6.2 Experimental results of bearing with 0.2 mm defect

In this section, six tests on a bearing with 0.2 mm defect were performed. With the start of each new test the applied loads were increased by 20 kg. The first test started at 0 kg and the last test ended with an applied load of 100 kg. During each test the motor speed was increased from 0 rpm to 1500 rpm and back to 0 rpm. During each test the dBm values were recorded. This was done to determine if the dBm value would stay constant irrespective of the speed and load changes. The tests were carried out under controlled conditions as discussed in Chapter 3. In each test, there are three graphs displayed, see Figures 4.24 to 4.29. The bottom graph in pink displays the speed of rotation of the bearing, the blue graph displays dBc values and the black graph displays the dBm. Each reading was taken at a respective speed as indicated in the bottom speed graph.

4.6.2.1 Test one

In this experiment, the no load was applied and the speed was varied between 0 rpm and 1500 rpm. In Figure 4.24 the dBm value stabilised at 200 rpm and remained constant for the duration of the acceleration cycle. The recorded results indicated an average of 20 dBm as seen in Appendix 4. The dBm value fluctuated in the deceleration stage. This fluctuation in the dBm value was caused by the changing thrust loads in the bearing during deceleration. The dBc value was 10 and very stable, which indicated a well-lubricated bearing.

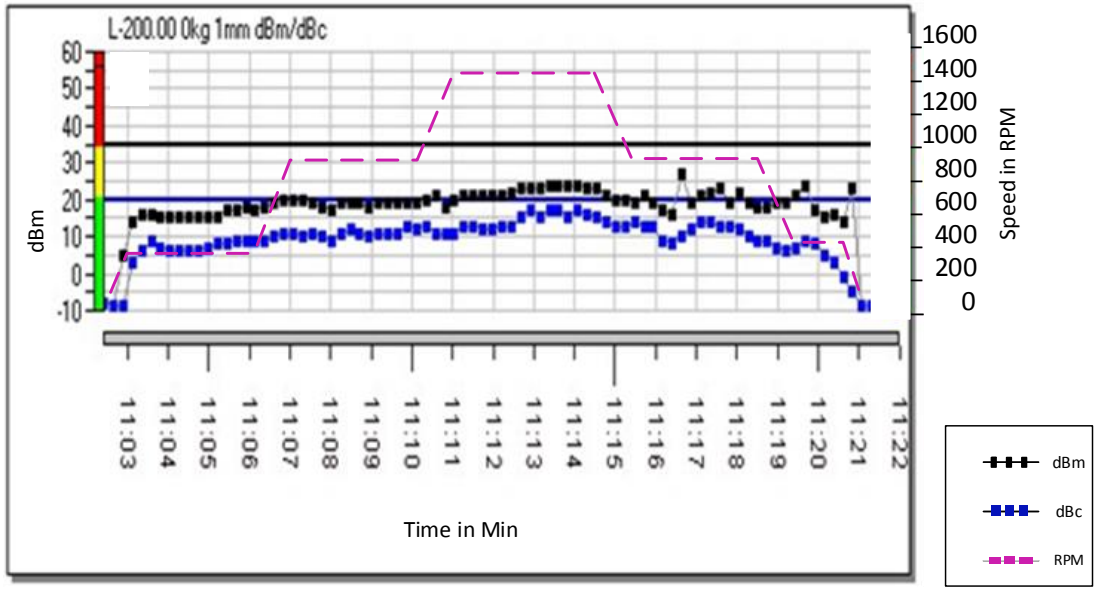

Figure 4.24 dBm values with no load and speed variation

4.6.2.2 Test two

In this experiment the load was kept at 20 kg and the speed was varied between 0 rpm and 1500 rpm. In Figure 4.25, the dBm value stabilised at 200 rpm and remained constant for the duration of the test. An average dBm of 22 was calculated from the test data as indicated in Appendix 5. Some peaks are evident in the dBm graph. This was attributed to the larger cavity in the bearing. The dBc value was 10 and very stable, which indicated a well-lubricated bearing.

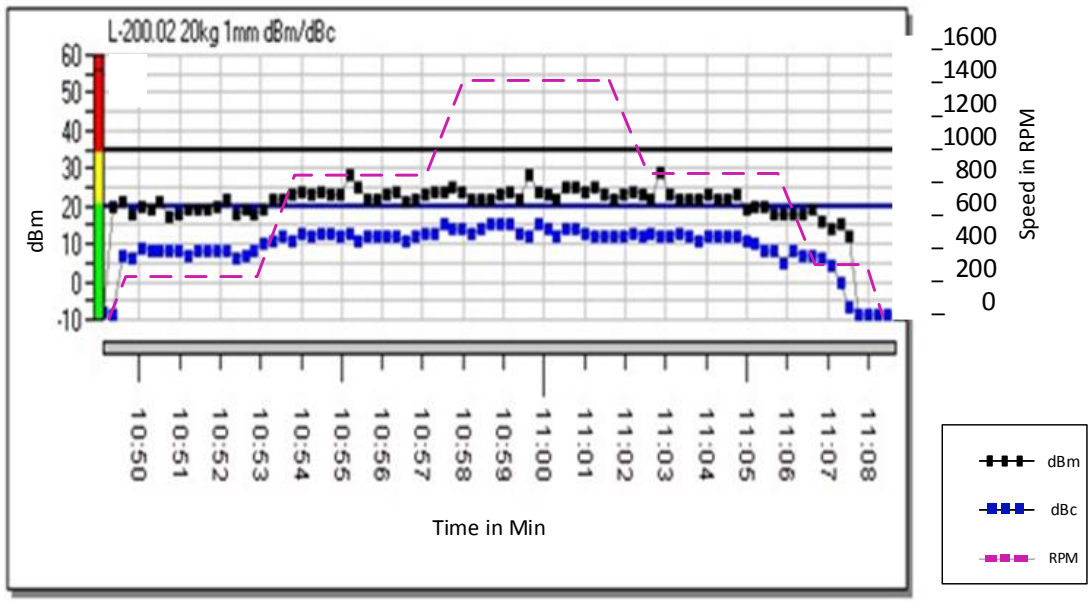

Figure 4.25 dBm values with 20 kg load and speed variation

4.6.2.3 Test three

In this experiment, the load was kept at 40 kg and the speed was varied between 0 rpm and 1500 rpm. In Figure 4.26, the dBm value stabilised at 200 rpm and remained constant for the duration of the test. An average dBm of 24 was calculated from the test data as indicated in Appendix 5. Some peaks are evident in the dBm graph. This was attributed to the larger cavity in the bearing. The dBc value was 12 and stable, which indicated a well-lubricated bearing.

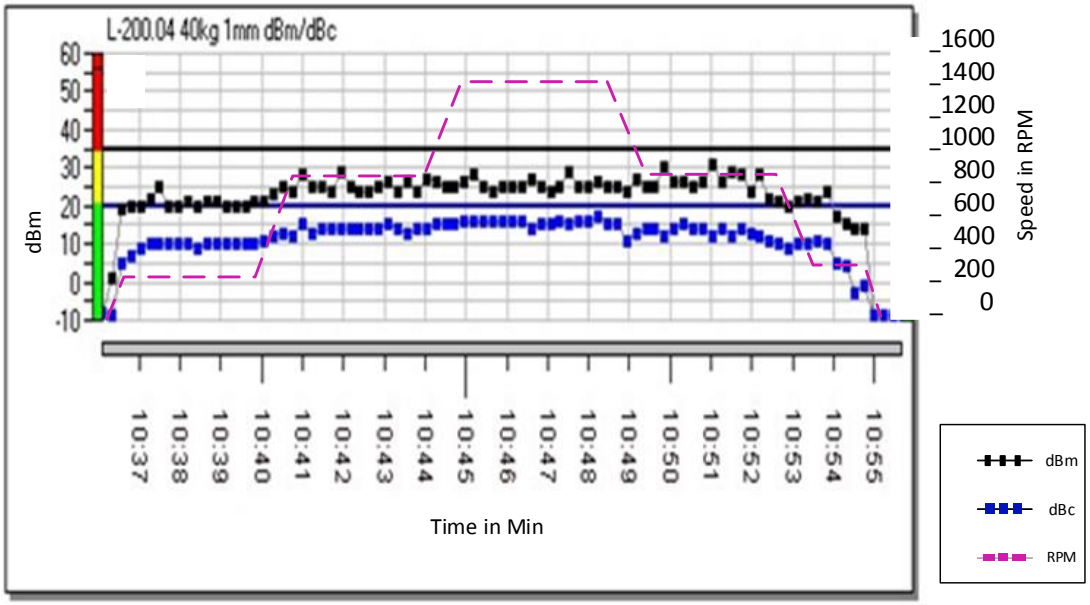

Figure 4.26 dBm values with 40 kg load and speed variation

4.6.2.4 Test four

In this experiment, the load was kept at 60 kg and the speed was varied between 0 rpm and 1500 rpm. In Figure 4.27, the dBm value stabilised at 200 rpm and remained constant for the duration of the test. An average dBm of 26 as calculated from the test data as seen in Appendix 5. Some peaks are evident in the dBm graph. This was attributed to the larger cavity in the bearing. The dBc value was 15 and stable, which indicated a well-lubricated bearing.

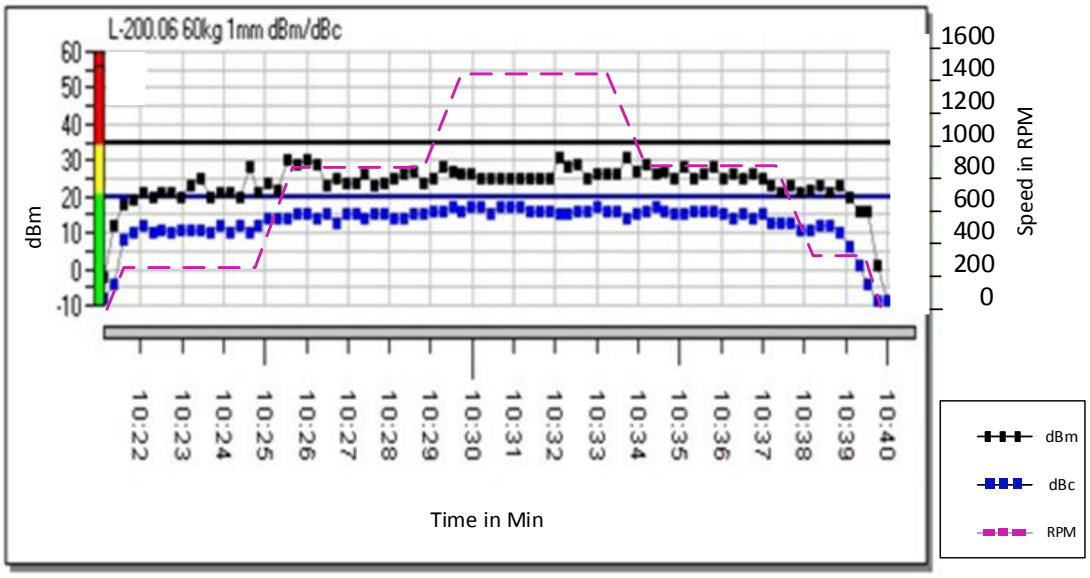

Figure 4.27 dBm values with 60 kg load and speed variation

4.6.2.5 Test five

In this experiment, the load was kept at 80 kg and the speed was varied between 0 rpm and 1500 rpm. In Figure 4.28, the dBm value stabilised at 200 rpm and remained constant for the duration of the test. An average dBm of 24 calculated from the test data as seen in Appendix 5. Some peaks are evident in the dBm graph. This was attributed to the larger cavity in the bearing. The dBc value was 15 and stable, which indicated a well-lubricated bearing.

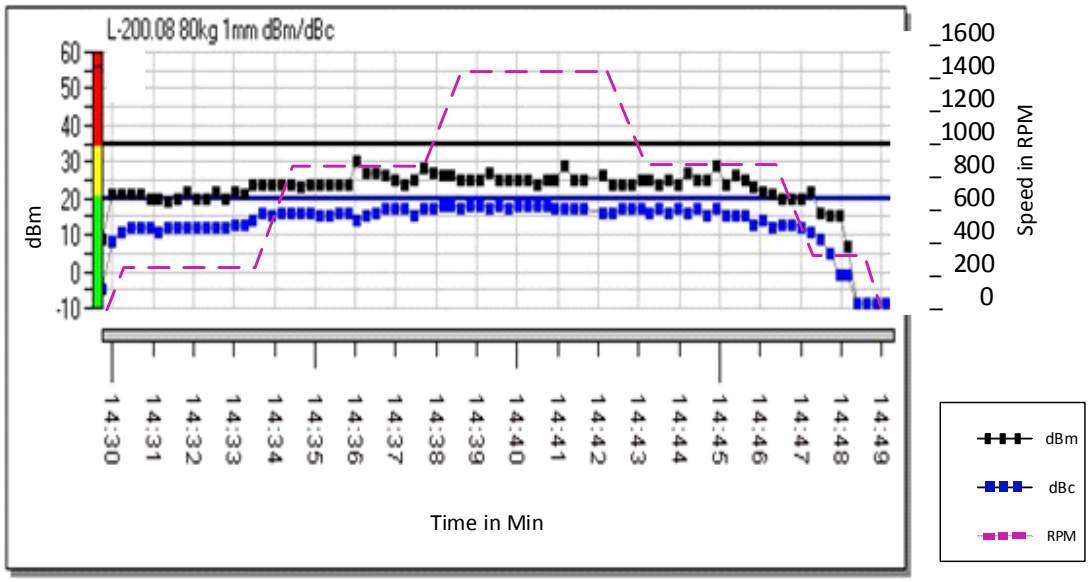

Figure 4.28 dBm values with 80 kg load and speed variation

4.6.2.6 Test six

In this experiment, the load was kept at 100 kg and the speed was varied between 0 rpm and 1500 rpm. In Figure 4.29, the dBm value stabilised at 200 rpm and remained constant for the duration of the test. An average dBm of 24 was calculated from the test data as seen in Appendix 5. Some peaks are evident in the dBm graph. This was attributed to the larger cavity in the bearing. The dBc value was 10 and very stable, which indicated a well-lubricated bearing.

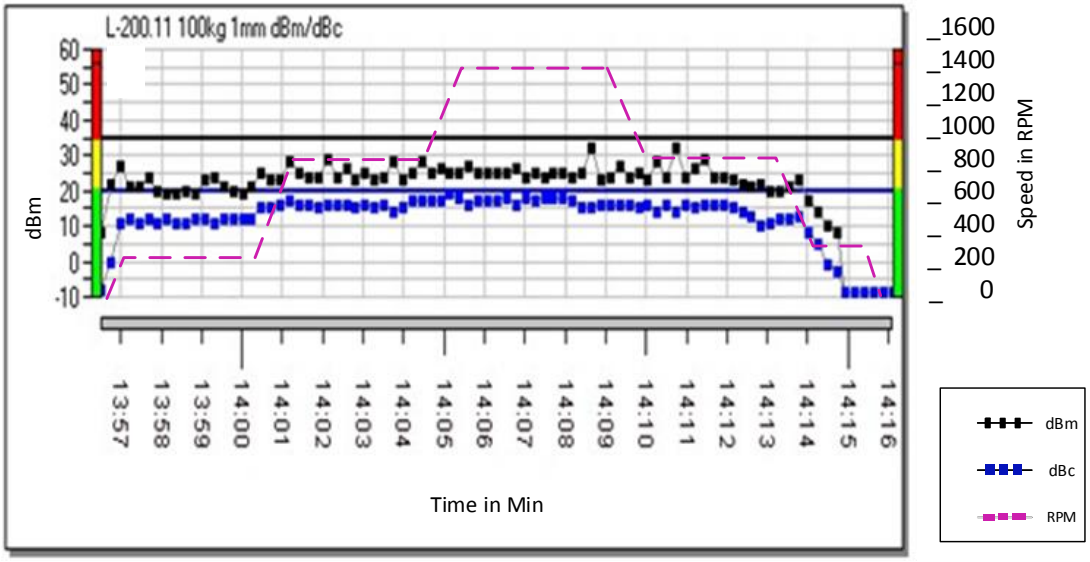

Figure 4.29 dBm values with 100 kg load and speed variation

4.6.2.7 Discussion of results in Sections 4.6.2.1 to 4.6.2.6

The graph in Figure 4.30 below represents a combination of the above six graphs as displayed in Figures 4.24 to 4.29. In Figure 4.30, it was evident that a 0 kg to 20 kg changed in load caused a change of 5dBm. However, a 20 kg to 100 kg change in load caused change of 3 dBm. A value of 3 dBm is small for a load change of 80 kg. The dBc, which represents the condition of the bearing raceway surface, shows that the lubrication during the test is adequate.

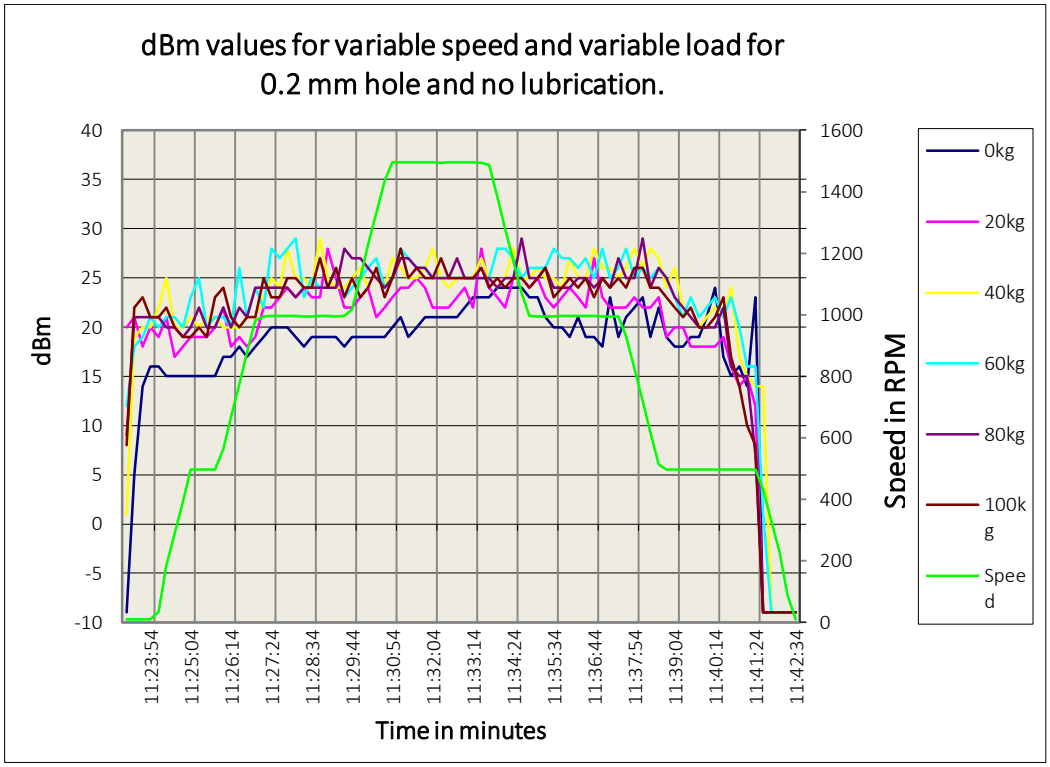

Fig 4.30 Measured dBm values of a damaged bearing for variable speed and load

4.6.3 Conclusion

From the two graphs, one for the 0.1 mm defect in Figure 4.23 and other for the 0.2 mm defect in Figure 4.30, it was clear that the 0.2mm defect bearing gave similar shock values throughout the test. The results for the various loads and speed gave a constant pattern throughout the test, with slight increase in shock values as the load increased and the speed increased.

The 0.2 mm defect bearing had a slightly more erratic dBm graph, and it could be speculated that it is due to the larger cavity, but it was not required to be proven by these research.

The graph in Figure 4.30 gives a clear indication that for a damaged bearing the dBm value for bearing with mass load of 20kg gives very similar values as that of an 80kg load bearing. The no load condition value are much lower and more erratic, which will always be the case due to the no load conditions that cause looseness in bearings.

CHAPTER 5: DISCUSSION OF RESULTS

5.1

It was shown in Section 4.2 of this thesis that the dBsv measured over time could not be used to monitor the condition of the bearing under variable speed applications. This was because the dBsv changed as the speed increased, as seen in Figure 4.1, Section 4.2.

It was further shown in this section that if the dBi value is calculated for the bearing using Equation 3.16 in Section 3.2 the dBm value could be obtained by subtracting the dBi value from the dBsv value, as shown by Equation 3.17 in Section 3.2. of this thesis. The resultant graph of the dBm values is presented in Figure 4.1. of this thesis stayed constant for the duration of the test and this allowed the condition of the bearing to be measured under variable speed conditions. This implied that the dBm value could be used to monitor the condition of a bearing under various acceleration and deceleration conditions.

5.2

In Sections 4.3 to 4.6 of this thesis, the dBm value was determined in various tests to monitor the condition of a bearing. The dBm values were constant and in one area of the acceleration phases, but during the deceleration phases, they were erratic and scattered. These erratic conditions could be seen in Section 4.4.1, Figures 4.7 to 4.9, Section 4.6.1, Figures 4.17 to 4.22, and in Section 4.6.2, Figures 4.24 to 4.29. This phenomenon occurred in the bearings due to looseness in the bearings, caused by changing thrust loads during deceleration. Erratic results in the dBm values were also experienced at very low speeds. Only once the 200 rpm speed was passed did the dBm values stabilise. This is due to the centrifugal forces in bearings that are too weak to induce any shock value. Once the dynamic forces increase, the lubrication moves into the hydrostatic mode, and the rolling elements in the bearing become static and the erratic results stabilise (Barkov *et al.* 1997; Smith, 1993). Thus, only the result from 200 rpm and higher was considered. It was concluded that the dBm value recorded the best results only when the machine is accelerating and it is near the maximum acceleration period, or when the machine reached maximum

speed of 1500 rpm. The dBm did fluctuate during the speed range from 200 rpm to 1500 rpm. The value was 4 dBm and this was minimal, and therefore, it was concluded that irrespective of the roller bearing speed and acceleration period, the dBm stayed constant.

5.3

In section 4.6.1.1, the dBm value was measured while the applied load was varied. There were two exceptions in the monitoring period that gave poor results. The first being under no-load conditions the overall value was 6 dBm lower than with any load, see Figure 4.17 Section 4.6.1.1 compared to Figure 4.18 Section 4.6.1.1. The results were, therefore, not a true reflection of the bearing condition. Therefore, the dBm cannot be used to measure the condition of bearing under no-load conditions. The load increase from 20 kg to 100 kg, only gave an increase of 3 dB, and this was not a large difference. Small loads would then only change the dB value slightly. The second exception was when the speed was below 200 rpm. In this stage of the run cycle, the centrifugal forces within the bearing are not big enough to induce centrifugal loading on the bearing roller surface. This was evident in all the graphs. It can be concluded that the operating condition of the bearing could be recorded if there is a load on the bearing and the load only changes in small increments of load.

5.4

In Section 4.6.1, tests were performed at varying speeds and loads on a bearing with 0.1 mm defect on the raceway. These results were different from those performed on individual load and speed tests as seen in Sections 4.3, 4.4 and 4.5. During the variable speed cycle, Section 4.3, the dBm difference was 3 dB as seen in Figure 4.6. During the variable load cycle, Section 4.5 the dBm difference was 6 dB, as seen in Figure 4.16. During the combined variable speed and load tests in Figure 4.23 only gave a reading difference of 3 dB and this was an unexpected value.

5.5

The dBm measured over time was proven successful in providing diagnostic information of bearing conditions during variable speed and load. To prove this, a second test was performed on a bearing with a 0.2 mm defect on the bearing raceway. From the tests as seen in Section 4.6.2 it was clear that the 0.2 mm defected bearing resulted in higher shock values than the results as seen in Section 4.6.1. of a 0.1 mm defect.

CHAPTER 6 : CONCLUSION

Shock pulse monitoring was applied under variable speed and variable load conditions and the mechanical shock values in dBsv and dBm were measured, as stated in the objectives.

The following conclusions were obtained from re-occurring results:

- The first objective was to determine the response of dBsv, measured over time and how this measurement would provide diagnostic information of the condition of the bearing. It was found that the dBsv measured over time could not be used to monitor the condition of the bearing under variable speed applications because the dBsv varied as the speed was increased.

- The second objective was to determine how the dBn, measured over time, will provide diagnostic information of bearing conditions during acceleration and deceleration. It was found that the dBn trended over time could be used to determine the condition of a bearing when accelerating but could not determine the condition of the bearing during deceleration because the centrifugal forces in bearings during deceleration are too weak to induce constant shock values and this affected the results.

- The third objective was to determine how the dBm, measured over time, will provide diagnostic information of bearing conditions when the applied load is varied. It was found that the dBm measured over time could be used to determine the condition of the bearing when the applied load was varied. Under no-load conditions the components in the bearing induced no shock values because the centrifugal forces in bearings are too weak during deceleration and this affected the results.

- The fourth objective was to determine how, the dBm, measured over time, will provide diagnostic information of the bearing conditions, during variable speed and varying load conditions. It was found that the dBm measured over time could provide diagnostic information of bearing conditions during variable speed and load conditions.

Finally, the dBm value can be used under variable speed and load conditions but the dBm value should be measured over time and not be used as once-off values.

It was observed that that varying speeds and loads had no influence on the dBm value, and thus it would be possible to measure the condition of the bearings if the abovementioned conditions are applied.

The results also indicated that the larger the defect on the bearing raceway, the higher the dBm values were. Multipil defects on the bearing race ways were not part of this thesis and this gives an opertunity for futher research.

In conclusion, this research results obtained here demonstrated that SPM can be used to monitor the condition of bearings. Monitoring is however limited to the acceleration stage of the machine.

BIBLIOGRAPHY

ALFREDSON, R.J. & MATHEW, M.I.E. October 1985. Time domain methods for monitoring the condition of rolling element bearings. *Institution of Engineers*, ME10(2):102-107.

ANON. 1984. Holiday detection of internal tubular coatings of less than 10 mils (0.25MM) dry film thickness. *Materials Performance*, 23(10):52-55.

AZOVTSEV, A.Y., BARKOV, V. & CARTER, D.L. 1996. Improving the accuracy of rolling element bearing condition assessment. [Online]. Available: <http://www.vibrotek.com/article.php?article=articles/abcvi96/ abcvi96.htm>.

BALDERSTON, H.L. 1969. The detection of incipient failure in bearings. *Material Evaluation*, 27:121-128.

BARKOV, A., BARKOVA, N. & AZOVTSEV, A. 1997. Peculiarities of slow rotating rolling element bearings condition diagnostics. [Online]. Available: <http://www.vibrotek.com/articles/slowbear/index.htm>.

BARKOV, A.V. 1998. The capabilities of the new generation of the monitoring and diagnostic systems. [Online] Available at: <http://www.vibrotek.com/articles/metal-e/index.htm>.

BARTHEL, K. 1977. Shock pulse method for measuring the condition of antifriction bearings. *Tappi*, 60(8):111-113.

BISBEE, G.A. 1994. Why do motor shafts and bearings fail? *Tappi Journal*, 77(9):251-252.

BLOCH, H.P. 2000. Use shock pulse methods to monitor bearings. [Online]. Available: <http://www.ludeca.com/casestudy/shockpulse.pdf>.

BLOUGH, J.R. 2003. Development and analysis of Time Variant Discrete Fourier transform order tracking. *Mechanical Systems and Signal Processing*, 17(6):1185-1199.

BOTO, P.A. 1971. Detection of bearing damage by shock pulse measurements. *The Ball Bearing Journal*, 167.

BRAUN, S. 1975. Signal analysis for rotating machinery vibrations. *Pattern Recognition*, 7:81-86.

BROWN, P.J. 1977. Condition monitoring of rolling element bearings. *Noise Control Vibration and Insulation*, 8(2):41-44.

BURCHILL, R.F., FRAREY, J.L. & WILSON, D.S. 1973. New machinery health diagnostic techniques using high-frequency vibration. *In* National Aerospace Engineering and Manufacturing Meeting, Los Angeles, California, 16-18 October. Society of Automotive Engineers.

BUTLER, D.E. 1973. The shock-pulse method for the detection of damaged rolling bearings. *Non-destructive Testing*, 6(2):92-95.

COLLACOTT, R.A. 1979. *Vibration monitoring and diagnosis*. New York: Wiley.

DAADBIN, A., WONG, J.C.H. 1990. Different vibration monitoring techniques and their application to rolling element bearings. *International Journal of Mechanical Engineering Education*, 19(4):295-305.

DYER, D. & STEWART, R.M. 1978. Detection of rolling element bearing damage by statistical vibration analysis. *Journal of Mechanical Design*, 100:229-235.

ELBESTAWI, M.A. & TAIT, H.J. 1985. A comparative study of vibration monitoring techniques for rolling element bearings. Mechanical Research Division: 1510-1517. Toronto. Canada.

ENGJA, H., RASMUSSEN, M. & LIPPE, J. 1977. Vibration analysis used for detection of roller bearing failures. *Norwegian Maritime Research*, 3:23-33.

GABERSON, H.A. 2002.The use of wavelets for analyzing transient machinery vibration. *Sound and Vibration*, 2002:12-17.

GLEW, C.A.W. 1974. Effectiveness of vibration analysis as a maintenance tool.*The Institute of Marine Engineers*, 86:29-51.

GLUZMAN, D. 2001. Recognizing impending bearing failure. *Reliability Magazine*, 2001:41-47.

HERON, R. 1985. Condition monitoring as a production tool. The Chartered Mechanical Engineer: The Journal of the Institute of Mechanical Engineers, 32(32):21-23.

IGARASHI, T., HAMADA, H. 1982. Studies on the vibration and sound of defective rolling bearings. *In* Vibration of ball bearings with one defect. *The Japan Society of Mechanical Engineers*, 25(204):994-1001.

KOELLNER, W. 2006. A new all AC gearless drive system for large mining draglines.IEEE.[Online].Available<http://ieeexplore.ieee.org/xpl/articleDetails.jsp?tp=&arnumber=4025387&queryText%3Da+new+all+ac+gearless+drive+system+for+large>.

KUHNELL, B.T. 1985. Correlation of vibration, wear debris analysis and oil analysis. *Maintenance Management International*, 5:105-115.

LI, B., MO-YUEN, C. & YODYIUM, T. 2000.Neural-Network-Based motor rolling bearing fault diagnosis. *Industrial electronics.* [Online] ws. 47(5):1060-1069. Available: <http://ieeexplore.ieee.org/xpl/articleDetails.jsp?tp=&arnumber=873214&matchBoolean%3Dtrue%26searchField%3DSearch_All%26queryText%3D%28p_Title%3Aneural-network-based+motor+rolling+bearing+fault+diagnosis%29>.

LIU, B., LING, S.F. & GRIBONVAL, R. 2001. Bearing failure detection using matching pursuit. NDT&E International. [Online] ws. 35:255-262. Available: <http://www.sciencedirect.com/science/article/pii/S0963869501000639>.

LIU, Y., CHEN, K.X. & ZHANG, S. 1991. Early detection of gearbox fault using frequency demodulation. *In* Proceedings of the 3rd International Machine Monitoring and Diagnostics Conference. Society for Experimental Mechanics, Bethel:72-76.

LOU, X. & LOPARO, K.A. 2003. Bearing fault diagnosis based on wavelet transform and fuzzy inference. *Mechanical Systems and Signal Processing*. [Online]ws.Available: <http://www.sciencedirect.com/science/article/pii/S0888327003000773>.

LOU, X., LOPARO, K.A., DISCENZO, F.M., YOO, J. & TWAROWSKI, A. 2002. A wavelet-based technique for bearing diagnostics. Rockwell Science Center. N00014-98-3-0012

LYON, D., SHERRARD, J. & SHERMAN, P. 2000. Justification for software-based order tracking an an integral component of an innovative predictive maintenance program. *PPM Technology*.

MARTINS, L.G. & GERGES, S.N.Y. 1984. Comparison between signal analysis for detecting incipient bearing damage. *In* International Condition Monitoring Conference. 1984:191-204. Swansea.

MCFADDEN, P.D. & SMITH, J.D. 1984. Model for the vibration produced by a single point defect in a rolling element bearing. *Journal of Sound and Vibration*, 96(1):69-82.

MCFADDEN, P.D. & SMITH, J.D. 1985. The vibration produced by multiple point defects in a rolling element bearing. *Journal of Sound and Vibration*, 98(2):263-273.

MCLAIN, D.A. & HARTMAN, D.L. 1980. Analysis of defective anti-friction bearings in the paper industry. *Tappi*, Winter.

MIYACHI, T., SEKI, K. 1986. An investigation of the early detection of defects in ball bearings using vibration monitoring: practical limit of detectability and growth speed of defects. *In* Proceedings of the International Conference on Rotordynamics, Tokyo, 14-17 September. IFTOMM: 403-408, 1986.

MONK, R. 1972. Vibration measurement gives early warning of mechanical faults. *Processing Engineering*, 53:135-137.

MORANDO, L.E. 1988. Measuring shock pulses is ideal for bearing condition monitoring. *Pulp & Paper,* 62(12):96-98.

MORANDO, L.E. 1996. Technology overview: shock pulse method. *In* Technology showcase: integrated monitoring, diagnostics and failure prevention. *In* Proceedings of a joint Conference, Mobile, DTIC: 1-10, Alabama.

MORI, K., KASASHIMA, N., YOSHIOKA, T. & UENO, Y. 1996. Prediction of spalling on a ball bearing by applying discrete wavelet transform to vibration signals. *Wear*, 195:162-168.

NAHRATH, T., BAUER, B. & SEELIGER, A. Vibration monitoring at unstable speeds. 1999. *In* International congress on condition monitoring and diagnostic engineering management. Coxmoor: 555-562
NEVILLE, W.E. 1979. Cost effective condition monitoring. *In* Symposium on availability and reliability. 1978. The Institution of Engineers, Sydney. Australia.

OSUAGWU, C.C. & THOMAS, D.W. 1982. Effect of inter-modulation and Quasi-periodic instability in the diagnosis of rolling element incipient defect. *Journal of Mechanical Design*, 104(2):296-302.

PAYA, B.A., ESAT, I.I. & BADI, M.N.M. 1997. Artificial neural network based fault diagnostics of rotating machinery using wavelet transforms as a preprocessor. *Mechanical Systems and Signal Processing*, 11(5):751-765.

PENG, Z.K. & CHU, F.L. 2004. Application of the wavelet transform in machine condition monitoring and fault diagnostics: a review with bibliography. *Mechanical Systems and Signal Processing*, 18(2):199-22.

PRABHAKAR, S., MOHANTY, A.R. & SEKHAR, A.S. 2002. Application of discrete wavelet transform for detection of ball bearing race faults. *Tribology International*, 35(12):793-800.

PRASHAD, H., GHOSH, M. & BISWAS, S. 1985. Diagnostic monitoring of rolling-element bearings by high-frequency resonance technique. *ASLE Transactions*, 28(4): 439-448.

QIAN, S. 2003. Gabor expansion for order tracking. *Sound and Vibration Journal*, 37(6):18-22.

RAI, V.K. & MOHANTY, A.R. 2007. Bearing fault diagnosis using FFT of intrinsic mode functions in Hilbert-Haung transform. *Mechanical Systems and Signal Processing.* [Online] ws*.* 21:2607-2615. Available:

<http://www.sciencedirect.com/science/article/pii/S0888327006002846>.
RANDALL, R.B. 2007. Handbook of noise and vibration control.

RANDALL, R.B. & ANTONI, J. 2011. Rolling element bearing diagnostics – a tutorial. Mechanical systems and signal processing. [Online] ws. 25: 485-520. Available<http://www.sciencedirect.com/science/article/pii/S0888327010002530>.

RAY, A.G. 1980. Monitoring rolling contact bearings under adverse conditions. *Institute of Mechanical Engineers,* 279:187-194.

RUSH, A.A. 1979. Kurtosis: a crystal ball for maintenance engineers. *Iron and Steel International*, 55:24-27.

SCHNEIDER, S.D. SEELIGER, A., MARTIN, W. & MACKEL, J. 2000. Analysis of oscillation bearings in universal joint shafts. *In* Proceedings of the International Conference on Quality Reliability and Maintenance. Professional Engineering Publishing: 175-178.

SCHOEN, R.R., HABETLER, T.G., KAMRAN, F. & BARTHELD, R.G. 1995. Motor bearing damage detection using stator current monitoring. IEEE. [Online] ws.31(6):1274-1279.Available: <http://ieeexplore.ieee.org/xpl/articleDetails.jsp?tp=&arnumber=345491&queryText%3Dmotor+bearing+damage+detection+using+stator+current>.

SEKER, S. & AYAZ, E. 2003. Feature extraction related to bearing damage in electric motors by wavelet analysis. *Journal of the Franklin Institute*. [Online] ws.340:125-134.Available: <http://www.sciencedirect.com/science/article/pii/S0016003203000152>

SHAWKI, G.S. 1979. Optinum grease quantity for roller bearing lubrication. *Tribology International*, 12(1):21-24.

SHIROISHI, J., LI, Y., LIANG, S., KURFESS, T. & DANYLUK, S. 1997. Bearing condition diagnostics via vibration and acoustic emission measurements. *Mechanical Systems and Signal Processing,* 11(5):693-705.

SMITH, J.D. 1993. A new diagnostic technique for asperity contact. *Tribology International*, 26(1):25-27.

SOHOEL, E.O. 1971. Method and arrangement for determining the mechanical state of machines. (US patent 3,554,012).

SOHOEL, E.O. 1984. Shock pulses as a measure of the lubricant film thickness in rolling element bearings. *In* Proceedings of an international conference on condition monitoring held at University College of Swansea, 10-13 April, 1984.

SOHOEL, E.O 1994. A complete set of tools for evaluating the running condition of operating rolling element bearings. (SPM Method August 1994). Sweden.

SPANJAARD, J.M., ELTON, S.D. 1996.Variable shaft rate estimation and the analysis of non-stationary signals from rotating machinery. *In* International Symposium on Signal Processing and its Applications. 1996. Organised by the Signal Processing Research Centre, QUT, Brisbane. Australia.

STACK, J.R., HABETLER, T.G. & HARLEY, R.G. 2004. Fault classification and fault signature production for rolling element bearings in electric machines. IEEE.[Online]ws.40(3):735-739.Available: <http://ieeexplore.ieee.org/xpl/articleDetails.jsp?tp=&arnumber=1300726&queryText%3Dfault+classification+and+fault+signature+production+for+rolling+element>.

STRONACH, A.F., CUDWORTH, C.J. & JOHNSTON, A.B. 1984. Condition monitoring of rolling element bearings. *In* International Condition Monitoring Conference. 1984:162-177. Swansea.

TANDON, N. & CHOUDHURY, A. 1999. A review of vibration and acoustic measurement methods for the detection of defects in rolling element bearings. *Tribology International*. [Online] ws. 32(8):469-480, Aug. Available: <http://www.sciencedirect.com/science/article/pii/S0301679X99000778>.

TANDON, N. & NAKRA, B.C. 1992. Comparison of vibration and acoustic measurement techniques for the condition monitoring of rolling element bearings. *Tribology International*, 25(3):205-212.

TAYLOR, J.I. 1980. Identification of bearing defects by spectral analysis. *American Society of Mechanical Engineers*, 102:199-204.

TAYLOR, J.I. & KIRKLAND, D.W. 2004. The bearing analysis handbook: a practical guide for solving vibration problems in bearings. USA: VCI. American Society of Mechanical Engineers, 92:100-154.

THORSEN, O.V. & DALVA, M. 1998. Methods of condition monitoring and fault diagnosis for induction motors. *ETEP*, 8(5):383-395.

THORSEN, O.V. & DALVA, M. 1999. Failure identification and analysis for high-voltage induction motors in the petrochemical industry. IEEE. [Online] ws.35(4):810-818.Available: <http://ieeexplore.ieee.org/xpl/articleDetails.jsp?tp=&arnumber=732309&queryText%3Dfailure+identification+and+analysis+for+high-voltage+induction+motors>

VOLD, H., MAINS, M. & BLOUGH, J. 1997. Theoretical foundations for high performance order tracking with the Vold-Kalman tracking filter. *SAE International*, 97NV164.

WEICHBRODT, B. & BOWDEN, J. 1970. Instrumentation for predicting bearing damage. *In* General Electric Co Schenectady NY Research and Development Center. DTIC.

WU, J.D., HUANG, C.W. & HUANG, R. 2004. An application of a recursive Kalman filtering algorithm in rotating machinery fault diagnosis.*NDT and E International*, 37(5):411-419.

ZHEN, L., ZHENGJIA, H., YANYANG, Z. & XUEFENG, C. 2008. Bearing conditioning monitoring based on shock pulse method and improved redundant lifting scheme. [Online] ws. 79:318-338. Available: <http://www.sciencedirect.com/science/article/pii/S0378475408000037>.

APPENDIX 1

Table 1

Experimental data captured and presented in Figure 4.1

Readings	dBm	dBsv	RPM	Time intervals
1	-9	-37.923314	10	15:37:00
2	-9	-37.923314	10	15:36:46
3	-9	-37.923314	10	15:36:32
4	-9	-37.923314	10	15:36:18
5	-9	-37.923314	10	15:36:04
6	7	-2.838464	90	15:35:50
7	21	18.0537474	199	15:35:36
8	20	20.6768247	302	15:35:22
9	23	26.268574	407	15:35:08
10	22	26.9863194	496	15:34:54
11	23	27.9863194	496	15:34:40
12	23	27.9863194	496	15:34:26
13	23	27.9863194	496	15:34:12
14	22	27.627511	534	15:33:58
15	22	29.186703	639	15:33:44
16	20	28.5081446	744	15:33:30
17	19	28.6446029	848	15:33:16
18	19	29.6585439	953	15:33:02
19	19	30.0331475	995	15:32:48
20	19	30.0331475	995	15:32:34
21	19	30.0418726	996	15:32:20
22	19	30.0418726	996	15:32:06
23	21	32.0244135	994	15:31:52
24	21	32.0331475	995	15:31:38
25	21	32.0331475	995	15:31:24
26	21	32.0331475	995	15:31:10
27	21	32.0331475	995	15:30:56

28	22	33.0418726	996	15:30:42
29	22	33.0418726	996	15:30:28
30	21	32.0156708	993	15:30:14
31	21	32.3670966	1034	15:30:00
32	21	33.2071603	1139	15:29:46
33	22	34.9730935	1244	15:29:32
34	22	35.6704837	1348	15:29:18
35	23	37.3219981	1453	15:29:04
36	22	36.5695097	1495	15:28:50
37	23	37.5753177	1496	15:28:36
38	22	36.5695097	1495	15:28:22
39	22	36.5753177	1496	15:28:08
40	22	36.5753177	1496	15:27:54
41	20	34.5636978	1494	15:27:40
42	21	35.5753177	1496	15:27:26
43	22	36.5695097	1495	15:27:12
44	24	38.2680297	1444	15:26:58
45	21	34.9494706	1392	15:26:44
46	21	34.6122974	1339	15:26:30
47	23	36.2682568	1287	15:26:16
48	21	33.9029891	1234	15:26:02
49	20	32.5216838	1181	15:25:48
50	22	34.1382547	1130	15:25:34
51	21	32.7129313	1076	15:25:20
52	21	32.2911632	1025	15:25:06
53	21	32.0331475	995	15:24:52
54	19	30.0418726	996	15:24:38
55	20	31.0418726	996	15:24:24
56	21	32.0244135	994	15:24:10
57	21	32.0331475	995	15:23:56
58	21	32.0331475	995	15:23:42
59	22	33.0331475	995	15:23:28

60	21	32.0418726	996	15:23:14
61	21	31.5945086	946	15:23:00
62	21	30.926768	876	15:22:46
63	21	30.4057648	825	15:22:32
64	20	28.8402757	773	15:22:18
65	22	30.2233358	720	15:22:04
66	21	28.5852082	669	15:21:50
67	21	27.8823891	617	15:21:36
68	21	27.0868538	563	15:21:22
69	22	27.2620851	512	15:21:08
70	20	25.0038136	497	15:20:54
71	19	24.0038136	497	15:20:40
72	18	23.0038136	497	15:20:26
73	17	22.0038136	497	15:20:12
74	17	22.0038136	497	15:19:58
75	17	22.0038136	497	15:19:44
76	19	24.0038136	497	15:19:30
77	18	22.7556285	483	15:19:16
78	19	22.7662313	431	15:19:02
79	20	22.6265219	378	15:18:48
80	22	23.3143531	325	15:18:34
81	23	22.8316971	274	15:18:20
82	22	20.0037453	222	15:18:06
83	23	18.7366081	171	15:17:52
84	25	17.7323933	121	15:17:38
85	14	-14.923314	10	15:17:24
86	6	-22.923314	10	15:17:10
87	-9	-37.923314	10	15:16:55
	21	29.7646	----	Averages

APPENDIX 2

Table 2

Experimental data captured and presented in Figure 4.6

Readings	9MIN	6MIN	3MIN	2MIN	
1	dBm	dBm	dBm	dBm	RPM
2	20	22	22	24	1610
3	22	22	21	19	1540
4	22	21	21	21	1470
5	21	21	20	20	1400
6	22	22	21	20	1330
7	21	21	22	21	1260
8	22	21	22	20	1190
9	21	21	21	20	1120
10	22	22	23	21	1050
11	19	22	21	21	980
12	23	22	21	20	910
13	21	21	21	21	840
14	20	20	21	20	770
15	20	20	20	20	700
16	21	20	20	21	630
17	20	20	21	20	560
18	21	19	21	19	490
19	20	20	22	20	420
20	20	20	20	19	350
21	19	21	21	20	280
22	20	21	20	19	210
23	21	18	21	20	140
24	21	15	23	19	70
25	10	9	20	20	0
	20.4	20	21.1	20.2	Averages

APPENDIX 3

Table 3

Experimental data captured and presented in Figure 4.1

	0kg	20kg	50kg	80kg	Time
Readings	dBm	dBm	dBm	dBm	
1	38	38	44	46	20:58:50
2	37	40	44	47	20:58:44
3	36	39	44	46	20:58:38
4	35	35	44	45	20:58:32
5	37	40	44	46	20:58:26
6	37	40	45	46	20:58:20
7	37	38	45	46	20:58:14
8	37	39	45	47	20:58:08
9	36	40	44	47	20:58:02
10	36	36	44	46	20:57:56
11	36	39	44	46	20:57:50
12	35	39	45	45	20:57:44
13	35	35	45	47	20:57:38
14	36	38	45	47	20:57:32
15	35	40	45	46	20:57:26
16	35	39	45	47	20:57:20
17	37	42	44	47	20:57:14
18	36	35	44	47	20:57:08
19	35	38	44	47	20:57:02
20	37	39	43	46	20:56:56
21	37	37	45	47	20:56:50
22	34	39	44	47	20:56:44
23	36	39	45	48	20:56:38
24	35	37	44	47	20:56:32
25	34	40	44	47	20:56:26

26	37	40	44	47	20:56:20
27	34	39	45	47	20:56:14
28	39	38	44	47	20:56:08
29	36	37	44	46	20:56:02
30	36	37	44	46	20:55:56
31	35	39	42	47	20:55:50
32	37	40	44	46	20:55:44
33	36	34	45	45	20:55:38
34	37	39	44	46	20:55:32
35	39	40	44	47	20:55:26
36	37	39	44	46	20:55:20
37	36	39	43	47	20:55:14
38	37	40	43	46	20:55:08
39	36	37	44	47	20:55:02
40	36	39	45	47	20:54:56
41	36	40	43	47	20:54:50
42	35	40	44	46	20:54:44
43	34	39	44	47	20:54:38
44	36	40	43	47	20:54:32
45	36	40	42	47	20:54:26
46	35	38	43	46	20:54:20
47	36	40	44	48	20:54:14
48	35	35	44	45	20:54:08
49	33	40	44	47	20:54:02
50	35	41	43	47	20:53:56
51	34	40	44	47	20:53:50
52	35	40	44	48	20:53:44
53	36	40	44	47	20:53:38
54	35	38	44	47	20:53:32
55	34	40	43	46	20:53:26
56	36	40	43	48	20:53:20
57	34	36	45	46	20:53:14

58	37	39	45	46	20:53:08
59	36	39	44	46	20:53:02
60	34	39	43	45	20:52:56
	35.817	38.7	44.02	46.55	Averages

APPENDIX 4

Table 4

Experimental data captured and presented in Figure 4.1

	100kg	80kg	60kg	40kg	20kg	0kg		
Readings	dBm	dBm	dBm	dBm	dBm	dBm	RPM	Time
1	-8	-4	-8	-8	-8	-8	10	11:42:34
2	11	-4	-9	-9	13	-9	10	11:42:20
3	17	14	11	-9	18	4	136	11:42:06
4	17	16	15	15	19	9	276	11:41:52
5	19	17	19	18	20	12	380	11:41:38
6	20	18	18	17	21	12	486	11:41:24
7	21	20	19	19	21	13	497	11:41:10
8	21	20	21	22	22	11	497	11:40:56
9	21	19	21	20	21	8	497	11:40:42
10	20	18	21	20	20	7	565	11:40:28
11	19	19	20	21	20	8	670	11:40:14
12	17	19	21	19	18	8	790	11:40:00
13	17	18	20	21	18	18	909	11:39:46
14	16	17	20	21	18	12	995	11:39:32
15	17	17	19	19	19	12	996	11:39:18
16	18	16	21	23	19	13	996	11:39:04
17	19	18	21	23	19	12	996	11:38:50
18	17	18	22	21	19	13	995	11:38:36
19	18	19	19	22	18	13	996	11:38:22
20	18	19	18	21	19	12	996	11:38:08
21	17	18	18	21	19	15	996	11:37:54
22	18	18	22	22	19	14	995	11:37:40
23	18	18	20	21	19	13	996	11:37:26
24	18	18	22	22	19	18	996	11:37:12
25	19	18	21	21	19	9	996	11:36:58
26	17	19	19	21	19	12	994	11:36:44

27	19	19	19	21	18	8	1081	11:36:30
28	17	16	19	20	21	11	1186	11:36:16
29	18	17	21	22	20	14	1291	11:36:02
30	16	17	22	21	19	15	1395	11:35:48
31	18	16	21	22	20	15	1496	11:35:34
32	17	20	22	22	19	15	1496	11:35:20
33	18	19	23	22	21	15	1494	11:35:06
34	17	16	20	21	19	15	1496	11:34:52
35	18	18	21	22	20	15	1495	11:34:38
36	17	18	23	23	20	14	1496	11:34:24
37	16	19	23	23	19	12	1496	11:34:10
38	18	19	21	23	19	12	1495	11:33:56
39	18	19	22	22	22	15	1472	11:33:42
40	18	20	21	22	21	13	1421	11:33:28
41	17	20	21	22	20	13	1367	11:33:14
42	20	18	21	23	19	14	1316	11:33:00
43	17	20	21	23	20	13	1264	11:32:46
44	17	19	21	22	20	12	1209	11:32:32
45	17	20	21	22	21	14	1157	11:32:18
46	18	18	21	22	20	13	1107	11:32:04
47	17	18	21	21	20	12	1054	11:31:50
48	18	18	23	22	19	11	994	11:31:36
49	18	18	21	21	19	14	995	11:31:22
50	18	18	19	21	19	16	996	11:31:08
51	18	18	18	20	19	13	996	11:30:54
52	19	19	20	21	19	14	996	11:30:40
53	18	19	20	20	19	14	996	11:30:26
54	18	18	20	19	19	17	995	11:30:12
55	18	18	20	19	19	14	996	11:29:58
56	17	18	19	20	19	14	967	11:29:44
57	18	19	21	21	20	14	913	11:29:30
58	18	17	20	20	20	15	862	11:29:16

59	18	19	20	21	19	12	802	11:29:02
60	18	18	20	20	18	11	750	11:28:48
61	18	18	21	20	18	10	698	11:28:34
62	19	18	20	22	19	13	646	11:28:20
63	19	19	22	22	20	12	593	11:28:06
64	20	20	22	22	20	13	541	11:27:52
65	21	20	22	22	20	13	497	11:27:38
66	19	19	21	22	20	12	497	11:27:24
67	20	19	19	20	21	13	497	11:27:10
68	20	19	21	20	20	14	497	11:26:56
69	19	18	20	21	19	12	498	11:26:42
70	18	18	20	21	18	13	498	11:26:28
71	19	17	19	21	19	11	456	11:26:14
72	18	17	20	21	19	15	404	11:26:00
73	19	17	21	22	17	13	351	11:25:46
74	19		20	19	19	13	300	11:25:32
75	19		20	20	19	14	247	11:25:18
76	18		20	21	19	15	195	11:25:04
77	19		22	20	21	16	145	11:24:50
78	21		20	22	22	9	90	11:24:36
79	6		11	13	9	5	10	11:24:22
80	5		11	14	18	-3		11:24:08
	18.23	18	20.51	21.07	19.44	12.89	-----	Averages

APPENDIX 5

Table 5

Experimental data captured and presented in Figure 4.1

100kg	80kg	60KG	40KG	20KG	0KG		Time
dBm	dBm	dBm	dBm	dBm	dBm	RPM	
-9	-9	-9	-9	-9	-9	10	11:42:34
-9	-9	-9	-9	-9	-9	10	11:42:20
-9	-9	-9	-9	-9	-9	10	11:42:06
-9	-9	-9	-9	-9	-9	10	11:41:52
-9	-9	1	14	-9	-9	34	11:41:38
8	7	16	14	12	23	184	11:41:24
10	15	16	15	15	14	289	11:41:10
14	15	20	17	14	16	393	11:40:56
17	16	23	24	16	15	497	11:40:42
23	22	21	21	19	17	497	11:40:28
21	20	23	22	18	24	497	11:40:14
20	20	22	21	18	21	496	11:40:00
20	20	21	20	18	19	563	11:39:46
22	21	23	21	18	19	668	11:39:32
21	22	21	22	20	18	773	11:39:18
22	23	23	26	20	18	878	11:39:04
23	25	25	24	19	19	982	11:38:50
24	26	26	27	23	22	995	11:38:36
24	24	25	28	22	19	996	11:38:22
26	29	26	26	22	23	996	11:38:08
26	25	25	28	23	22	996	11:37:54
24	25	28	26	22	21	996	11:37:40
25	27	26	25	22	19	994	11:37:26
24	24	25	26	22	23	995	11:37:12
25	25	28	26	23	18	996	11:36:58

23	24	25	28	27	19	996	11:36:44
25	25	27	25	22	19	994	11:36:30
24	25	26	25	23	21	996	11:36:16
25	24	27	27	24	19	1017	11:36:02
24	24	27	24	23	20	1122	11:35:48
23	24	28	25	22	20	1227	11:35:34
26	26	26	25	23	21	1332	11:35:20
25	25	26	26	25	23	1436	11:35:06
24	25	26	25	24	23	1496	11:34:52
25	29	25	25	25	24	1495	11:34:38
25	25	27	28	25	24	1496	11:34:24
24	25	28	25	22	24	1495	11:34:10
25	24	28	24	23	24	1496	11:33:56
24	25	25	25	24	23	1495	11:33:42
26	25	25	27	28	23	1494	11:33:28
25	25	25	25	22	23	1496	11:33:14
25	25	25	25	24	22	1495	11:33:00
25	27	25	25	23	21	1496	11:32:46
25	25	25	24	22	21	1496	11:32:32
27	25	25	25	22	21	1494	11:32:18
25	25	25	28	22	21	1488	11:32:04
25	26	26	26	24	21	1384	11:31:50
26	26	26	25	25	20	1279	11:31:36
25	27	27	25	24	19	1175	11:31:22
28	27	28	26	24	21	1069	11:31:08
25	25	25	27	23	20	996	11:30:54
23	24	24	24	22	19	994	11:30:40
26	25	27	26	21	19	995	11:30:26
24	26	26	24	24	19	995	11:30:12
23	27	25	26	23	19	996	11:29:58
25	27	24	25	22	19	996	11:29:44
23	28	23	24	22	18	996	11:29:30

26	24	26	24	25	19	996	11:29:16
24	24	24	25	28	19	996	11:29:02
27	24	24	29	23	19	994	11:28:48
24	24	25	24	23	19	994	11:28:34
24	24	23	25	24	18	995	11:28:20
25	23	29	25	23	19	930	11:28:06
25	24	28	28	24	20	826	11:27:52
23	24	27	24	23	20	720	11:27:38
23	24	28	25	22	20	617	11:27:24
25	24	22	23	22	19	513	11:27:10
21	24	24	21	19	18	497	11:26:56
21	21	21	21	18	17	497	11:26:42
20	22	26	20	19	18	497	11:26:28
21	20	20	20	18	17	497	11:26:14
24	22	21	20	22	17	497	11:26:00
23	20	21	21	20	15	497	11:25:46
19	20	20	21	19	15	497	11:25:32
20	22	25	20	19	15	497	11:25:18
19	20	23	21	19	15	497	11:25:04
19	19	20	20	18	15	497	11:24:50
20	20	21	20	17	15	497	11:24:36
22	20	21	25	21	15	497	11:24:22
21	21	20	22	19	16	433	11:24:08
21	21	21	20	20	16	328	11:23:54
23	21	19	20	18	14	226	11:23:40
22	21	18	19	21	5	89	11:23:26
8	9	12	1	20	-9	10	11:23:12
24	24	25	24	22	20	-----	Averages

APPENDIX 6

Test bearing configuration, design specifications and lubrication properties used in this thesis.

The bearing in Figure 5.1 was a standard SKF ball bearing unit with a Y- unit design arrangement. These units comprise of a single row deep groove ball bearing with convex sphered outside housing.

Y-bearing units are easy to mount and enable initial errors of alignment to be compensated for.

Figure 5.1 Test bearing configuration.

The Y bearing is mounted in a collar take-up housing unit as illustrated in Figure 5.2. It is designed for quick, easy and safe mounting.

Figure 5.2. Bearing mounted in collar take-up housing.

In Figure 5.3 and in table 5 the configuration and design specifications are given.

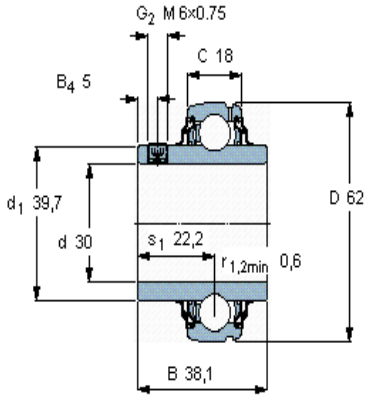

Hexagonal key size [mm]
3

Rec. tightening torque [Nm]
4

Appropriate rubber seating ring
RIS 206 A

Calculation factor
f_0 14

Figure 5.3 Bearing configuration

Table 5.1 Bearing design specifications

Principal dimensions				Basic load ratings		Fatigue load limit	Limiting speed	Mass	Designation
				dynamic	static				
D	D	B	C	C	C0	Pu			
mm				kN		kN	r/min	kg	-
30	62	38,1	18	16,3	11,2	0,475	3800	0,29	YAR 206-2RF/HV

Table 5.2 Lubrication properties of the oil used in this thesis.

Property	Value in metric unit	
Density at 60°F (15.6°C)	0.872 *10^3	kg/m^3
Kinematic viscosity at 104°F (40°C)/100°F (38°C)	108.5	cSt
Kinematic viscosity at 212°F (100°C)/210°F (99°C)	15.4	cSt
Viscosity index	149	
CCS viscosity at -13°F (-25°C)	6270	cP
Flash point	220	ºC
Pour Point	-33	ºC
Sulphated ash	0.86	%
Neutralization No. (TBN-E)	7.1	

APPENDIX 7

Bearing defect specifications as mentioned in section 3.3.5.

Figure 6.1 show the test bearing with the 0.1 mm defect induced in the raceway for the experiments performed in Section 4.6.1.

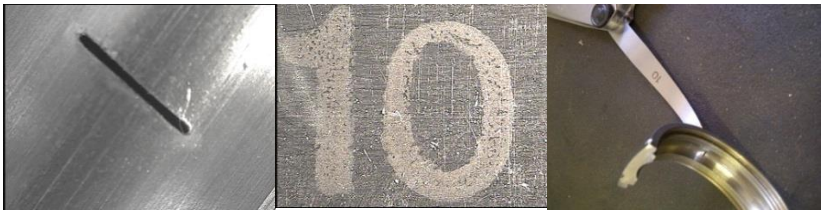

Figure 6.1. 10 Micron feeler gauge inserted into the 0.1mm defect.

Figure 6.2 show the test bearing with the 0.2 mm defect induced in the raceway for the experiments performed in Section 4.6.2.

Figure 6.2. 20 Micron feeler gauge inserted into the 0.2mm defect.